Novel Planning and Market Models for Energy Storage Systems in Smart Grids

by

Ahmed Awad

A thesis
presented to the University of Waterloo
in fulfillment of the
thesis requirement for the degree of
Doctor of Philosophy
in
Electrical and Computer Engineering

Waterloo, Ontario, Canada, 2014

AUTHOR'S DECLARATION

I hereby declare that I am the sole author of this thesis. This is a true copy of the thesis, including any required final revisions, as accepted by my examiners.

I understand that my thesis may be made electronically available to the public.

Abstract

The increasing deployment of distributed generation, especially renewable-based due to feed-in-tariff programs, has led to a revolution in the use of distribution systems and the emergence of smart-grid concepts. Smart grids are intended primarily as a means of facilitating the integration of renewable energy sources and of achieving greater system reliability and efficiency. Energy storage systems (ESSs) offer a number of benefits that can help utilities move toward achieving those goals. However, ESSs are very expensive in capital and operation costs. Consequently, utilities are very conservative in deploying ESSs into their networks because they are not certain about the economic benefit of integrating ESSs into their networks over their high costs. The research work presented in this thesis addresses this barrier through analysis and quantification of the potential benefits of installing ESSs for distribution companies, thus increasing the interest of adopting ESSs in distribution networks. Moreover, this thesis aims to investigate the impact of integrating large-scale ESSs on electricity markets.

The first goal of this thesis is to develop a comprehensive planning framework for allocating distributed storage (DS) units in distribution networks in order to achieve several benefits that include improving distribution system reliability, deferring network upgrades, and making benefit of the price arbitrage. The use of DS allows for successful islanding operation, thus preventing loss of load or minimizing the loss of energy supplied to non-affected customers during network disturbances. Moreover, the application of DS helps in shifting the peak demand into off-peak times, thus deferring the network upgrades. On the top of that, charging and discharging the DS units during off-peak and peak times, respectively, represents another benefit due to the price arbitrage between those different times. In this framework, the installation and maintenance costs of DS units are optimized with respect to the economic value of the benefits mentioned above. The output of the planning framework is the optimal size and location of DS units to be installed, the optimal operation of DS at each load state, and the load points to be shed during contingencies.

The second goal of this thesis is to present a mathematical model for determining the optimal operation of ESS as well as the market prices in a perfectly competitive environment. Controlling ESS operation usually depends on electricity-market prices so as to charge when the price is low and discharge when the price is high. On the other hand, the market-clearing price itself is determined based on the energy storage output. The problem is formulated as a mixed complementarity problem.

The proposed model is useful for power system operators dealing with large-scale ESSs at their networks. Furthermore, the impact of energy storage size and location on market price, total generation cost, energy storage arbitrage benefit, and total consumer payment is investigated using the model proposed.

Acknowledgements

All praise is due to Allah almighty, who taught humans what they knew not and whose countless bounties have enabled me to complete this thesis successfully.

I would not have finished my dissertation without the guidance of my committee members, help from my friends, and support from my family.

I would like to express my deepest gratitude to my advisors, Professor M. Salama and Dr. T. El-Fouly, for their guidance, care, and patience, and providing me with such a wonderful environment for conducting research.

I also offer my gratitude to my parents. My research work would not have been possible without their help, their constant support and encouragement, and their never-failing good wishes.

Finally, I would like to thank my siblings and fiancée Alyaa for always standing by me through both the good times and the bad.

Dedication

To my beloved father, Samir,

To my precious mother, Saadia,

To my dear siblings, Manal, Naglaa, and Mohamed,

To my beloved fiancé, Alyaa,

in recognition of your endless love, care, support, and encouragement.

Table of Contents

List of Figures

List of Tables

Nomenclature

Acronyms

CAES	Compressed air energy storage
CAS	Compressed air in vessels
CDF	Cumulative distribution function
CDFN	Customer damage function
DER	Distributed energy resource
DG	Distributed generation
DS	Distributed storage
ECOST	Expected interruption cost
EENS	Expected energy not supplied
ESS	Energy storage system
GA	Genetic algorithm
GAMS	General algebraic modeling system
IESO	Independent electricity system operator
KKT	Karush-Kuhn-Tucker
LA	Lead-acid battery
LMP	Locational marginal price
LP	Linear programming
MCP	Mixed complementarity problem
MCS	Monte Carlo simulation
MINLP	Mixed integer non-linear programming
MPC	Model predictive controller
Na/S	Sodium-sulfur battery
Ni/Cad	Nickel-cadmium battery
NLP	Non-linear programming
NPV	Net present value
O&M	Operation and maintenance
PCS	Power conversion system

PDF	Probability distribution function
PV	Photovoltaic
PVF	Present value function
RES	Renewable energy source
RTS	Reliability test system
SC	Super capacitor
SMES	Superconducting magnetic energy storage
SOP	Standard offer program
VR	Vanadium redox
WTP	Willingness to pay

Indices

d	Interruption event index
hr	Hour index
i, j	System bus indices
k	Faulty line (contingency) index
l	Load state index
min	Script referring to minimum values
max	Script referring to maximum values
q	Constraint index
s	Combined load-DG state index
u	Reinforcement index
w	Wind speed state index
yr	Year index
y_u	Index of the year by which reinforcement u is required

Parameters

B_{ij}	Imaginary part of bus admittance matrix element (i,j), pu siemens
c	Scale index of Weibull PDF
C_E	Capital energy cost of the ESS
C_E^*	Annualized capital energy cost of the ESS

C_M	Annual operation and maintenance cost of the ESS
C_O	Operational cost of the ESS
$c_{\text{off-peak}}$	Average off-peak electricity price, \$/pu kWhr
c_{peak}	Average peak electricity price, \$/pu kWhr
C_P	Capital power cost of the ESS
C_P^*	Annualized capital power cost of the ESS
e	Shape index of Weibull PDF
E_{ESS}^{rated}	Rated capacity of the ESS, pu kWhr
F	Inflation rate
FR	Future value of replacement cost
G_{ij}	Real part of bus admittance matrix element (i,j), pu siemens
IR	Interest rate
IR'	Effective interest rate
M	Total number of required upgrades
$MTTF$	Mean time to fail, hour
$MTTR$	Mean time to repair, hour
n	Lifetime of the equipment
N	Total number of system buses
N_c	Total number of constraints
N_y	Number of years generated by Monte Carlo simulation
N_{yr}	Number of years in the planning period
P_D	Demand active power, pu kW
P_G	Generated active power, pu kW
P_r	Rated output power of the wind turbine, pu kW
Q_D	Demand reactive power, pu kW
Q_G	Generated reactive power, pu kW
S_{ESS}^{rated}	Rated charging/discharging power of the ESS, pu kW
v_{ci}	Cut-in speed of the wind turbine, m/s
v_{co}	Cut-out speed of the wind turbine, m/s
v_{mean}	Mean wind speed in a given site, m/s

v_r	Rated speed of the wind turbine, m/s
Y	Magnitude of bus admittance matrix element, pu siemens
θ	Angle of bus admittance matrix element, degree
$\rho_{(\bullet)}$	Probability of state $(\bullet)$
$\alpha, \beta,$ and γ	Generation cost function parameters in \$/MWhr^2, \$/MWhr, and \$, respectively
η	Round-trip efficiency of the ESS
η^{ch}	Energy storage charging efficiency
η^{dis}	Energy storage discharging efficiency

Sets

$\mathcal{E}$	Set of candidate buses for energy storage installation
$\mathcal{G}$	Set of system buses equipped with generators
$\mathcal{L}$	Set of load states
$\mathcal{L}_{ch}$	Set of candidate load states for ESS charging
$\mathcal{L}_{dis}$	Set of candidate load states for ESS discharging
$\mathcal{M}_k$	Set of system buses equipped with ESS units for contingency k
$\mathcal{S}$	Set of combined load-DG states
$\mathcal{S}_{ch}$	Set of candidate combined load-DG states for ESS charging
$\mathcal{S}_{dis}$	Set of candidate combined load-DG states for ESS discharging

Variables

CE_{loss}	Cost of energy losses
C_R	Net present value of the replacement cost of the ESS
E_{ESS}	Energy stored at the ESS, pu kWhr
NPV_{AR}	Net present value of the arbitrage benefit
NPV_{LO}	Net present value of the energy losses costs
NPV_{UP}	Net present value of the system upgrade costs
P	Net active power generated, pu kW
P_{ESS}^{ch}	Energy storage charging active power, pu kW
P_{ESS}^{dis}	Energy storage discharging active power, pu kW
P_{flow}	Power flow of the line, pu kW

P_g	Generated active power, pu kW
P_{loss}	Total power losses in the distribution network, pu kW
P_{SH}	Portion of load to be shed that is equal to 1 if the load is totally shed
Q_{ESS}	Energy storage output reactive power, pu kVAR
Q_g	Generated reactive power, pu kVAR
r	Replacement period of the ESS
R_u	Cost of reinforcement u
T_d	Duration of interruption d, hour
t_q	Binary variable associated with constraint q, which equals to zero if the corresponding constraint is satisfied, or otherwise equals to one
T_{repair}	Repair time, hour
T_{up}	Up time, hour
V	Bus voltage magnitude, pu Volt
x	Integer decision variable controlling the power size of ESS to be installed
y	Integer decision variable controlling the energy capacity (size) of ESS to be installed
z	Integer decision variable controlling the load to be shed
δ	Bus voltage phase angle, degree
$\delta_{ij,hr}$	Difference in phase angles of buses i and j at hour hr, i.e., $\delta_{i,hr} - \delta_{j,hr}$, degree
λ	Locational marginal price, $/pu kWhr
Λ	Highest locational marginal price in the system, $/pu kWhr

Chapter 1
Introduction and Objectives

1.1 Preface

The recent deployment of distributed generation (DG) has led to a revolution in the use of distribution systems. Distribution systems have become active, and hence they are referred to as "active distribution networks". Furthermore, renewable portfolio standards place obligations to have certain penetration percentage from renewable energy sources (RESs), e.g. state of California requires that 33% of the supply mix should be provided from RESs by 2020 [1]. Customers are also becoming interested in participating in electricity-market operations to reduce their energy bills. This practice is referred to as "load management or demand response". Load management can be achieved by implementing two-way communication infrastructure between utilities and customers [2].

As a consequence of all of the above, it is crucial that the distribution system is operated in a fundamentally different manner. One of the initiatives that have been proposed to manage this new environment is the concept of "smart grid". Smart grids could be defined from different perspectives; they are defined as the two-way flow of electricity and information between supply and demand. Another definition is the application of intelligent devices and communication technologies in power systems [2]. Smart grids are intended primarily as a means of facilitating the integration of RESs and achieving greater system reliability and efficiency.

Energy storage systems (ESSs) offer a number of benefits that can help utilities move toward achieving the goals of smart grids. Some of these benefits are enumerated as follows:

- facilitating the integration of RESs;
- improving the reliability of distribution systems;
- deferring the upgrade of assets in distribution networks;
- mitigating the power quality issues found in modern distribution networks.

Reference [3] represents the benefits of ESSs in monetary value, i.e., dollars per installed capacity of energy storage ($/kW), as shown in Figure 1-1. More than 20 benefits are considered in this work, and they are categorized into six main applications; electric supply, ancillary services, grid system, end user/utility customer, renewables integration, and incidental. The benefits are calculated based on the present worth value for 10 years with 2.5% inflation rate and 10% discount rate.

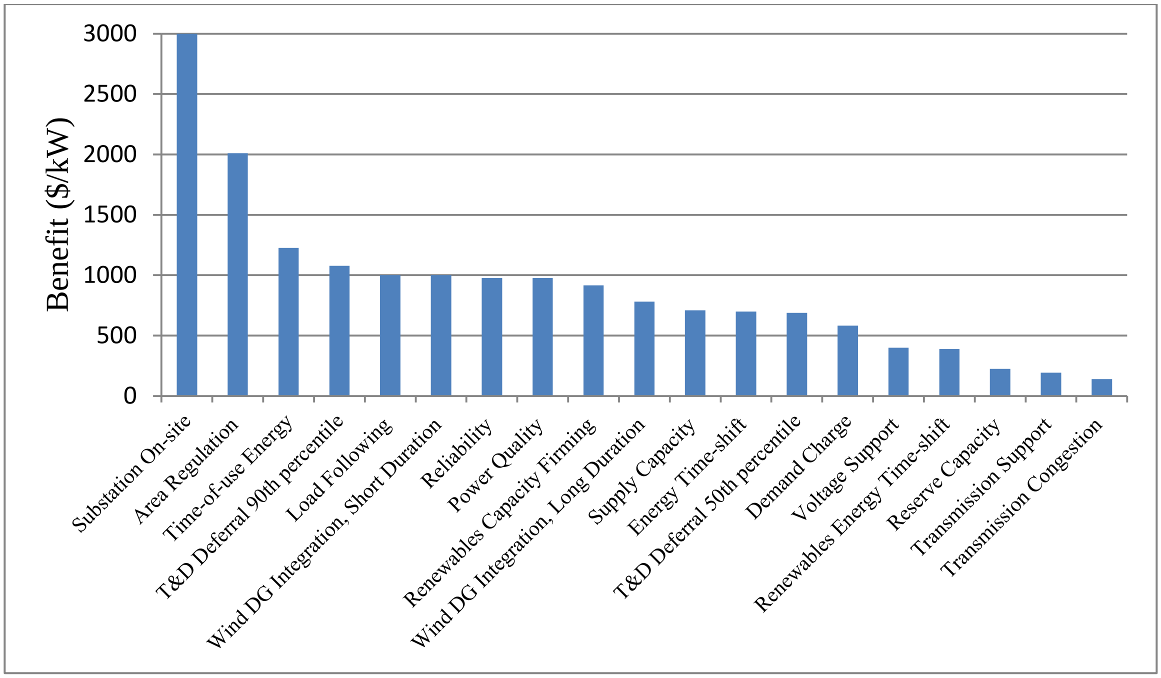

Figure 1-1 Application-specific 10-year benefit estimates for the U.S. [3]

Today, the worldwide capacity of energy storage is about 90 GW, which is almost 2.6% of the total electricity production (3400 GW) [4]. In Canada, the first battery storage project (2×1 MW) has been installed near Golden substation in 2012; the project, funded by both British Columbia (BC) Hydro and Natural Resources Canada (NRCan), aims to shave the peak load at Golden substation and to reduce the interruption durations for customers in "Field" area [5]. Another battery-storage project was recently installed by Toronto Hydro with rating of 500 kW-250 kWh [6]. According to Ontario's long-term energy plan, 50 MW of energy storage is to be procured by the end of 2014 [7]. In 2007, the American electric power has launched three energy storage projects, each is 2 MW-14 MWhr sodium-sulfur batteries, for the purpose of improving distribution system reliability [8]. Moreover, state of California has adopted the United States' first energy-storage mandate, requiring the state's three major power companies to have 200 MW of electricity-storage capacity in place by the end of 2014 and 1325 MW by 2020 [9].

ESSs are very expensive in capital, operation, and maintenance costs. As observed in Figure 1-2, the installation costs of energy storage have declined by almost 50% in the last decade. They are further expected to decrease in the future and become less than $600 per kW by 2020 [10]. As cheaper and more effective storage technologies appear, large-scale ESSs would deem more cost effective for grid applications.

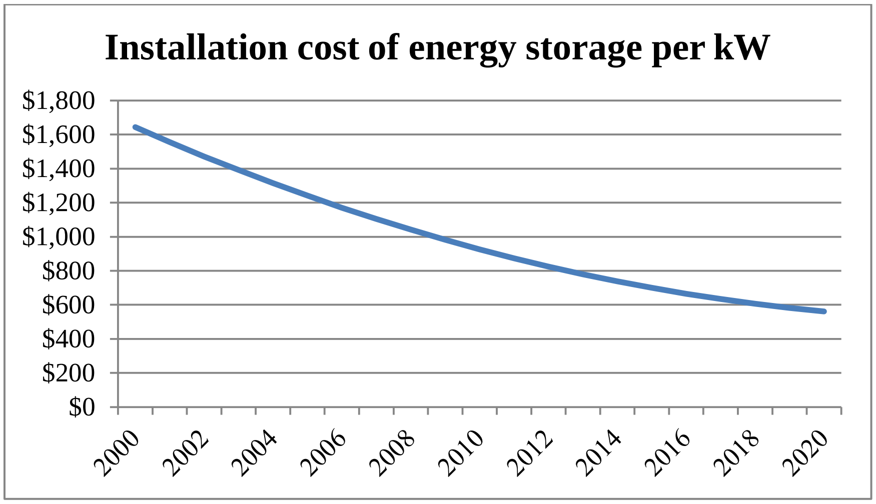

Figure 1-2 Historical and projected costs of energy storage [10]

1.2 Research Motivation

As concluded from the previous section, ESSs are one promising technology that can support the incorporation of smart grids because of their capacity to improve system reliability and to facilitate the integration of high penetration levels of RESs. Thus, distribution companies would be interested in allocating ESSs in their networks in order to achieve several benefits. However, the main obstacle of integrating ESSs into power systems is the high capital costs of the current storage technologies. Therefore, planning frameworks need to be developed that include maximization of the benefits of installing ESSs with respect to their capital and operation costs. Such frameworks would be useful for distribution companies, which are assumed to be the candidate owner of ESSs. As well, governments may consider special incentives for ESS operation in order to encourage private investment. Thus, mathematical models are required for electricity markets incorporating large-scale ESSs under such incentives. These models would be beneficial for system operators to determine the market equilibrium, in the presence of large-scale ESSs, and to study the impact of energy storage size and location on the various market variables.

1.3 Research Objectives

The rationale behind the work presented in this thesis is to assess and quantify the benefits of integrating ESSs into distribution networks and to study the impact of large-scale ESSs on electricity-market equilibrium. Thus, the proposed research has two main objectives; the first objective is to propose a planning framework for the allocation of ESSs, while the second one is to develop energy-market based tool for electricity markets incorporating large-scale ESSs.

In more details, the first objective of the proposed research is to develop planning framework for allocating distributed storage (DS)[1] units via optimizing the installation costs with respect to the benefits of DS application. Therefore, this planning framework ascertains the most cost-effective siting and sizing of DS units in distribution systems in order to achieve several benefits as follows:

- Improving distribution system reliability—a value-based reliability approach is adopted as a means of improving distribution system reliability from an economic perspective. In that approach, the willingness of some customers to pay more for greater reliability is taken into consideration.
- Arbitrage benefit and system upgrades deferral—the application of energy storage to shave peak load is similar to demand side management programs that shift demand use of energy from peak to off-peak periods. In this application, some energy is stored within DS during off-peak times and is released when the load is high (i.e., peak). Two benefits basically arise from this application. The first one, namely arbitrage benefit, is the direct benefit from buying and storing energy with an inexpensive price during off-peak periods, and selling the energy stored back, after accounting of the losses in the DS, with a high price at peak times. The second benefit is to defer system upgrades; system upgrades are usually required in order to account for the annual load growth in a given distribution system. Through peak load shaving, system upgrades can be deferred to later years, and the net present value of system upgrades can be then reduced.

The second objective is to propose energy-market based tool for electricity markets incorporating large-scale ESSs. Controlling ESS operation usually depends on electricity-market prices so as to charge when the price is low and discharge when the price is high. On the other hand, the market-clearing price itself is determined based on the net demand, i.e., including energy storage output, at

[1] The terms ESS and DS are used interchangeably in this thesis.

every hour. Therefore, the primary goal is to develop a mathematical model that determines the optimal ESS operation as well as the equilibrium market prices in a perfectly competitive environment. This model is very useful for power system operators dealing with large-scale ESSs in their networks.

1.4 Thesis Outline

As can be seen in Figure 1-3, the remainder of this thesis is organized in six chapters as follows:

Chapter 2 presents the background and literature review on the previous work in the field of planning and electricity-market models with ESSs. This chapter also provides the approaches adopted in the literature for modeling the various system components.

Chapter 3 provides the mathematical formulation for the cost-effective improvement of distribution system reliability through integrating DS units.

Chapter 4 discusses the methodology of allocating DS units for the purpose of deferring distribution system upgrades and making benefit of the price arbitrage.

Chapter 5 presents a comprehensive planning framework for the allocation of DS units that includes combination of the models presented in the previous two chapters.

Chapter 6 develops the electricity-market model for electricity-markets incorporating large-scale ESSs. This chapter further studies the impact of large-scale ESSs on electricity-market equilibrium.

Chapter 7 summarizes the conclusions and contributions of this thesis. This chapter further gives some directions for future research work.

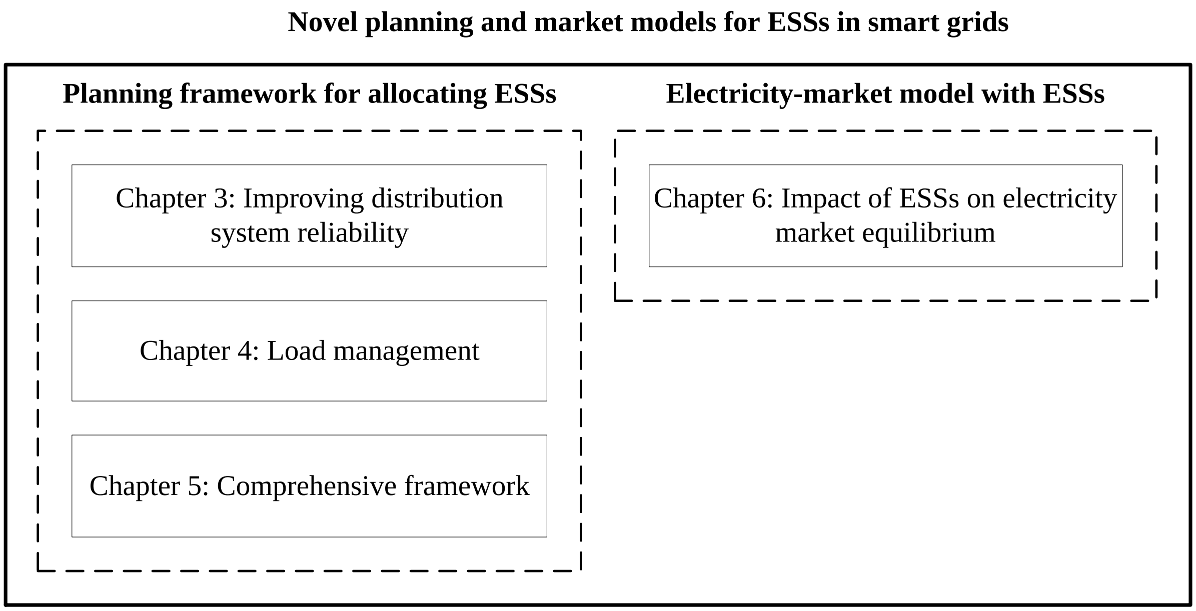

Figure 1-3 Thesis outline

Chapter 2
Background and Literature Review

2.1 Introduction

Chapter 1 presented the motivation to this research work and summarized the research objectives. In this chapter, the background information of ESSs is introduced, followed by a literature survey of the previous research conducted in the field of planning and market models with ESSs. Moreover, the various approaches used for modeling the stochastic nature of different system components are provided in this chapter. Finally, this chapter summarizes the drawbacks of the previous work addressed in the literature.

2.2 Energy Storage Technologies

There are several technologies for energy storage; each has its own characteristics, and hence it economically sounds for one or more applications. Basically, any ESS consists of energy storage reservoir and power conversion system (PCS). The PCS is either a dc-ac converter as in case of superconducting magnetic energy storage (SMES) and batteries, or a motor-generator set as in case of pumped hydro, compressed air energy storage (CAES), and flywheels [11], [12].

ESSs can be classified into three main categories, according to their applications as follows: power quality, bridging power, and energy management [13]. Power quality applications use the energy stored for time durations of seconds or less in order to mitigate power quality problems, such as voltage and frequency variations. Bridging power is to ensure continuity of power supply during switching from one power source to another, i.e., about seconds to minutes. Finally, energy management implies energy being stored during off-peak periods so that it can be used at the times of peak load. The classification of ESS technologies, according to each application, is shown in Figure 2-1 [13].

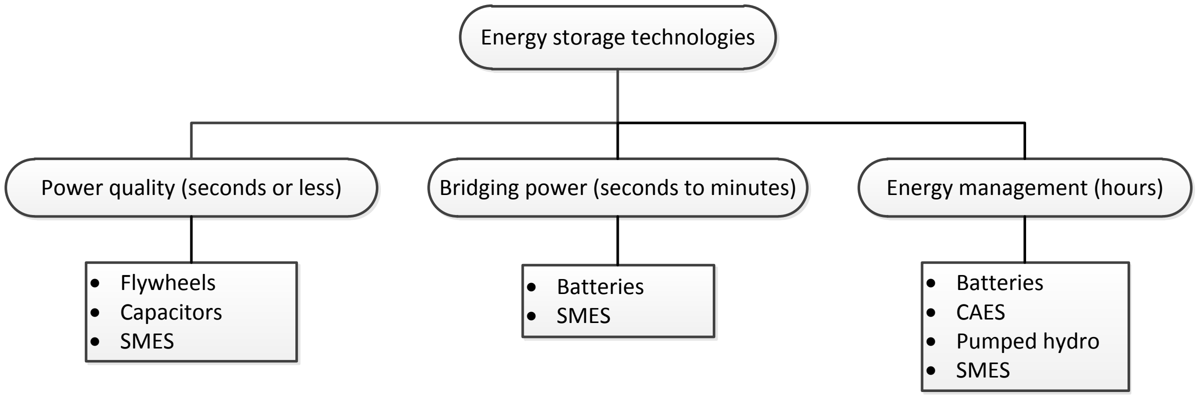

Figure 2-1 Classification of ESSs according to the application

From the physical construction point of view, ESSs can be classified into static and dynamic devices, as presented in Figure 2-2. Static devices include SMES, capacitors, and batteries, whereas dynamic storage includes flywheels, CAES, and pumped hydro. Static devices have relatively low operation and maintenance (O&M) costs compared to the dynamic ones since there are no moving parts associated with static-based ESSs. Moreover, the efficiency of dynamic ESSs is less than that of static devices due to mechanical and friction losses [14].

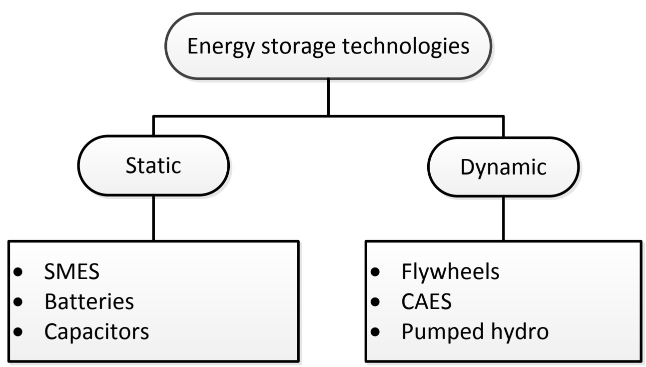

Figure 2-2 Classification of ESSs according to the physical construction

The physics behind each energy storage technology and the advantages/disadvantages of each technology are described briefly as follows [11], [15], [14], [16]:

- Superconducting magnetic energy storage (SMES): the energy is stored in the form of magnetic field produced by the current flowing through a superconducting coil. The coil is made of special alloys and cooled down to cryogenic temperature (i.e., -269°C) in order to have negligible resistance [16]. SMES has high efficiency and long life, and it provides a wide range of energy access time. On the other hand, it is the most expensive technology due to the need for coil refrigeration.

- Capacitors: they store energy in the form of electrical charge between two plates separated by a dielectric. Capacitors have long life cycle, high efficiency, and immediate recharge capability; however, they provide short-term storage. Improvements of capacitor designs have led to what is called “super capacitor (SC)”. Commercial sizes of SC are up to 100 kW with time duration up to 10 seconds [15].

- Batteries: they store energy in electrochemical form for wide range of time durations. The major drawback of batteries is that they have relatively low life cycle; life cycle is mainly a function of the frequency of charging/discharging [17]. They also have relatively low efficiency between 60-80% [15]. The main types of battery storage are lead-acid (LA), sodium-sulfur (Na/S), nickel-cadmium (Ni/Cad), and vanadium redox (VR) batteries.

- Flywheels: the energy is stored in the form of kinetic energy in rotating masses. Electrical energy is exchanged through a variable frequency motor/generator set using a cyclo-converter. Flywheels have long life cycle, moderate efficiency, and fast response; on the other hand, they have short energy access time [17], [18].

- Compressed air energy storage (CAES): it stores energy via compressing air within a reservoir. Natural aquifers are usually utilized as the reservoir for CAES, otherwise pressure vessels can be used; however, this artificial system, termed as “compressed air in vessels” (CAS) is more expensive than CAES [11]. Nevertheless, during discharging, the compressed air is burnt within a conventional combustor in order to produce electrical power. Therefore, it can be considered to be a hybrid energy storage and generation technology. It has moderate efficiency and response time. The only drawback is that it produces CO_2 emissions due to fuel burning during discharge periods.

- Pumped hydro storage: the energy is stored via pumping the water to a high altitude (high potential energy), and then this water is used to drive hydro-turbines at a lower level as needed. Pumped hydro storage is a mature technology. The only challenges are siting considerations and environmental issues due to dams building.

Table 2-1 summarizes the typical power and energy capital costs, O&M costs, maximum industrial sizes, and efficiency of each technology, based on statistics presented around the end of the last century [11], [19], [20]. Figure 2-3 shows the power ratings and the discharge times for different energy storage technologies, as published by the electricity storage association [21]. It is worthwhile to mention that the selection of a certain energy storage technology is mainly dependent on the application under consideration. In this thesis, the main focus is on energy management application, i.e., improving the reliability of distribution systems, and deferring the network upgrades. Therefore, batteries are selected as the candidate storage technologies since their power and discharge time capacities are suitable for the application under study.

Table 2-1 Capital and operation costs, efficiencies, and industrial ratings for the various storage technologies [11], [19], [20]

	SMES	Batteries	Capacitors	Flywheels	CAES	Pumped hydro
Power capital cost ($/kW)	300	300	300	220	425	600
Energy capital cost ($/kwh)	up to 500,000	200	3600	800	10	16.8
Fixed annual O&M cost ($/kW)	1	1.55	5% of capital costs	7.5	1.35	4.3
Efficiency (%)	95+refrigeration	75	95	80-85	85+fuel	75
Maximum power (MW)	1000	100	1	90	290	2000
Maximum energy (MWh)	5000	200	0.001	0.002	3000	20000

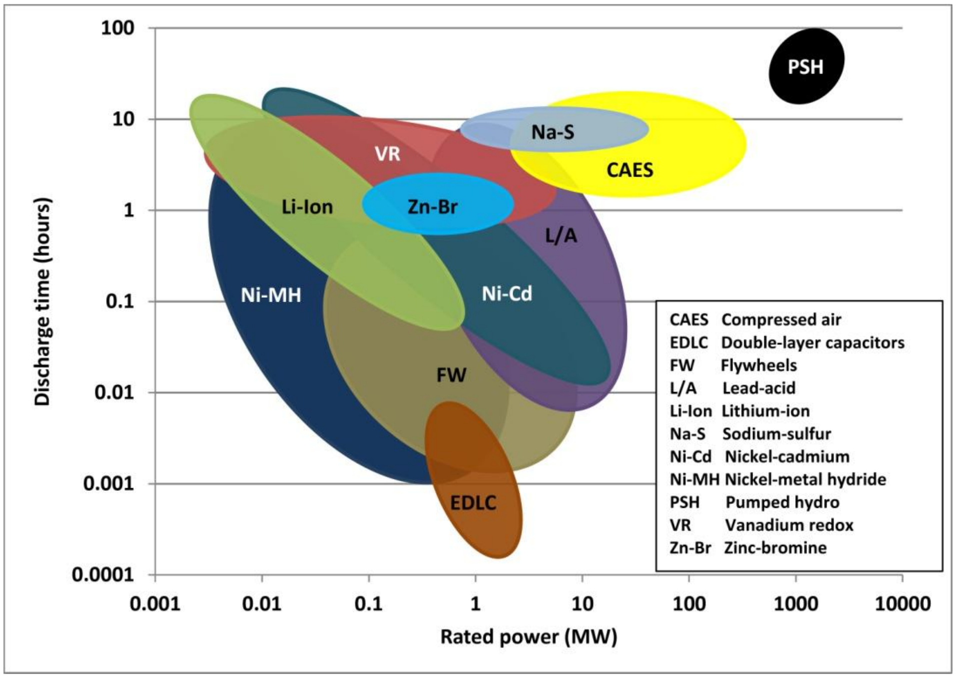

Figure 2-3 Power ratings and discharge time for the different storage technologies [21]

2.3 Optimal Allocation of Distributed Storage Units

What are the optimal locations and sizes for installing DS units? What is the optimal operation strategy (i.e., charging and discharging) of these DS units? These are the basic questions that typically arise when dealing with the integration of distributed energy resources (DERs) into electrical power systems. In the past few decades, many researchers have proposed algorithms for ascertaining the most cost effective sizing and siting of DG units in distribution networks. On the other hand, few research studies have investigated determining the optimal allocation of DS units in distribution systems. In these few studies, the following objectives have been considered:

- enhancement of the system reliability;
- deferral of the network upgrades;
- suppression of the fluctuations in the output electrical power of RESs;
- minimization of the curtailed output power from renewable-based DG units.

With respect to the enhancement of distribution system reliability, all of the work presented in this area is based on the assumption that islanding is allowed. Although utilities currently force DERs to be disconnected in case of islanding detection, this requirement would most likely change in the next few years due to the trend toward evolving the traditional grid into smart grids. According to [22], DERs can provide power to the system loads during planned or un-planned network outages. Basically, successful islanding operation improves system reliability by preventing loss of load or by minimizing the loss of energy supplied to non-affected customers during network disturbances. Thus, when a disturbance occurs, the formation of islands may help improve system reliability if DERs are available and are able to operate in islanded mode. However, because of the stochastic nature of the power generated from renewable-based customer-owned DG, e.g., wind turbines and photovoltaic (PV) arrays, distribution utilities cannot rely solely on such sources as a means of improving system reliability. They might utilize DS units as a backup source for addressing network disturbances. The primary challenge in introducing this concept of non-volatile distribution systems is the high installation cost associated with DS, which means that to minimize installation costs and maximize the associated improvement in reliability, distribution utilities must calculate the optimal size of the DS units to be installed.

Several research works have addressed the problem of optimal allocation of DG units to enhance the reliability of distribution systems, as in [23], [24], [25], [26]. In [23], DG units and circuit reclosers are allocated in order to minimize a composite reliability index. The results proved that the more reclosers and the higher DG sizes used, the less reliability index can be obtained. However, the authors did not consider the cost effectiveness of the solution since adding more reclosers and/or DG units may be more expensive than the benefits achieved form gaining higher reliability levels. This drawback was mitigated in [24], [26], wherein the authors have utilized a value-based reliability approach so that the costs associated with the levels of reliability play a role in the allocation decisions of DG units. Nevertheless, reliability evaluation of distribution systems has been conventionally done using segmentation concept, as in [23], [26], [27]. In this concept, the distribution system is divided into a number of segments according to the positions of protection devices. A failure of any component in one segment leads to isolating the whole segment from the entire system; however, self-healing capability necessitates that the system should detect and isolate the faulty part only, and restore the service in the healthy sections of the system, thus improving system reliability. Every fault scenario thus divides the system into a different configuration of grid connected and isolated buses. Therefore, all fault scenarios should be considered in order to determine the best fit allocation of DG units and/or ESSs as proposed in this thesis.

Like the research work conducted in reliability enhancement using DG, the feasibility of battery storage plants to enhance the power system reliability has been discussed in [28]. In [29], a Monte Carlo simulation (MCS) based method was proposed for evaluating the improvement of power system reliability using ESS but without including cost-benefit analysis that could justify the installation of ESS for such application. Moreover, the evaluation of distribution systems reliability with ESSs has been previously addressed in the literature [30], [31], [32]. A mathematical formulation was derived for the sizing of backup energy storage in order to meet specific reliability targets for critical customers [30], but since the formulas developed did not correspond to the network model, the impact of the location of the storage was not considered, nor did the authors optimize the economic benefit of achieving the reliability target relative to the storage cost. The authors in [31] compared the reliability and economic benefits of two different control strategies for energy storage in distribution systems: standby and model predictive controllers (MPCs). With a standby strategy, during islanding, an ESS is assumed to release its stored energy in order to supply isolated nodes, thus eliminating loss of load or minimizing loss of energy for the isolated customers. Once the network is restored following a disturbance, the ESS is immediately charged and put on standby in preparation for the next disturbance. The drawback of this strategy proposed is that the charging of the ESS was not included in the analysis, which was also based on the assumption that it can be fully charged between any two successive failures. However, the charging cycle of the ESS must be considered in order to determine whether it can be charged during acceptable operating states, i.e., without violating system constraints. On the other hand, an MPC-based strategy implies the forecasting of load demands and electricity prices, followed by a determination of the optimal charging and discharging power levels that enable the utility to benefit from the electricity price difference between off-peak and peak periods. The latter strategy is implemented in normal operation; however, during islanding, the proposed strategy behaves in a manner similar to that of the standby approach. The authors therefore concluded that standby control provides greater reliability than the MPC-based approach, but at the expense of more costly energy drawn from the substation. In [33], a systematic approach was presented for clustering distribution systems into virtual microgrids based on minimizing energy flows between these microgrids. The impact of allocating pre-specified amount of DS units and distributed reactive sources on maximizing the self-adequacy of formed microgrids was further studied in this reference.

Moreover, few research works have discussed the economic feasibility of DS integration with distribution substations in order to achieve other benefits, such as upgrade deferral, arbitrage benefit maximization, etc., in [34], [35]; however, the distribution network model has not been represented, thus the upgrade deferral has been evaluated by means of empirical formulas that consider the investment cost of distribution substation only.

In order to integrate high penetration levels from renewable-based DG units, measures should be taken in order to suppress the fluctuations associated with the output power of such DG. In this context, ESS can be controlled so as to minimize the difference between the forecasted and the actual output power of a wind farm [36]. In this reference, several strategies were proposed for controlling the ESS; a simple controller commands the ESS to source/sink an output power equal to the difference between forecasted and actual wind powers, if and only if this difference exceeds +/- 4%. The size of ESS was varied in steps, and simulations were adopted to calculate the total cost function in order to select the optimal solution with each control strategy. However, based on Ontario's standard offer program (SOP), DG units are only paid based on their output power, and there is no penalty for any power mismatch since DG units do not bid into the electricity market. According to this SOP, there is no benefit for the owners of renewable-based DG units to install ESSs with their DG units; however, such policies may change in the future when large penetration levels of RESs are integrated in the system [37].

Moreover, according to Ontario regulations, the utility has the right to curtail the power of renewable-based DG units when the reverse power flow exceeds 60% of the substation rating. The work introduced in [37] included determining the optimal size and location of ESSs that minimize the energy curtailment from wind-based DG units in distribution networks. Thus, the methodology proposed aims to maximize the benefits for both the DG owners and utilities via minimizing the DG energy to be curtailed. The results concluded that the economic benefits of installing ESSs are slightly higher than their installation costs. However, the authors could not identify the candidate owner of the allocated ESSs since the benefits are shared between two entities, i.e., the DG owners and utilities. Therefore, taking into account several benefits for utilities, e.g., improving system reliability and deferral of system upgrades, should be sufficient to justify the high costs that utilities would pay for installing ESSs. According to the best of the author's knowledge, combining more than one benefit for the implementation of ESSs has not been addressed yet in the literature.

2.4 Optimization Techniques for Planning Studies

In the literature, there are numerous techniques proposed for the allocation of DERs. The authors in [38] summarized all techniques used in DG planning and allocation problems into three categories: analytical analysis, numerical programming, and metaheuristics. Some of these techniques have been also used for the sizing and siting of DS units.

Analytical analysis is to find closed-form formulas for the optimal capacity of DG, at a certain location, that minimizes or maximizes a certain objective (e.g., power losses in distribution networks) [39]. The main drawback of such technique is that it only takes into account a given demand-generation snapshot scenario. Another limitation is that only a single DG location can be evaluated at a time; therefore, sequential analysis is required for evaluating multiple DG connections.

Numerical programming methods have been proposed to address the capacity allocation and optimization issues [37], [40]. Numerical programming is based on solving a modified formulation of the optimal power flow (OPF) problem, which is basically a non-linear programming (NLP) problem. Numerical programming can incorporate multiple periods in order to consider the variability in demand and generation, but at the expense of adding many variables and constraints to the problem formulation, thus increasing the computational time and effort. When dealing with integer decisions, for instance discrete sizes and locations of DG or DS units, a mixed integer NLP (MINLP) approach should be used. However, this approach could potentially limit the size of the problem according to the capabilities of the solution method [38]. Moreover, this classical optimization formulation may restrict the consideration of some technical aspects, e.g., using MCS for evaluating one or more terms within the objective function or constraints.

Metaheuristics are iterative generation techniques that combine intelligent concepts for exploring and exploiting the search space in order to find near-optimal solutions. One great advantage of metaheuristics is the flexibility of optimization-problem formulation, thus allowing for the consideration of complex technical aspects that cannot be handled using classical optimization formulations. Moreover, metaheuristics can be applied to any type of problems (e.g., NLP, MINLP, etc.). On the other hand, metaheuristics do not guarantee global optimal solutions. There are several metaheuristic optimization algorithms: genetic algorithm (GA), particle swarm optimization, Tabu search, etc. These algorithm are emerging as efficient optimization techniques to solve complicated problems such as DG planning [26] and unit commitment [41]. GA has been extensively used in the literature as in [23], [26], [42], [43], [44], and it has showed superior performance compared to other metaheuristic techniques in terms of the solution error and the execution time [45].

2.5 Probabilistic vs. Time-Series Modeling Approaches

Allocating DERs in distribution networks requires proper modeling for the system components, i.e., loads and DG units. In some works introduced in the literature, deterministic approaches have been adopted whereby the loads and DERs are represented as constant power elements, usually based on their average or maximum ratings. Although these approaches can be easily implemented, adopting them in allocation problems may lead to inaccurate or non-realistic results, or even degrade system performance under realistic conditions [40]. Therefore, considering the stochastic nature of system components is necessary in order to obtain more realistic results. Two approaches can be used to include the consideration of the stochastic nature of system components, namely time-series and probabilistic modeling approaches.

The literature includes numerous accounts of the use of time-series models for modeling the stochastic nature of a variety of components, such as RES-based DG and load demand, as in [36], [37], [46], [42]. These models usually imply one year-ahead forecasting for all loads and generation units. The forecasted profiles are then used for determining the charging/discharging cycle of the ESS at each hour, based on which the size of the ESS is optimized or the adequacy of the power systems with the ESS is assessed. Despite the difficulties associated with forecasting highly stochastic components, such as wind speed and solar irradiance, the application of time-series models in planning studies provides an optimal solution that is valid only for the time-series pattern that is applied. Consequently, the solution obtained is not guaranteed to be the global optimal for other possible patterns. A preferable solution would therefore be to derive probabilistic models that take into account all possible system states, as applied in this thesis.

The key of probabilistic modeling is that available historical data are utilized so that each component is represented by a specific probability distribution functions (PDF). Continuous PDFs are further divided into several states with associated probabilities, thus creating a probabilistic model for every component. The number of states for each component should be carefully selected so that the simplicity and accuracy of the analysis are not compromised: a large number of states increases accuracy but at the expense of also adding to the complexity, and a small number of states has the opposite effect. A combined load-DG model can then be generated by convolving all of the individual probabilistic models assuming that these individual models of the load and DG sources are independent (uncorrelated) as in [33], [40]. Such a model combines all possible operating states for the available DG units and the different load levels. The total number of states is therefore equal to the product of the number of states for each component. In the following subsections, the different models of system components are introduced.

2.5.1 Dispatchable DG modeling

Dispatchable DG units are represented with constant output power generation [33], [47], which equals to the rating of the DG installed and utilizing constant power factor (i.e., unity according to Hydro One regulations [48]). This representation is valid for normal (i.e., grid connected) mode of operation. In islanding mode of operation, on the other hand, dispatchable DG units supply the required active and reactive powers [26].

2.5.2 Intermittent-based DG modeling

Unlike dispatchable DG, intermittent-based DG units cannot be represented with constant output power due to the high degree of uncertainty of their power generation. Analytical probabilistic models are therefore necessary to model the variability of power production from such DG sources. In this subsection, the modeling of wind-based DG is only presented; however, similar approaches can be applied to model PV arrays.

Generally, Weibull PDF (2.1) represents a very good expression for modeling wind speeds (v) [40]. In this distribution, two parameters, namely the shape index (e) and scale index (c), are used to fit the probability distribution to the wind speed data of a given site. Figure 2-4 shows the Weibull PDF for different values of the shape and scale indices.

$$f(v) = \frac{e}{c} \times \left(\frac{v}{c}\right)^{e-1} \times \exp\left[-\left(\frac{v}{c}\right)^{e}\right] \tag{2.1}$$

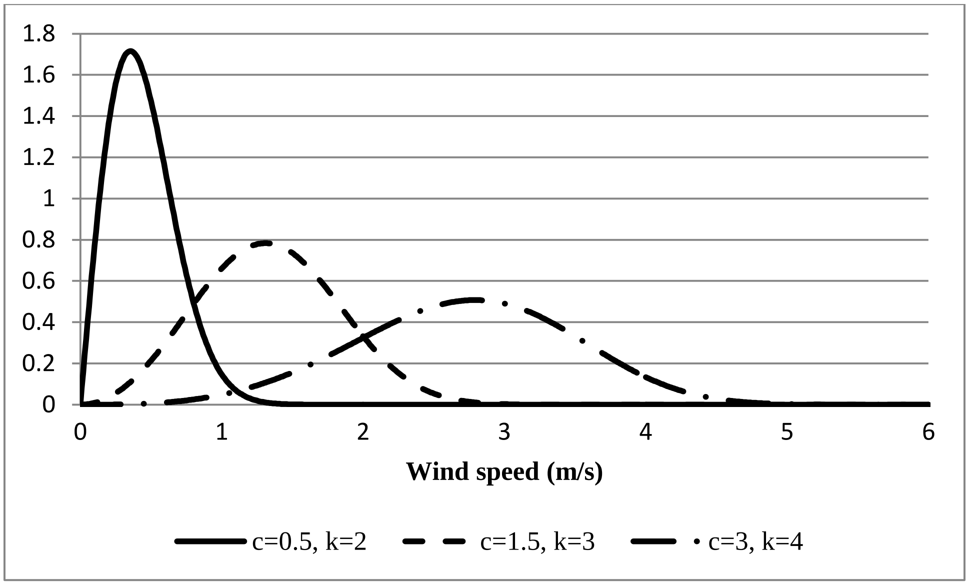

Figure 2-4 Weibull distribution with different values of the scale and shape indices

The Rayleigh PDF is a special case of Weibull distribution, in which the shape index is equal to two as in (2.2), that mimics the distribution of most wind speed profiles.

$$f(v) = \frac{2v}{c^2} \times \exp\left[-\left(\frac{v}{c}\right)^2\right] \tag{2.2}$$

The scale index (c) can be calculated from the mean wind speed (v_{mean}) for a given site as follows:

$$v_{mean} = \int_0^\infty v\, f(v)\, dv = \frac{\sqrt{\pi}}{2} c \cong 0.886\, c \tag{2.3}$$

The historical data of wind speeds can be utilized to estimate the mean wind speed, thus finding the corresponding Rayleigh PDF. Two approaches were reported in the literature for estimating the parameters of any PDF: annual or hourly based approaches [40], [49]. In the first approach, the historical data are processed to calculate the annual mean wind speed. The second approach divides the entire year into four seasons; each season is represented by a typical day. Every day is further divided into 24 hours. Then, the mean wind speeds are calculated, from the historical data, thus defining a unique PDF for each hour in each typical day for every season. It is worth mentioning that the hourly based approach provides better representation because it preserves the chronological characteristics of the data collected, especially for modeling the solar irradiance. Nevertheless, wind speeds can be efficiently represented via the annual based approach, thus minimizing the computational effort.

2.5.3 Load modeling

The normal electrical load is highly dependent on human activities; therefore, it varies with a high degree of uncertainty from one system to another. Unlike the modeling of wind speeds and solar irradiance, there is no unique PDF that can be used for representing the variability of the electrical demand. Thus, several PDFs have been adopted in the literature for modeling the stochastic nature of electrical load, such as uniform PDF, Weibull PDF [50], normal PDF [51], lognormal PDF [51], and beta PDF [52]. A more accurate representation is based on discretizing the load duration curve into a defined number of states, according to the desired accuracy and speed of simulation, using the central centroid sorting process developed in [53].

2.6 Electricity-Market Models with ESSs

Several research works have addressed the problem of determining the optimal operation strategy of ESSs, i.e., when and how much power is to be charged or discharged, as in [54], [55], [56]. In these works, the storage devices were modeled as "price-taker" firms knowing the electricity price at each hour for some period ahead. Such modeling is based on the assumption that storage capacities are too small to affect the market price. However, the increased potential of adopting large central storage facilities in power systems would contradict that assumption.

Mathematical models were further developed in [57] to find the optimal capacity and the optimal dispatch[2] of a hybrid system comprised of generation and storage facilities. This was achieved through minimizing the annual capital and operation costs of the system. The impact of adopting large-scale energy storage on system price has been also investigated, but since the developed models did not represent the power network, the impact of storage location was not considered. In [58], the authors evaluated the arbitrage benefit of small-size energy storage via optimizing its operation during two weeks period and assuming perfect market price foresight during that period. The impact of large-scale energy storage was further discussed through representing the price as an econometrically estimated non-decreasing function of the net power demand including storage output,

[2] In this thesis, the term dispatch is used for determining the optimal ESS operation in day-ahead markets, in which unit commitment is usually performed, contrary to the usual meaning of dispatch that is typically conducted in short-time periods ahead of the actual operation.

aggregated over the whole network. That representation does not actually optimize the market price at every hour nor is the storage location represented. Nevertheless, the results showed lower and higher prices during peak and off-peak periods, respectively. As a result, the arbitrage value was found to be 10-20% less than that calculated considering constant prices at every hour. The results further revealed an increase in consumer surplus which was larger than the decrease in producer surplus, and thus resulting in a net increase in the social welfare. Similarly, the authors in [59] investigated the impact of large-scale energy storage operation on the wholesale electricity price. However, no mathematical models were described for determining either the optimal operation strategy of the storage units or the market-clearing price. The impact on electricity price was instead approximated via observing the effect of storage units on the generation cost of marginal conventional plants. Like [57], [58], the work in [59] did not model the power network, so locational effects were not considered.

2.7 Summary

From the literature review presented in this chapter, it is revealed that some research works have been conducted in the fields of allocating ESSs in distribution networks and determining the optimal operation of large-scale ESSs in day-ahead markets. However, major concerns are still unresolved and have provided the rationale of the work presented in this thesis. Regarding the allocation of ESSs in distribution networks, the following research gaps have been noticed:

- Sufficient work has been conducted with respect to evaluating the reliability of distribution systems with ESSs. However, the literature reveals that the problem of improving system reliability by ascertaining the most cost-effective siting and sizing of DS units in distribution networks has not yet been addressed.
- Few studies have investigated other benefits of ESS implementation in distribution networks, such as peak load shaving and upgrade deferral, without modeling the distribution network. Therefore, the benefit of deferring the upgrades of distribution lines has not been considered.
- No comprehensive planning framework has been presented for determining the size and location of ESSs in order to consider various benefits for ESS implementation in distribution networks.

It is also clear from the discussion in section 2.6 that some work has addressed the problem of determining the optimal operation strategy of ESSs assuming forecasted market prices for some period ahead. The impact of large-scale energy storage operation on market prices and generation costs has been further investigated assuming either a historical ESS operation or a price function of the net power demand, without modeling the network. These two problems of determining the optimal energy storage dispatch and the market-clearing price were de-coupled to mitigate the complexity of the analysis.

The above research gabs have provided the motivation to the work presented in this thesis. The next four chapters describe the work proposed to address these shortcomings. Chapter 3 presents a methodology for the cost-effective improvement of system reliability through the allocation of distributed storage units in distribution systems. Chapter 4 proposes a planning framework for allocating ESSs in distribution systems in order to defer system upgrades, minimize system losses, and take advantage of the price arbitrage. Chapter 5 introduces a comprehensive planning framework that combines the aforementioned benefits of installing ESSs in distribution systems. Chapter 6 develops a mathematical model for determining not only the optimal charging/discharging strategy of ESSs but also the optimal market price in a perfectly competitive environment.

Chapter 3
Optimal ESS Allocation and Load Shedding for Improving Distribution System Reliability

3.1 Introduction

This chapter proposes a methodology for the cost-effective improvement of system reliability through the allocation of distributed storage units in distribution systems. The costs of energy storage installation are optimized with respect to the reliability value expressed as customers' willingness to pay (WTP) in order to avoid power interruptions. The primary goal of this methodology is thus to determine the optimal combination of storage units to be installed and the loads to be shed so that all possible contingencies can be effectively addressed.

The main contributions of the work presented in this chapter are summarized as follows:

- A methodology is proposed that considers the WTP of customers in determining the most cost-effective siting and sizing of DS units in distribution networks.
- The approach presented includes determining the load points to be shed, during contingencies, which minimizes the total interruption cost via increasing the probability of successful islanding operation.
- Unlike previous work that applied time-series patterns for optimizing the size of DS units, a probabilistic approach is utilized in order to consider the uncertainty of system components.

In the next sections, the problem description, problem formulation, case study, and results are presented. Finally, some concluding remarks are discussed in the last section.

3.2 Problem Description

In this research, a value-based reliability approach is adopted as a means of improving distribution system reliability from an economic perspective. In practice, distribution utilities set arbitrary targets rather than obligatory standards as objectives of their reliability indices [60]. These targets usually depend on the utilities' perception of customer tolerance levels with respect to interruptions. However, the expensive investments that characterize the planning stage mean that planning decisions should not rely on such rule of thumb criteria for reducing the costs associated with customer interruption. In other words, achieving those arbitrary targets may cost the distribution utilities much more than the customers would actually pay as interruption costs. In such a case, the reliability target would be overestimated and would result in unnecessary extra costs. As well, in most cases, no reward/penalty system forces distribution utilities to target specific reliability levels despite the willingness of some customers to pay more for greater reliability. WTP therefore represents the reliability value that utilities might lose if they fail to achieve the desired reliability level for those customers. It is consequently crucial to apply optimization approaches that include economic considerations in order to determine the optimal investment plan as well as the optimal reliability level.

Based on the above discussion, the rationale behind the work presented in this chapter is the optimization of the investment costs associated with DS installation relative to the reliability value expressed as the customers' WTP. In reliability-based planning studies as in [61], all load points in a given island are usually shed during unsuccessful islanding operation, i.e., when the total generation is insufficient to supply the isolated loads. This practice has been proposed due to the difficulty of determining the optimal load points to be shed, for each contingency and every state, in order to guarantee successful islanding operation.

In this chapter, the goal is thus to determine the optimum combination of DS units to be installed and the loads to be shed for the most cost-effective improvement in distribution system reliability. The proposed problem then includes some planning decisions, such as determining the sizes and locations of DS units to be installed, as well as other contingency planning decisions, such as the load points to be shed during contingencies. The contingency planning decisions basically aim to increase the overall probability of successful islanding operation, and thus to minimize the total interruption cost. It is worth mentioning that the exact (optimal) amount of load shedding and the corresponding load points to be shed would be determined in the operational stage, and thus they are out of scope of this thesis.

Due to the difficulty of determining the price that customers would pay for reliability, in reliability assessment studies, the interruption costs usually adopted are a reflection of customers' WTP in order to receive the reliability level required [62]. Interruption costs generally depend on the customer classification, e.g., residential, industrial, or commercial, and on the characteristics of the interruption, e.g., duration and frequency. Since the mid-1980s, numerous surveys have been conducted by US and Canadian utilities as a means of estimating the price at which the load would be curtailed in an effort to address a contingency state (i.e., interruption cost). In the case of commercial/industrial customers, this cost basically depends on the revenue/production lost; for residential customers, it is their WTP to avoid service interruption. One of those surveys is the Canadian survey conducted in order to estimate customer damage functions (CDFNs), which represent the interruption cost as a function of the duration of the interruption [63]. In 2008, the US department of energy funded several studies targeted at estimating interruption costs, or CDFNs, for a variety of customer categories, as shown in Figure 3-1 [64]. In this figure, the CDFN is represented as interruption cost per unserved kWh.

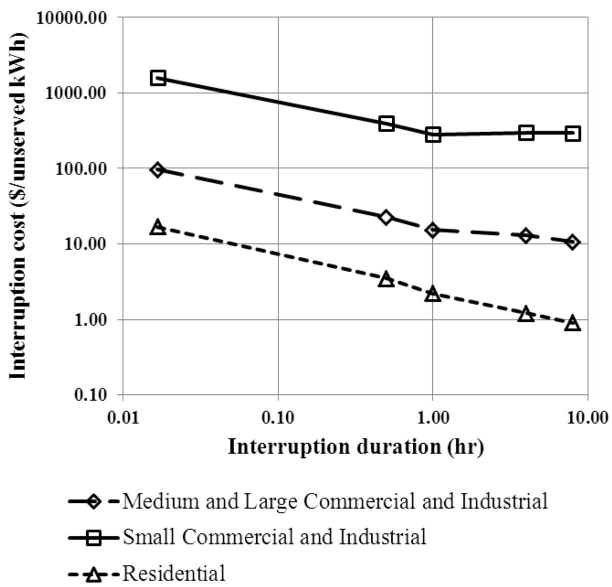

Figure 3-1Customer damage function (CDFN) for a variety of customers

3.3 DG and Load modeling

This section presents the probabilistic models of DG and normal load, which are used in the proposed problem formulation in this chapter and the next two chapters.

3.3.1 Dispatchable DG modeling

As discussed in section 2.5.1, the output power of dispatchable DG is assumed to be either fixed, during normal mode of operation, or variable in order to supply the required active and reactive powers, during islanding mode of operation.

3.3.2 Wind-based DG modeling

The wind speed data for the site under study are assumed to reveal a mean wind speed of 6 m/s. The data of the wind turbine is further given in Table 3-1. Both wind speed and wind turbine data are utilized in the development of the probabilistic wind-based DG model, which is based on the adoption of a Rayleigh PDF as discussed in section 2.5.2. The Rayleigh PDF has been further divided into several states in which each step is bounded by certain limits. The step size affects both the complexity and accuracy of the analysis. In this work, 1 m/s step size is selected to generate the probabilistic wind-based DG model as given in Table 3-2. In this table, similar states are grouped together to form one state, e.g., all wind speeds up to cut-in speed and wind speeds greater than cut-out speed are aggregated to form the last state since all of them result in zero output power.

Table 3-1 Parameters of the wind turbine

Cut-in speed (m/s)	4
Rated speed (m/s)	14
Cut-out speed (m/s)	25

Table 3-2 Probabilistic wind-based DG model

Wind state number	**Wind speed limits (m/s)**	**Output power (% of rated power)**	**Probability**
1	14-25	100	0.1240
2	13-14	95	0.0226
3	12-13	85	0.0257
4	11-12	75	0.0292
5	10-11	65	0.0333
6	9-10	55	0.0379
7	8-9	45	0.0431
8	7-8	35	0.0491
9	6-7	25	0.0558
10	5-6	15	0.0636
11	4-5	5	0.0723
12	0-4 and > 25	0	0.4434

In Table 3-2, the output power of the wind turbine is calculated via (3.1), which represents a linear approximation for the output power characteristics of the wind turbine as shown in Figure 3-2 [65], using the average speed for each state.

$$P_{o/p}(v) = \begin{cases} 0 & 0 \le v < v_{ci} \\ P_r \times \dfrac{v - v_{ci}}{v_r - v_{ci}} & v_{ci} \le v < v_r \\ P_r & v_r \le v < v_{co} \\ 0 & v_{co} \le v \end{cases} \tag{3.1}$$

Moreover, the probability of each state (ρ_w) is calculated using (3.2) as follows:

$$\rho_w = \int_{v_{w_1}}^{v_{w_2}} f(v)\, dv \tag{3.2}$$

where v_{w_1} and v_{w_2} are the speed limits of state *w*.

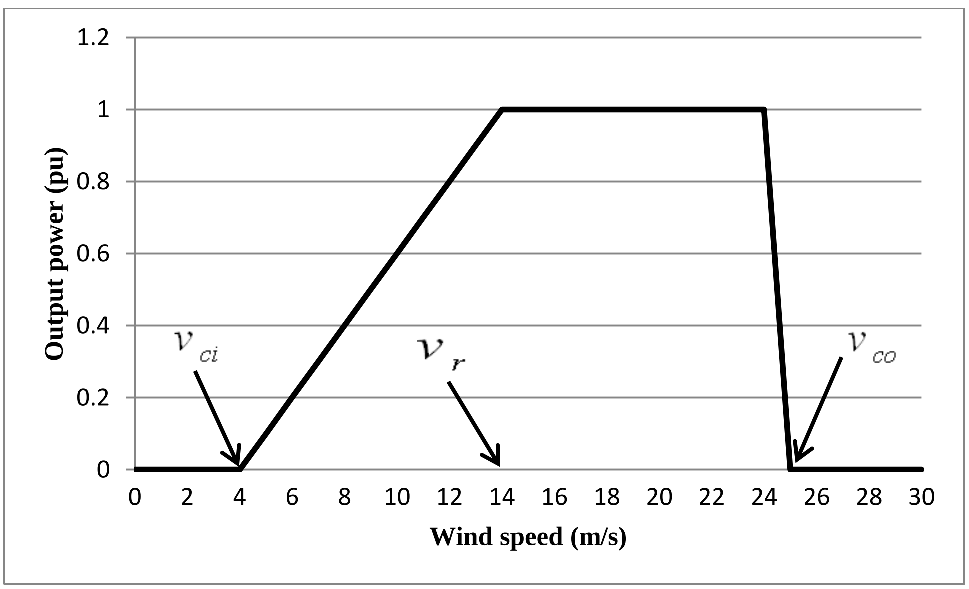

Figure 3-2 Power characteristics of the wind turbine

3.3.3 Load modeling

The load demand is assumed to follow the hourly load shape of the IEEE-reliability test system (RTS) as in [66]. The hourly load data has been clustered into 10 load states that have proved a good trade-off between complexity and accuracy of the analysis, as shown in Table 3-3 [40].

Table 3-3 Probabilistic load model

Load state number	**Load magnitude (% of peak load)**	**Probability**
1	100	0.01
2	85.3	0.056
3	77.4	0.1057
4	71.3	0.1654
5	65.0	0.1654
6	58.5	0.163
7	51.0	0.163
8	45.1	0.0912
9	40.6	0.0473
10	35.1	0.033

3.4 Problem Formulation

This section presents the general methodology adopted in this chapter. A two-stage algorithm is proposed, which is then combined with GA for minimizing the objective function under study. The main step in the GA is chromosome encoding; each solution (chromosome) consists of integer variables that represent the discrete size of DS units and discrete portion of load-shedding decision variables at each bus, as shown in Figure 3-3.

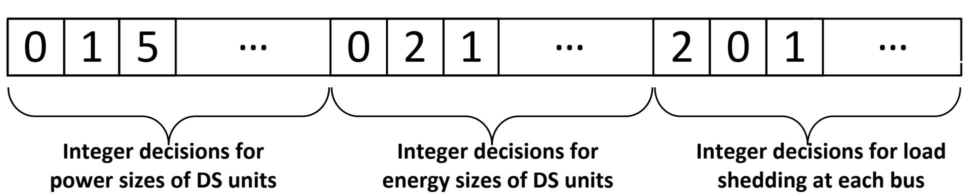

Figure 3-3 A sample structure of the chromosome encoding

For every population generated by the GA, the first stage implies a contingency analysis of the distribution system in order to determine how much power is required from each allocated DS unit in order to supply the demand power required for all possible island formations. The second stage utilizes a sequential Monte Carlo simulation (MCS) for an evaluation of the reliability of the distribution system through the estimation of the expected energy not supplied (EENS) and the interruption cost (ECOST) indices [67]. It is worth mentioning that the ECOST index is used primarily so that consideration of the reliability value can be included in the evaluation of the objective function, whereas the EENS is utilized as a measure of the improvement in the reliability. All solutions (chromosomes) of each population are then evaluated by means of the fitness (objective) function. Finally, a new population is generated, and the entire process is repeated until the stopping criterion is met. The mathematical formulation is explained in the following subsections.

3.4.1 Contingency Analysis

In the first stage, a combined load-DG model is utilized as discussed in section 2.5. This stage performs an N-1 contingency analysis that considers the failure of every single line in the distribution system. When such a disturbance occurs, the protection system isolates the faulty section so as to ensure the healthy operation of the rest of the system. This practice results in the formation of islands if DG and/or DS units are available and capable of supplying the load demand in those islands. The contingency analysis implies the solving of the load flow equations (3.3) to (3.9) for all possible islands in order to determine the power requirements from every DS unit for all combined load-DG states, taking into account the load-shedding decision variables at each bus. It is worth mentioning that the power values calculated in (3.8) and (3.9) may be less or more than the DS power size, thus leading to successful or unsuccessful islanding operation, respectively, as will be explained later on in the second stage.

All system buses are modeled as either P-Q or P-V nodes except the nodes that are connected to DS units. In every island, only one DS unit should act as a slack (reference) bus for all other nodes in that island, and any other available DS units should be treated as voltage-frequency controlled buses, as described in [68]. The latter bus type implies that two additional equations that represent the droop characteristics be added to the basic load flow equations. For the sake of simplicity, it is assumed that all droop controller parameters are identical and that the terminal voltage of each DS unit is set at one per unit. Applying these assumptions results in equal net active power generated from every DS node, as represented in (3.7). Figure 3-4 summarizes the flowchart of the first stage.

System constraints, i.e., nodal voltages and the power flow limits of the lines, along with DS size constraints, are further given in (3.10) to (3.18). Constraints (3.10) to (3.12) are added to the objective function (3.26) using penalty functions (terms), according to which every term equals zero if the corresponding constraint is satisfied or equals a large positive value otherwise. Basically, there are several techniques mentioned in the literature to handle constraints in evolutionary algorithms, e.g., eliminating or repairing infeasible chromosomes, and penalty terms applied to the objective function. Eliminating or repairing infeasible chromosomes are inefficient and problem dependent. On the other hand, the approach of penalty terms is simple and generally works well with all problems [69].

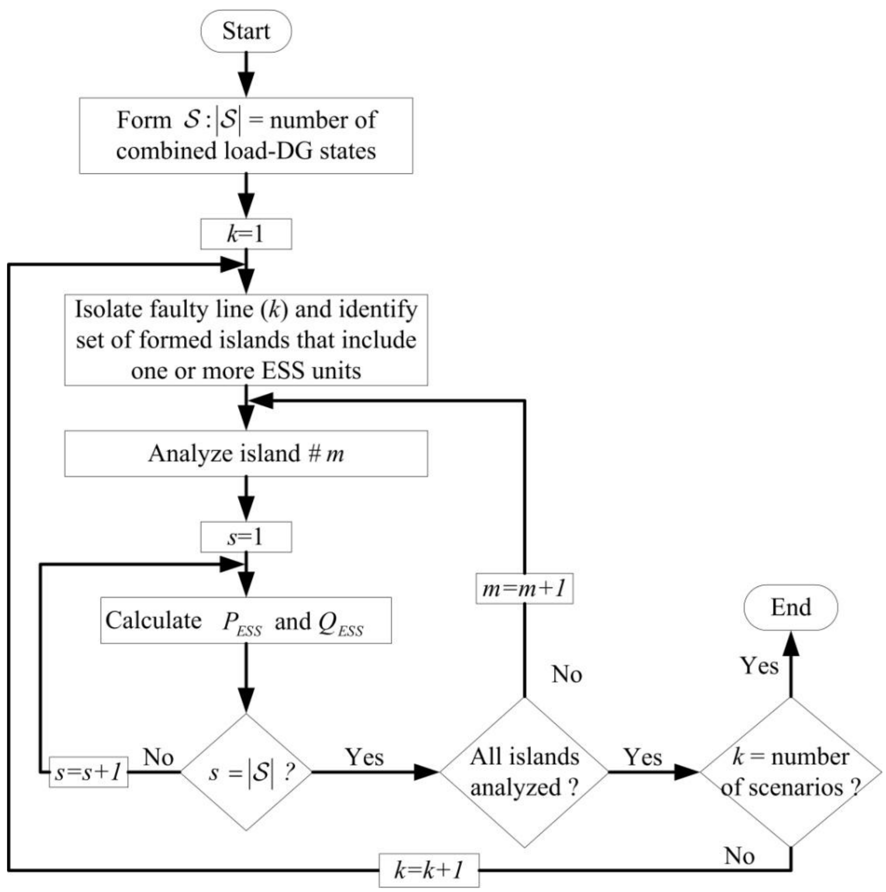

Figure 3-4 Flowchart of the first stage

This study is based on a number of islanded operating strategies as assumptions:

- Only dispatchable DGs are allowed to supply reactive power so that their terminal voltages can thus be regulated. Other types of DG are assumed provided with VAR compensators, e.g., capacitor banks, in order to support their operation in islanded mode. Dispatchable DGs are therefore modeled as P-V nodes, while other DGs are treated as P-Q buses.
- Charging ESS units in islanded mode is not permitted, and all DGs are hence assumed to be controllable in order to avoid any excess generation.

Load flow equations:

- For no ESS installed at bus *i* during contingency *k* and state *s*:

$$P_{G_{i,s}} - P_{D_{i,s}}\left(1 - P_{SH_i}\right) = \sum_{j=1}^{N} V_{i,k,s} \times V_{j,k,s} \times Y_{ij,k} \times \cos\left(\theta_{ij,k} + \delta_{j,k,s} - \delta_{i,k,s}\right) \quad \forall i,k,s \tag{3.3}$$

$$Q_{G_{i,s}} - Q_{D_{i,s}}\left(1 - P_{SH_i}\right) = -\sum_{j=1}^{N} V_{i,k,s} \times V_{j,k,s} \times Y_{ij,k} \times \sin\left(\theta_{ij,k} + \delta_{j,k,s} - \delta_{i,k,s}\right) \quad \forall i,k,s \tag{3.4}$$

- For ESS installed at bus *i* during contingency *k* and state *s*:

$$V_{i,k,s} = 1 \qquad \forall i = \min\left(\mathcal{M}_k\right) : \left|\mathcal{M}_k\right| = M_k, \text{and } \forall k,s \tag{3.5}$$

$$\left|V_{i,k,s}\right| = 1 \qquad \forall i \neq \min\left(\mathcal{M}_k\right) : \left|\mathcal{M}_k\right| = M_k, \text{and} \forall k,s \tag{3.6}$$

$$P_{i,k,s} = P_{j,k,s} \qquad \forall i,j \in \mathcal{M}_k, i \neq j, \text{and} \forall k,s \tag{3.7}$$

$$P_{ESS_{i,k,s}}^{dis} = \sum_{j=1}^{N} V_{i,k,s} \times V_{j,k,s} \times Y_{ij,k} \times \cos\left(\theta_{ij,k} + \delta_{j,k,s} - \delta_{i,k,s}\right) - \left[P_{G_{i,s}} - P_{D_{i,s}}\left(1 - P_{SH_i}\right)\right] \quad \forall i,k,s \tag{3.8}$$

$$Q_{ESS_{i,k,s}} = -\sum_{j=1}^{N} V_{i,k,s} \times V_{j,k,s} \times Y_{ij,k} \times \sin\left(\theta_{ij,k} + \delta_{j,k,s} - \delta_{i,k,s}\right) - \left[Q_{G_{i,s}} - Q_{D_{i,s}}\left(1 - P_{SH_i}\right)\right] \quad \forall i,k,s \tag{3.9}$$

Voltage limits:

$$V_{min} \le V_{i,k,s} \le V_{max} \qquad \forall i,k,s \tag{3.10}$$

$$V_{1,k,s} = 1 \qquad \forall k,s \tag{3.11}$$

Line flow limits:

$$0 \le P_{flow_{ij,k,s}} \le P_{flow_{ij}}^{\max} \qquad \forall i \ne j,k,s \tag{3.12}$$

DS size constraints:

$$S_{ESS_i}^{rated} = x_i \times \text{certain discrete size} \qquad \forall i \in \mathcal{E} \tag{3.13}$$

$$S_{ESS_i}^{rated} \le S_{ESS}^{\max} \qquad \forall i \in \mathcal{E} \tag{3.14}$$

$$E_{ESS_i}^{rated} = y_i \times \text{certain discrete size} \qquad \forall i \in \mathcal{E} \tag{3.15}$$

$$E_{ESS_i}^{rated} \le E_{ESS}^{\max} \qquad \forall i \in \mathcal{E} \tag{3.16}$$

Load shedding constraints:

$$P_{SH_i} = z_i \times \text{certain discrete size} \qquad \forall i \tag{3.17}$$

$$P_{SH_i} \le 1 \qquad \forall i \tag{3.18}$$

3.4.2 Reliability Evaluation of the Distribution System

After the power requirements of each DS unit are determined, a sequential MCS is performed for the system. The basic idea of the MCS is to generate an artificial operating history for the system under study. To this end, the probabilistic model for every component (i.e., DG and load demand) is utilized to derive the corresponding cumulative distribution function (CDF). The components' states can be then generated through the generation of a uniformly distributed random number between 0 and 1, and rounding it to the nearest cumulative probability in the corresponding CDF.

As well, system feeders (lines) are represented using a two-state model (up state and down state), in which up and repair times are calculated based on the generation of a random number that follows an exponential distribution, as in (3.19) and (3.20) [70].

$$T_{up} = -MTTF \times \ln U \tag{3.19}$$

$$T_{repair} = -MTTR \times \ln U' \tag{3.20}$$

where U and U': two uniformly distributed random numbers between 0 and 1.

After a synthetic study period (N_y years) is generated for all system components, the study period is divided into segments (hours). The system is then simulated hour by hour for the entire study period. For each hour (hr), the system state is checked to determine whether it operates in normal (grid connected) mode or in islanded mode. During the latter mode, every DS unit in the island supplies the demand power only if the energy stored is sufficient and the power required is less than the rated DS power. The power required from every DS unit at each hour is recalled from the contingency analysis that corresponds to the combined load-DG state at that hour. If the energy stored is insufficient or the power required is larger than the rated DS power at a specific hour, islanding operation fails, and all loads must be disconnected during that hour. In addition, if no DS units are allocated in a given island, the load-shedding variables are adjusted at each hour, based on the total generation, total demand, and power losses (P_{loss}) in that island. The assumption is therefore that the islanding operation may fail if the total generation is insufficient to satisfy the load demand plus losses for a particular scenario, and hence all loads must be disconnected [61]. When the system is restored, DS units are permitted to be charged up to their maximum power rates as long as system constraints are not violated. Each study period starts with all DS units fully charged; however, the characteristic equations that govern the energy stored in each DS unit at a given hour are as follows:

$$E_{ESS_{i,hr}} = E_{ESS_{i,hr-1}} + P^{ch}_{ESS_{i,hr}} \times \eta - P^{dis}_{ESS_{i,hr}} \qquad \forall i, hr \tag{3.21}$$

$$0 \le E_{ESS_{i,hr}} \le E^{rated}_{ESS_i} \qquad \forall i, hr \tag{3.22}$$

$$\sqrt{\left(P^{ch}_{ESS_{i,hr}} - P^{dis}_{ESS_{i,hr}}\right)^2 + \left(Q_{ESS_{i,hr}}\right)^2} \le S^{rated}_{ESS_i} \qquad \forall i, hr \tag{3.23}$$

The process is then repeated for several periods (samples) until the ratio of the standard deviation of the sample mean of the reliability index of interest to the sample mean of the same index becomes less than a predetermined tolerance. This process is summarized in Figure 3-5. The expected energy not supplied (EENS) per year is calculated by summing the energy interrupted at all nodes over the entire study period, as calculated in (3.24). The expected interruption cost (ECOST) per year is also computed as in (3.25) by utilizing the CDFN shown in Figure 3-1, which is basically a function of the duration of the interruption (T_d). In the final step, the ECOST is utilized in order to evaluate the objective function in (3.26).

$$EENS = \frac{1}{N_y} \sum_{hr=1}^{8760*N_y} \sum_{i=1}^{N} P_{SH\,i,hr} \times P_{D\,i,hr} \tag{3.24}$$

$$ECOST = \frac{1}{N_y} \sum_{i=1}^{N} \sum_{\forall d} \sum_{hr=1}^{T_d} CDFN\,(T_d) \times P_{SH\,i,hr} \times P_{D\,i,hr} \tag{3.25}$$

$$\sum_{i=1}^{N} \left\{ \left(C_P^* + C_M \right) \times S_{ESS_i}^{rated} + C_E^* \times E_{ESS_i}^{rated} \right\} + ECOST + 10^8 \times \sum_{q=1}^{N_c} t_q \tag{3.26}$$

The above objective function minimizes the total cost comprised of the annual installation and maintenance costs of the DS units in addition to the annual interruption costs. In this formula, the fixed capital costs are annualized by dividing them by the present value function (*PVF*), which is expressed in terms of the interest rate (*IR*), inflation rate (*F*), and lifetime of the equipment (*n*), as calculated in (3.27) and (3.28) [71].

$$PVF\,(IR',n) = \frac{\left(1+IR'\right)^n - 1}{IR'\left(1+IR'\right)^n} \tag{3.27}$$

$$IR' = \frac{IR - F}{1+F} \tag{3.28}$$

It should also be mentioned that the above objective function inherently minimizes energy losses for all contingency scenarios because the DS units are sized to supply load demands and system losses during those scenarios. It is also obvious that the DS installation costs are paid independently based on how many times faults occur per year. On the other hand, interruption costs are paid annually according to fault incidence rates. Therefore, for systems with low reliability that are characterized by numerous fault occurrences per year, DS integration is economically desirable as a means of minimizing the total annual costs.

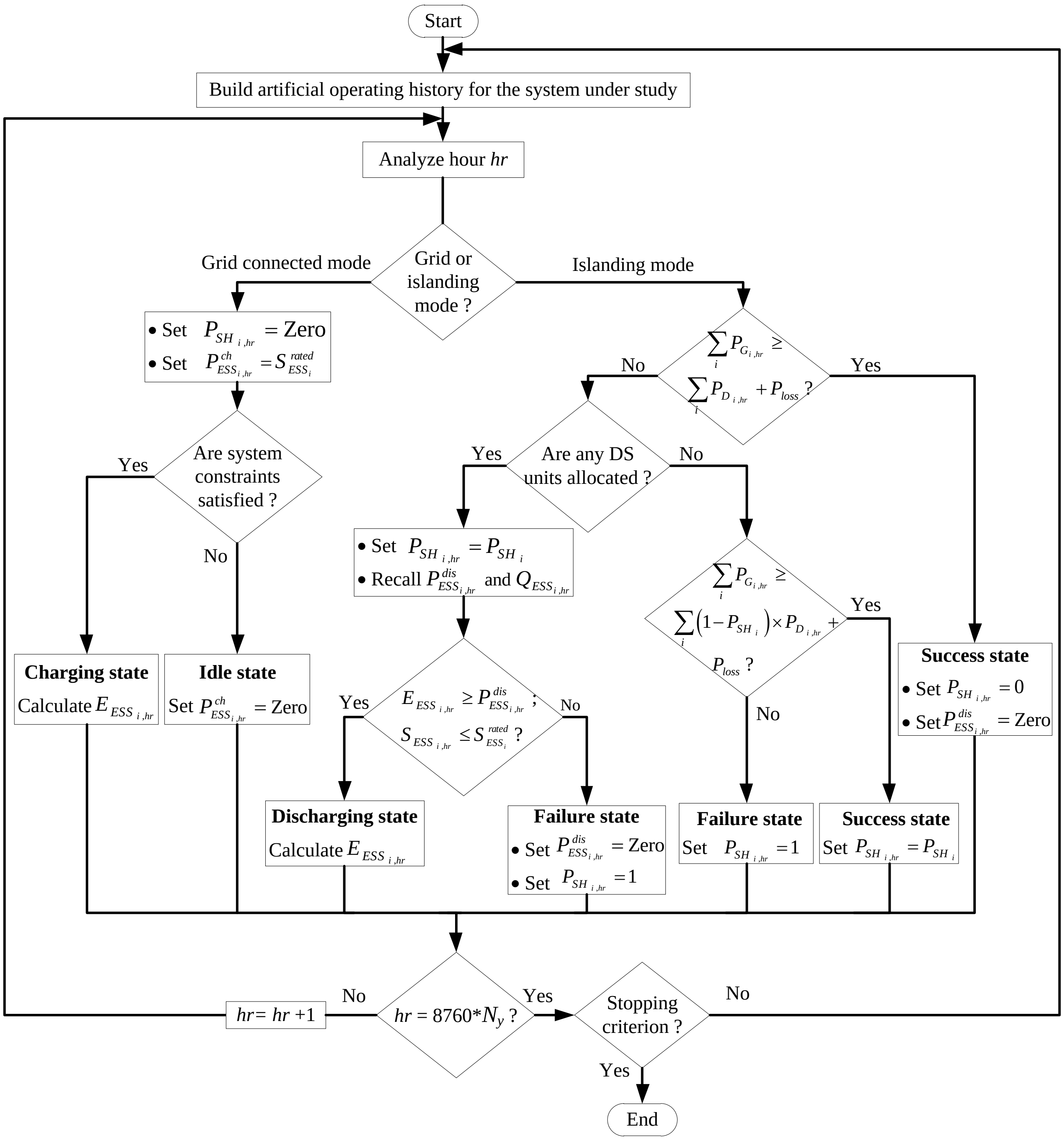

Figure 3-5 Flowchart of the second stage

3.5 Case Study

The system used for the case study is a 33-bus radial distribution system, as shown in Figure 3-6. The rated active and reactive power levels of the load points as well as the feeder data are given in Appendix A [72]. The reliability parameters of the substation and the system feeders are further summarized in Table 3-4 [27].

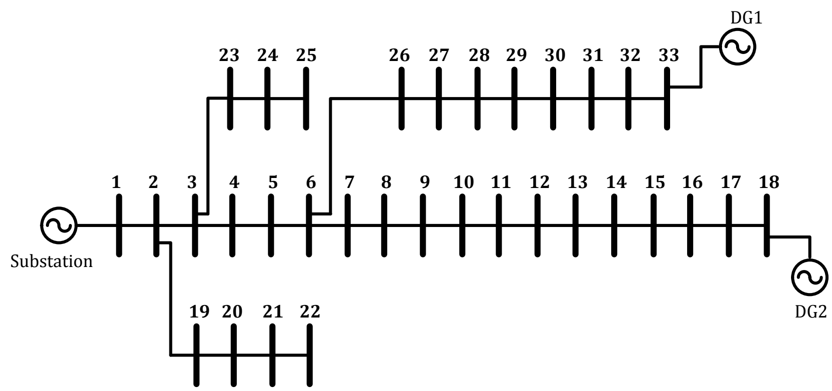

Figure 3-6 System under study

Table 3-4 Component reliability data

	Sustained failure rate (failures/year)	Repair time (hr)
Substation	0.6/100	24
Cables	3.5/100	18

Two different DG types are assumed in the system under study: dispatchable DG (DG_1) based on natural gas and intermittent DG (DG_2) based on wind. DG_1 and DG_2 are placed at buses 33 and 18, respectively. DG_1 is a 500 kVA synchronous generator that operates at 500 kW (unity power factor) during grid connected mode and supplies the active and reactive powers required during islanded mode. DG_2 is a 1 MW wind turbine with power curve parameters as shown in Table 3-1. The sum of the rated DG power levels is confirmed as meeting the Hydro One capacity requirement that limits installed DG ratings to 60% of the substation capacity plus the minimum station load [48]. The wind-based DG and load demands are assumed to follow the probabilistic models presented in Table 3-2 and Table 3-3, respectively.

For this case study, the following financial parameters are assumed: 5% interest rate and 1% inflation rate. The distribution system is assumed to contain a mix of 70% residential and 30% small commercial and industrial customers. These percentages are used for the estimation of the customers' WTP through the weighting of the corresponding CDFNs shown in Figure 3-1. As well, the DS installation costs are subdivided into three main parts: the capital power cost of the rotating machine/converter interface (in $/kVA), the capital energy cost of the storage capacity (in $/kWh), and the annual fixed O&M costs (in $/kVA). A lead-acid (LA) battery, a sodium-sulfur (Na/S) battery, and a vanadium redox (VR) battery were selected as candidate storage technologies because their power and discharge time capacities are suitable for the application under study. It is assumed that the candidate storage technologies are available in discrete sizes in steps of 100 kVA/kWh. Table 3-5 lists the annual capital and maintenance costs for the three candidate technologies, based on an assumed 30-year life cycle. Depending on land availability and/or utility regulations, the candidate buses for DS installation are assumed to be included in set $\mathcal{E}$: (16, 17, 21, 22, 25, and 32). The setting parameters and termination criteria of GA are further given in Table 3-6.

Table 3-5 Annual capital and maintenance costs of DS technologies [11], [73]

	LA	**Na/S**	**VR**
Rated output power (kVA)	2500	2500	2500
Round-trip efficiency (%)	75	77	70
Capital and maintenance costs			
Capital power cost ($/kVA)	175	1000	See note below
Capital energy cost ($/kWh)	305	500	740
Annual O&M cost ($/kVA)	15	20	20
Annual capital costs: *IR*=5%, *F*=1%, and *n*=30 years			
Annual capital power cost	10.07	57.55	--
Annual capital energy cost	17.55	28.78	42.59
Note: Capital power cost for VR battery is included in capital energy cost.			

Table 3-6 GA parameters

Population size	50
Selection criteria	Roulette wheel
Crossover algorithm and probability	Scattered – 0.6
Mutation probability	0.01
Termination criteria and value	Stall generations – 50

3.6 Results

This section summarizes the findings of this case study, in which DS units are optimally allocated, with consideration of all possible island formations, in order to improve system reliability. Two cases are compared in this section regarding the load shedding scheme applied, namely binary and discrete load shedding. It is worthwhile to mention that GA performs well when the decisions variables are binary. Therefore, the binary case has been firstly solved, and the results obtained have been used as initial population for the discrete case in order to accelerate the convergence of GA. Moreover, the impact of DG locations on the results obtained has been further investigated in the third case. Finally, the last case provides a sensitivity analysis for the impact of the value of interruption cost on the optimal solutions.

3.6.1 Binary Load Shedding

In this case, the load shedding decision variables (z_i) are binary (i.e., either 0 or 1). For each storage technology, the optimal DS locations and sizes as well as the load points to be shed are presented in Table 3-7. As can be seen, all technologies result in the same allocation of DS units and loads to be shed. Consequently, interruption costs are found to be the same, while the total cost varies based on the cost of each technology. However, these results are system dependent, which means that different results might be obtained if system parameters and costs are changed. Figure 3-7 provides a comparison of the total annual costs for the different technologies relative to the base case (i.e., without DS integration). In the base case, the annual cost is comprised of only the costs associated with the interruptions during the contingencies. Figure 3-7 reveals that LA batteries provide the least expensive solution: interruption costs were decreased from \$0.78 million (base case) to \$0.275 million. Figure 3-8 depicts the reliability level measured in EENS for each storage technology compared to the base case. Again, since the loads to be shed are the same for each technology, the same EENS values are depicted in each case.

Table 3-7 Optimal DS allocation and load shedding (binary load shedding)

		LA	Na/S	VR
Optimal DS sizes at each bus (kVA, kWh)	16	100, 100	100, 100	100, 100
	32	100, 100	100, 100	100, 100
Load points to be shed (Bus number)		22, and 29	22, and 29	22, and 29

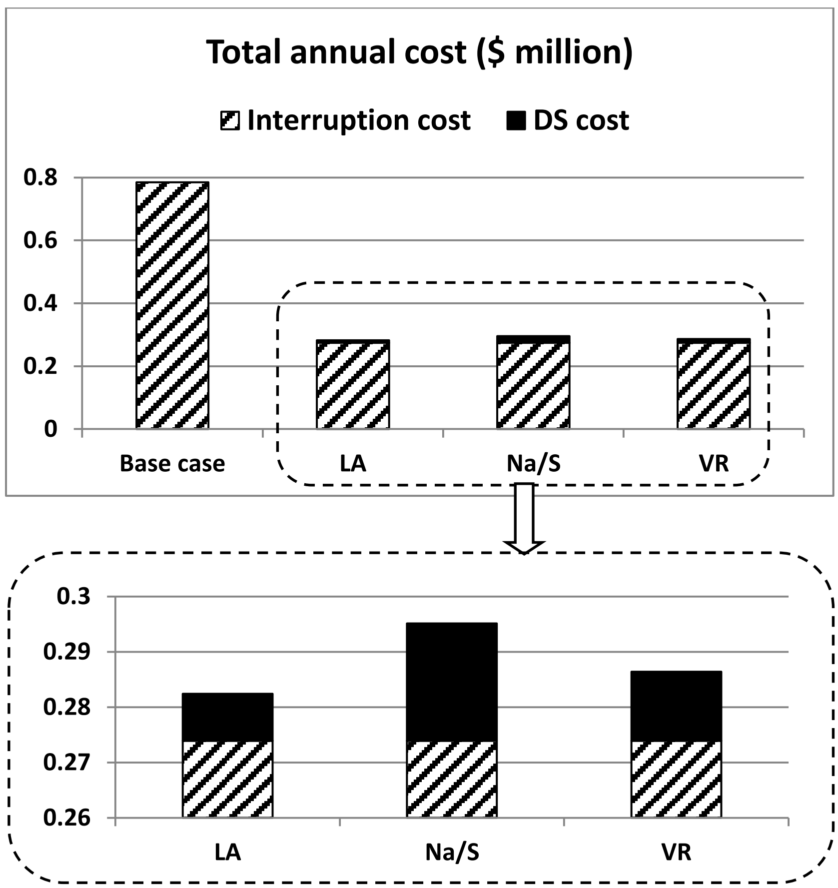

Figure 3-7 Total annual costs for the base case and different storage technologies (binary load shedding)

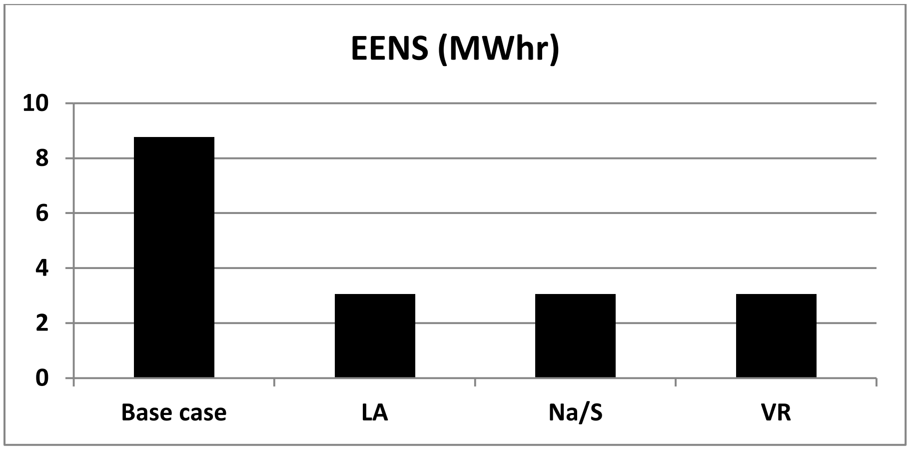

Figure 3-8 EENS for the base case and the different storage technologies (binary load shedding)

As an example, Figure 3-9 shows a graphical representation of LA battery allocation during a failure at the line between buses 1 and 2. The two DS units allocated at buses 16 and 32 are utilized in order to supply the island formed. Further, load points 22 and 29 should be disconnected by the utility operator in a timely manner in order to avoid overloading the allocated DS units and to guarantee the continuity of the supply in the isolated system. Another example is shown in Figure 3-10 for a disturbance between buses 7 and 8. As can be seen, the allocated DS unit at bus 16 and DG_2 only supply the formed island, while no load points have to be shed in this island.

After studying the impact of each technology on the total annual costs, another case study is conducted that investigates the allocation of combination of the three candidate DS technologies. This case study is implemented via adding an integer decision variable that represents the type of DS unit to be installed. The results obtained are confirmed with those of LA batteries allocation given in Table 3-7. Again, this conclusion depends on the system parameters and different costs of DS units.

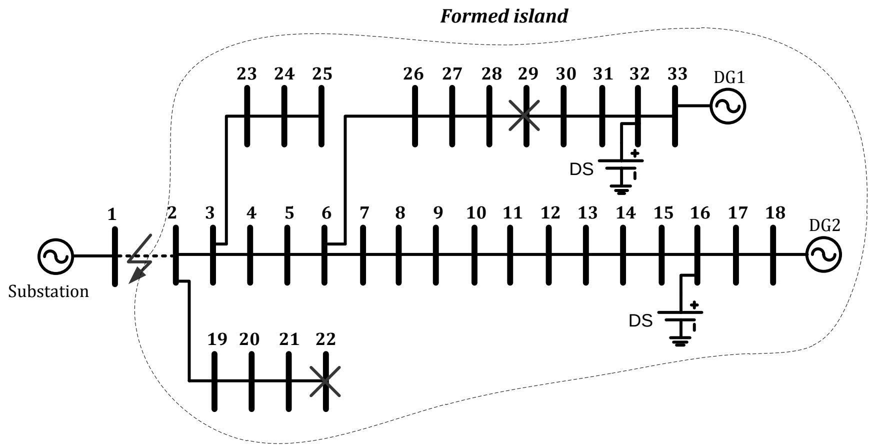

Figure 3-9 Graphical representation of DS allocation and load shedding during a contingency at the line between buses 1 and 2

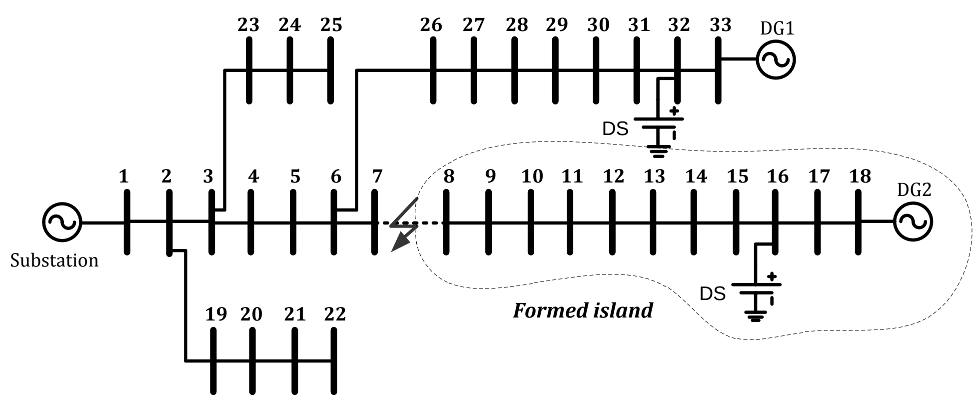

Figure 3-10 Graphical representation of DS allocation and load shedding during a contingency at the line between buses 7 and 8

3.6.2 Discrete Load Shedding

In this case, the load shedding decision variables (z_i) are discrete values between 0 and 1 with step size of 0.1. Table 3-8 shows the optimal type, location, and size of DS units, and portions of load points to be shed. The total annual cost is further given in Table 3-8. Through comparing these results to the binary case, it can be concluded that discrete load shedding only reduces the interruption costs by almost $30,000. This reduction is due to the advantage of discrete load shedding, i.e., flexible portion of load to be shed at each bus. This flexibility can be noticed in the amount of load to be shed at bus 29, i.e., 90%, compared to total load shedding in the binary case. However, these results depend on the system data and rated power levels of the load points.

Table 3-8 Optimal DS allocation and load shedding (discrete load shedding)

Optimal type and size of DS at each bus (type, kVA, kWh)	16	LA, 100, 100
	32	LA, 100, 100
Load points to be shed (Bus number, % of load to be shed)		22 (100%) 29 (90%)
Total annual cost ($ million)		0.279

3.6.3 Impact of DG Locations

DG_1 and DG_2 are re-allocated, in this case, to buses 25 and 22, respectively, in order to investigate the impact of DG locations. The optimal DS locations and sizes as well as the load points to be shed are given in Table 3-9. As can be seen, no load points have to be shed compared to the previous cases, which implies that the probability of successful islanding operation is not affected by disconnecting some load points. Moreover, neither the sizes nor the locations of the allocated DS units are affected with the new DG locations. However, these results are system dependent, thus they might be changed using different rated power levels of DGs and/or load points.

Moreover, Table 3-9 compares the total annual cost of the optimal solution with respect to the new base case, which corresponds to the new DG locations. It is revealed that interruption costs are increased in this case since the DG units are now closer to the substation, and thus more load points are deprived from their output power during contingencies beyond bus 3. Similarly, EENS values are increased with the new DG locations, as shown in Table 3-9.

A graphical representation of the new DG locations and LA battery allocation is further illustrated in Figure 3-11 during a failure at the line between buses 1 and 2, as an example. As can be seen, no load points have to be shed in this case compared to Figure 3-9.

Table 3-9 Optimal DS allocation and load shedding (new DG locations)

		Base case (without DS units)	With DS units
Optimal type and size of DS at each bus (type, kVA, kWh)	16	0	LA, 100, 100
	32	0	LA, 100, 100
Load points to be shed (Bus number)		--	--
EENS (MWhr)		10.28	4.01
Total annual cost ($ million)		0.9197	0.3591

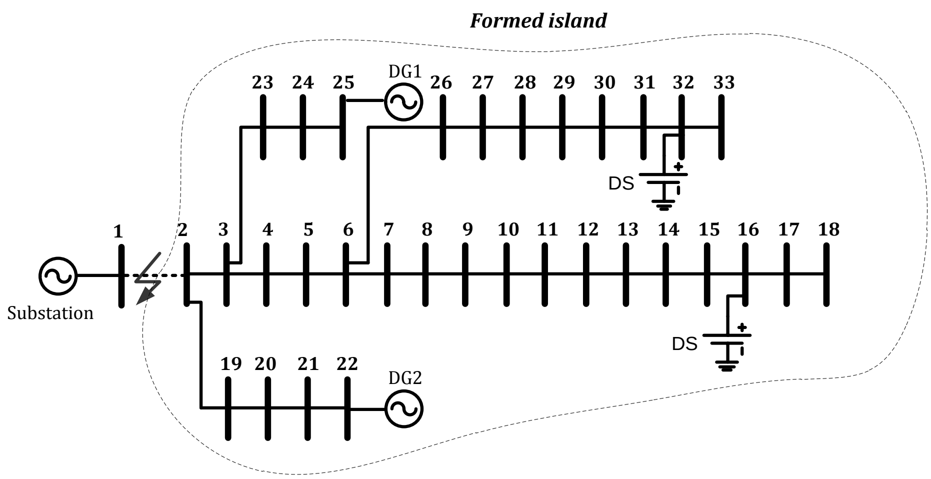

Figure 3-11 Graphical representation of DS allocation and load shedding during a contingency at the line between buses 1 and 2 (new DG locations)

3.6.4 Impact of the Value of Interruption Cost

This case investigates the impact of the value of interruption cost on the optimal size and location of DS units to be installed, as well as the load points to be shed. Table 3-10 presents several scenarios with different percentages of residential customers, and small commercial and industrial customers. The optimal solutions for each case are summarized in Table 3-10. As observed, the optimal DS allocation and load points to be shed are duly dependent on the value of the interruption cost. The higher the percentage of commercial and industrial customers is, which implies higher interruption cost, the larger sizes of DS units are required.

Table 3-10 Optimal DS allocation and load shedding (sensitivity analysis)

		10% I + 90% R	30% I + 70% R	50% I + 50% R	70% I + 30% R
Optimal DS size at each bus (kVA, kWh)	16	100, 100	100, 100	0	0
	17	0	0	100, 100	100, 100
	22	0	0	100, 100	100, 100
	25	0	0	100, 200	100, 200
	32	100, 100	100, 100	400, 3200	500, 4500
Optimal DS type		LA batteries			
Load points to be shed (Bus number)		22, 29	22, 29	4, 23	4, 23
R: residential customers, I: small commercial and industrial customers					

Moreover, Figure 3-12 and Figure 3-13 compare the total annual costs and the reliability level measured in EENS for the various cases.

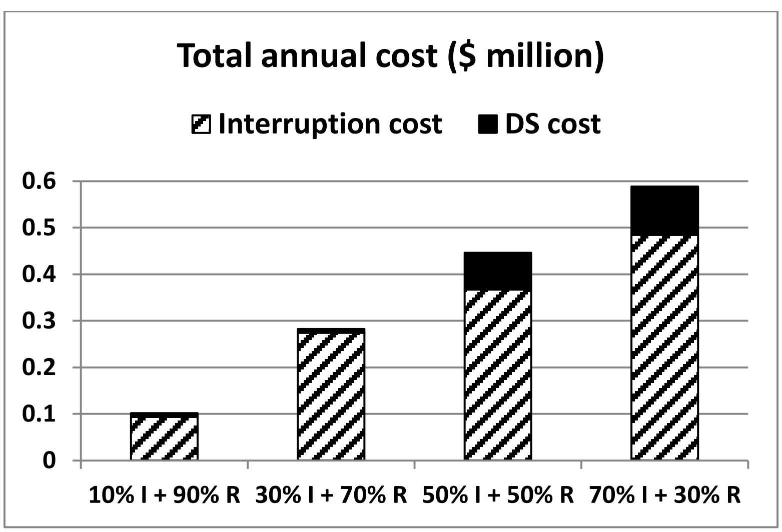

Figure 3-12 Total annual costs for the various scenarios of different customers

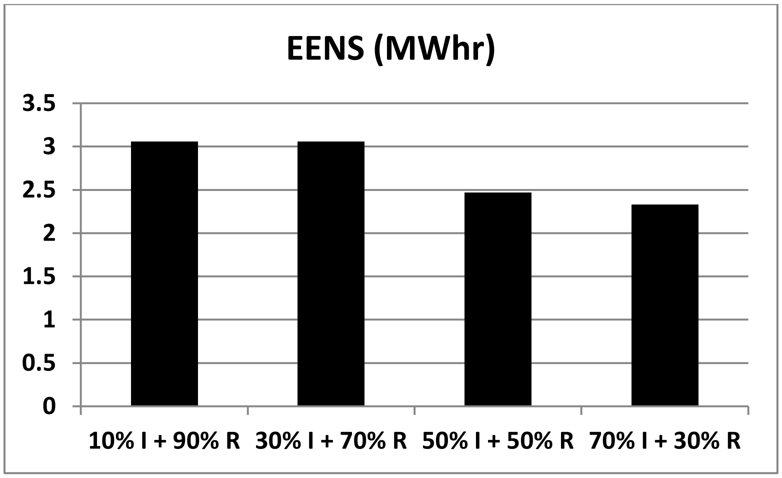

Figure 3-13 EENS for the various scenarios of different customers

3.7 Conclusions

In this chapter, a two-stage algorithm was proposed for the allocation of DS units in distribution systems as a cost-effective means of improving system reliability. A value-based reliability approach was adopted that includes consideration of customers' WTP as the reliability value benefit of improving system reliability. The total annual costs comprised of DS installation and maintenance costs as well as the interruption costs were then minimized in order to determine the optimal combination of DS units to be installed and the loads to be shed during all possible contingencies. For calculating the power requirements from the allocated DS units, a probabilistic approach was adopted that takes into account the stochastic nature of all of the system components: loads and existing DGs. A sample case study was presented, and three storage technologies were compared and measured against a base case with no DS installation. The results showed that integrating DS units with distribution systems reduces the utilities' annual costs because of their capacity to enable successful islanding and to minimize interruption costs, thus providing a cost-effective means of improving system reliability. A sensitivity analysis was further provided in order to investigate the impact of the value of interruption cost on the results obtained.

Chapter 4 Optimal ESS Allocation for Load Management Application

4.1 Introduction

This chapter proposes a methodology for allocating distributed storage units in distribution systems in order to defer system upgrades, minimize system losses, and take advantage of the price arbitrage. The cost and arbitrage benefit of energy storage installation are optimized with respect to system upgrade and energy losses costs. The primary goal of this methodology is to determine the optimal size and location of storage units to be installed, in addition to their optimal operation, so that total system costs are minimized, while system benefits are maximized.

The main contributions of the work presented in this chapter are summarized as follows:

- This chapter presents a planning framework that takes into account the distribution network model in ascertaining the most cost-effective siting and sizing of DS units in order to defer system upgrades by means of load management.
- The approach proposed further includes determining the optimized operation of DS units at each load state.
- Like the work proposed in the previous chapter, a probabilistic approach is proposed in order to consider the uncertainty of system components.

In the next sections, the problem description, problem formulation, case study, and results are presented. Finally, some concluding remarks are discussed in the last section.

4.2 Problem Description

The application of energy storage to shave peak load is similar to demand side management programs that shift demand use of energy from peak to off-peak periods. In this application, energy is stored within DS during off-peak times and is released when the load is high (i.e., peak). However, the economic feasibility of this usage of energy storage should be justified since DS units are expensive in installation and maintenance costs. To achieve this task, the benefits from integrating DS to attain demand side management need to be firstly identified as follows:

- Arbitrage benefit—this is the direct benefit from buying and storing energy with an inexpensive price during off-peak periods, and selling the energy stored back, after accounting of the losses in the ESS, with a high price at peak times.
- System upgrade deferral—system upgrades are usually required in order to account for the annual load growth in a given distribution system. Through peak load shaving, system upgrades can be deferred to later years, and the net present value (NPV) of system upgrades can be then reduced.
- Energy losses reduction—this is the secondary benefit from integrating DS units into distribution systems. By means of proper placement of energy storage units, the cost of energy losses in distribution systems can be minimized.

From the above discussion, the proposed methodology focuses on finding the optimal DS allocation in distribution systems that minimizes the NPV of system costs—i.e., system upgrades, energy losses, and DS installation and maintenance costs—and maximizes the NPV of arbitrage benefit. Allocating energy storage for this application involves determining the size and the location of DS units to be installed (planning decisions) as well as the control strategy of those allocated DS units (operational decisions). Controlling DS operation is the key for maximizing arbitrage benefit regardless of where the DS units are located. On the other hand, minimizing system upgrade and energy losses costs depends on both the planning and operational decisions.

4.3 Problem Formulation

This section presents the general methodology adopted in this chapter. The input to the methodology proposed is the different probabilistic models of load and DG units, while the output of this methodology is the optimal size and location of DS units as well as the optimized operation of DS units. The rationale behind the methodology proposed is the optimization of the investment costs by distribution companies through deployment and control of DS units. Due to the complexity of handling planning and operational planning decisions, GA combined with linear-programming (LP) solver is utilized for minimizing the objective function under study. In the following paragraphs, an overview of the methodology proposed is described, and the details are discussed in the next subsections.

The main step of the methodology proposed is the chromosome encoding of GA. In the presented work, each solution (chromosome) consists of integer variables that control the DS size (in kW and kWh) to be installed at every candidate system bus, as shown in Figure 4-1. For every population generated by GA, three steps are required to evaluate the objective (fitness) function of each individual, as shown in Figure 4-2. Multi-year planning approach is further proposed in this work in order to evaluate the NPV of both system expenses and benefits. The first step adopts a discrete load model, which implies certain load states with their magnitudes and the associated probabilities, in optimizing the charging/discharging DS operation at each state through a LP solver. The second step involves a MCS for the energy storage operation, utilizing the optimized operation from the previous step as an input, in order to estimate the annual arbitrage benefit and the number of charging-discharging cycles per year. Finally, load flow analysis is performed at each state in order to determine the required system upgrades and the corresponding energy losses. These steps are detailed in the next subsections and the associated mathematical formulations are presented.

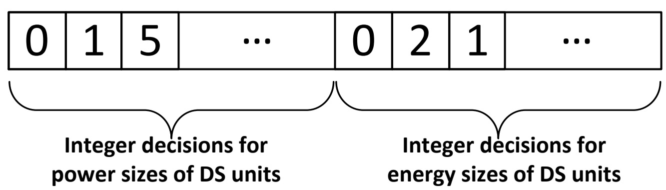

Figure 4-1 A sample structure of the chromosome encoding

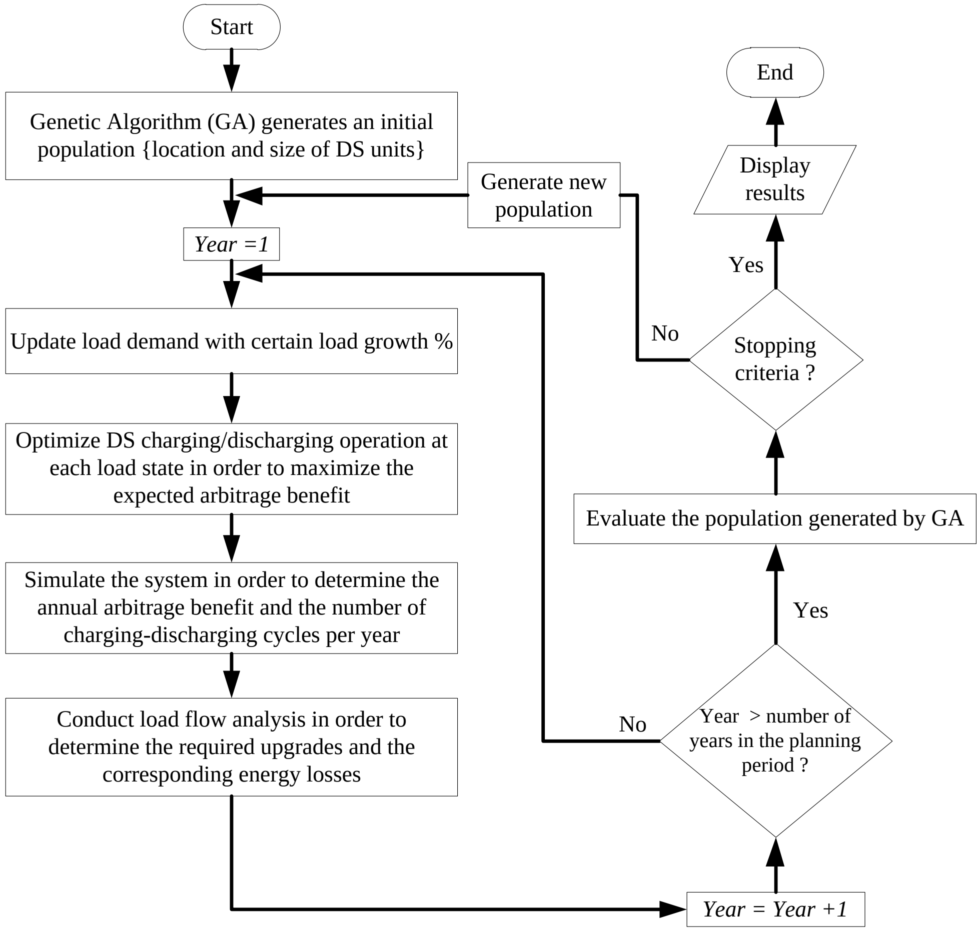

Figure 4-2 Flowchart of the proposed methodology

4.3.1 Optimize the Operation of DS Units

This step involves determining the optimal DS charging/discharging power at each load state. First of all, the load states are divided into candidate states for charging and discharging based on the magnitude of each load state. In particular, the last four states of the load probabilistic model in Table 3-3 (i.e., up to 51% of the peak load) are assumed to be off-peak states, and thus candidate states for charging, while the other six states (i.e., greater than 51% of the peak load) are considered to be candidate states for discharging. Furthermore, the electricity prices are assumed to follow the averaged off-peak and peak prices which are calculated from the hourly prices provided by the independent electricity system operator (IESO) [74]. This sub problem is formulated as a LP optimization problem that has an objective function of maximizing the expected arbitrage benefit in a certain period (i.e., one year) as follows:

$$\underset{P_{ESS_l}^{ch},P_{ESS_l}^{dis}}{\text{Maximize}} \quad c_{\text{peak}} \times \sum_{l \in \mathcal{L}_{dis}} 8760 \times \rho_l \times P_{ESS_l}^{dis} - c_{\text{off-peak}} \times \sum_{l \in \mathcal{L}_{ch}} 8760 \times \rho_l \times P_{ESS_l}^{ch} \tag{4.1}$$

In the above equation, the first and second terms represent the expected cost of energy to be sold and bought during peak and off-peak times, respectively. In each term, the probabilities of the corresponding load states are used to calculate the expected values of energy to be sold and bought. From this objective function, it is clear that this sub problem depends only on the electricity prices and the load states' probabilities as parameters. Although the load states' magnitudes (in MW) increase at every year over the planning period, each load state's probability can be assumed to remain constant. If we further assumed that off-peak and peak electricity prices may increase, or possibly decrease, with the same percentage over the planning period, then the above problem needs to be solved only once, thus leading to the same optimal DS operation at every year.

Nevertheless, the above objective is maximized subject to the following constraints. The first constraint implies that the expected stored energy in a certain period equals to the expected discharged energy in the same period. Moreover, the energy stored in a typical day is limited to the energy size of the DS in (4.3). The third constraint further enforces the discharging power at the most peak load state (i.e., state 1) to be equal to the power size of the DS in order to reduce the cost of system upgrades since the upgrades required are usually determined at this state as will be discussed later on.

subject to

$$\sum_{l \in \mathcal{L}_{dis}} 8760 \times \rho_l \times P_{ESS_l}^{dis} = \sum_{l \in \mathcal{L}_{ch}} 8760 \times \rho_l \times P_{ESS_l}^{ch} \times \eta \tag{4.2}$$

$$\sum_{l \in \mathcal{L}_{ch}} 24 \times \rho_l \times P_{ESS_l}^{ch} \times \eta \le E_{ESS}^{rated} \tag{4.3}$$

$$P_{ESS_1}^{dis} = S_{ESS}^{rated} \tag{4.4}$$

$$0 \le P_{ESS_l}^{dis}, P_{ESS_l}^{ch} \le S_{ESS}^{rated} \qquad \forall l \tag{4.5}$$

4.3.2 Determine the Annual Arbitrage Benefit and the Number of Operation Cycles

In this step, a sequential MCS is performed in order to estimate the annual arbitrage benefit and the number of charging-discharging cycles per year. This simulation takes into account the optimized DS operation from the foregoing stage. It is worth mentioning that the arbitrage benefit obtained from simulation is different from the expected value determined in the previous step. This difference is attributed to the fact that DS units might fail to operate as pre-planned if they are fully charged or discharged. The procedure for performing MCS is described as follows:

1- For each study period (i.e., one year), the load state at every hour (*hr*) is generated through the generation of a uniformly distributed random number between 0 and 1, and rounding it to the nearest value in the CDF that corresponds to the load probabilistic model in Table 3-3.

2- Based on the load state at every hour, recall the DS output power at each state from the foregoing stage. Then, calculate the energy stored at the DS (E_{DS}), taking into consideration the physical constraints of the DS at any time interval, via the following relations:

$$E_{ESS_{hr+1}} = E_{ESS_{hr}} + \eta \times P_{ESS_{hr}}^{ch} - P_{ESS_{hr}}^{dis} \qquad \forall hr \tag{4.6}$$

$$E_{ESS}^{\min} \le E_{ESS_{hr}} \le E_{ESS}^{rated} \qquad \forall hr \tag{4.7}$$

3- Determine the annual arbitrage benefit as in (4.8) in which, at a certain hour, only one term has a value while the other term equals to zero. The first term, with negative sign, represents the energy purchased at off-peak periods, while the second term, with a positive sign, corresponds to the energy sold at peak times. The DS efficiency is used to accurately account for the energy purchased at energy storage terminals.

$$\sum_{hr=1}^{8760} \left\{ -c_{\text{off-peak}} \times \max\left(0, E_{ESS_{hr+1}} - E_{ESS_{hr}}\right) / \eta + c_{\text{peak}} \times \max\left(0, E_{ESS_{hr}} - E_{ESS_{hr+1}}\right) \right\} \tag{4.8}$$

Afterwards, the NPV of the arbitrage benefit can be calculated as in (4.9) using the *PVF*, which is expressed in terms of *IR*, *F*, and N_{yr} as in (3.25) and (3.26) [71]

$$NPV_{AR} = \text{Annual arbitrage benefit} \times PVF \tag{4.9}$$

4- Calculate the number of annual operating (charge/discharge) cycles for each DS.

5- Stop if the ratio of the standard deviation of the sample mean of the index of interest (i.e., the arbitrage value) to the sample mean of the same index becomes less than a predetermined tolerance, otherwise go to step 1.

4.3.3 Evaluate System Upgrade and Energy Losses' Costs

In this step, a combined load-DG model is utilized as discussed in section 2.5. This step further applies multi-year probabilistic load flow analysis in order to evaluate system upgrade and energy losses' costs. The energy losses only account for the losses in the lines of the primary distribution system. Moreover, system upgrade involves the reinforcement of feeders (lines) and substation in order to account for the annual load growth. In this work, the distribution network's configuration is presumed fixed; therefore, upgrading network's equipment to larger sizes is considered to be the unique alternative for satisfying the growing demand. For radial distribution systems, system upgrades are usually evaluated at the condition of extreme power flow in the lines, i.e., the most peak load state. With the integration of DS units, however, the extreme power flow in the lines may not occur at the peak load state due to peak load shaving. Consequently, system upgrades should be determined based on the maximum upgrade required over all combined load-DG states. The procedure for evaluating system upgrade and energy losses costs is explained as follows:

1- For each year (*yr*), update load demand with a certain load growth percentage.

2- For each combined load-DG state (*s*), solve load flow equations as in (4.10) to (4.12), and calculate the corresponding upgrades for all equipment and the total power losses (P_{loss})

$$P_{G_{i,s,yr}} - P_{D_{i,s,yr}} - P_{ESS_s}^{ch} = \sum_{j=1}^{N} V_{i,s,yr} \times V_{j,s,yr} \times Y_{ij} \times \cos\left(\theta_{ij} + \delta_{j,s,yr} - \delta_{i,s,yr}\right) \quad \forall i, s \in \mathcal{S}_{ch}, yr \tag{4.10}$$

$$P_{G_{i,s,yr}} - P_{D_{i,s,yr}} + P_{ESS_s}^{dis} = \sum_{j=1}^{N} V_{i,s,yr} \times V_{j,s,yr} \times Y_{ij} \times \cos\left(\theta_{ij} + \delta_{j,s,yr} - \delta_{i,s,yr}\right) \quad \forall i, s \in \mathcal{S}_{dis}, yr \tag{4.11}$$

$$Q_{G_{i,s,yr}} - Q_{D_{i,s,yr}} = -\sum_{j=1}^{N} V_{i,s,yr} \times V_{j,s,yr} \times Y_{ij} \times \sin\left(\theta_{ij} + \delta_{j,s,yr} - \delta_{i,s,yr}\right) \quad \forall i, s, yr \tag{4.12}$$

3- For each piece of equipment, determine the maximum upgrade required.

4- For each year, determine the expected energy losses' costs as follows:

$$CE_{loss_{yr}} = 8760 \times \left\{ \sum_{s \in \mathcal{S}_{dis}} \rho_s \times P_{loss_s} \times c_{\text{peak}} + \sum_{s \in \mathcal{S}_{ch}} \rho_s \times P_{loss_s} \times c_{\text{off-peak}} \right\} \tag{4.13}$$

5- At the end of the planning period, determine the NPV of system upgrade and energy losses costs as in (4.14) and (4.15), respectively.

$$NPV_{UP} = \sum_{u=1}^{M} \frac{R_u}{(1+IR')^{y_u}} \tag{4.14}$$

$$NPV_{LO} = \sum_{yr=1}^{N_{yr}} \frac{CE_{loss_{yr}}}{(1+IR')^{yr}} \tag{4.15}$$

4.3.4 Evaluate the Objective Function

In this step, the objective (fitness) function is presented that minimizes the aforementioned costs and maximizes the arbitrage benefit. The problem constraints are further added to the objective function using penalty terms, as presented in the last term of (4.16).

$$\underset{x_i, y_i}{\text{Minimize}} \sum_{i=1}^{N} \left\{ \left(C_P + C_M \times PVF\right) \times S_{ESS_i}^{rated} + \left(C_E + C_R\right) \times E_{ESS_i}^{rated} \right\} + NPV_{UP} + NPV_{LO} - NPV_{AR} + 10^8 \times \sum_{q=1}^{N_c} t_q \tag{4.16}$$

If batteries are used as the energy storage technology, then they may need to be replaced once or more during the planning period; therefore, C_R is calculated as in (4.17) [37]

$$C_R = FR \times \left[\left(1+IR'\right)^{-r} + \left(1+IR'\right)^{-2r} + \cdots \right] \tag{4.17}$$

where r is the replacement period in years that can be calculated by dividing the battery's life time, i.e., the maximum number of charge/discharge cycles, by the number of operating cycles per year.

subject to

Voltage limits constraints:

$$V_{\min} \le V_{i,s,yr} \le V_{\max} \qquad \forall i, s, yr \tag{4.18}$$

DS size constraints:

$$S_{ESS_i}^{rated} = x_i \times \text{certain discrete size} \qquad \forall i \in \mathcal{E} \tag{4.19}$$

$$E_{ESS_i}^{rated} = y_i \times \text{certain discrete size} \qquad \forall i \in \mathcal{E} \tag{4.20}$$

$$S_{ESS_i}^{rated} \leq S_{ESS}^{\max} \qquad \forall i \in \mathcal{E} \tag{4.21}$$

$$E_{ESS_i}^{rated} \leq E_{ESS}^{\max} \qquad \forall i \in \mathcal{E} \tag{4.22}$$

DS installation constraints:

$$x_i \text{ and } y_i = 0 \qquad \forall i \notin \mathcal{E} \tag{4.23}$$

4.4 Case Study

The system used for the case study is the same 33-bus radial distribution system shown in Figure 3-6. The system peak demand is 3715 kW at base year, and it is assumed growing with a constant annual rate of 5%. For this case study, the planning period is considered to be 20 years. The following financial parameters are further assumed: 5% interest rate and 1% inflation rate. The capital fixed and variable upgrade costs of the system equipment are given in Table 4-1 [75]. Moreover, Table 4-2 lists the average off-peak and peak electricity prices calculated from the hourly prices provided by the IESO [74].

Table 4-1 Capital fixed and variable upgrade costs [75]

	Fixed cost	**Variable cost**
Feeder	$150,000 per km	$1000 per MW
Substation	$200,000	$50,000 per MW

Table 4-2 Average electricity prices [74]

	Peak	**Off-peak**
Energy price ($/MWh)	27	18

Like the case study in Chapter 3, two different DG types are used in the system under study: dispatchable DG (DG_1) based on diesel and intermittent DG (DG_2) based on wind. DG_1 and DG_2 are placed at buses 33 and 18, respectively. DG_1 is a 500 kVA synchronous generator that operates at 500 kW (unity power factor). DG_2 is a 1 MW wind turbine with power curve parameters as shown in Table 3-1. The wind-based DG and load demands are assumed to follow the probabilistic models presented in Table 3-2 and Table 3-3, respectively. The GA and linprog solvers in MATLAB optimization toolbox are used for solving the methodology proposed. The setting parameters and termination criteria of GA are given in Table 3-6.

In this case study, lead-acid (LA), sodium-sulfur (Na/S), and vanadium-redox (VR) batteries are selected as candidate storage technologies because their power and discharge time capacities are suitable for the application under study. It is assumed that the candidate storage technologies are available in discrete sizes in steps of 100 kW/kWh. Table 4-3 lists the capital and maintenance costs for the three candidate technologies. Again, the candidate buses for DS installation are assumed to be included in set $\mathcal{E}$: (16, 17, 21, 22, 25, 32).

Table 4-3 Capital and maintenance costs of DS technologies [11], [73]

	LA	**Na/S**	**VR**
Rated output power (kW)	2500	2500	2500
Round-trip efficiency (%)	75	77	70
Capital and maintenance costs			
Capital power cost ($/kW)	175	1000	See note below
Capital energy cost ($/kWh)	305	500	740
Capital replacement cost ($/kWh)	305	500	222
Annual O&M cost ($/kW)	15	20	20
Number of charge/discharge cycles	3200	2500	10000
Note: Capital power cost for VR battery is included in capital energy cost.			

4.5 Results

This section summarizes the findings of this study, in which DS units are optimally allocated in order to achieve load management, and thus defer system upgrades and minimize system losses. The impact of pre-allocated DG types is studied in this section through three different cases: the system without any DG, the system with intermittent DG type only (i.e., DG_2), and the system with both intermittent and dispatchable DG types (i.e., DG_1 and DG_2).

In each case, several scenarios representing the base case (i.e., without DS units) and the three different storage technologies, as shown in Table 4-4, are compared. The NPV of total costs are summarized for each scenario in Figure 4-3, and the details are shown in Table 4-5. Note that the percentage of savings in each scenario is calculated with respect to the corresponding base case.

Table 4-4 Different scenarios

Case	DG type	DG location	Scenario	
A	No DG	--	Base case	(A.0)
			LA	(A.1)
			Na/S	(A.2)
			VR	(A.3)
B	Wind-based	18	Base case	(B.0)
			LA	(B.1)
			Na/S	(B.2)
			VR	(B.3)
C	Wind-based	18	Base case	(C.0)
			LA	(C.1)
	Diesel	33	Na/S	(C.2)
			VR	(C.3)

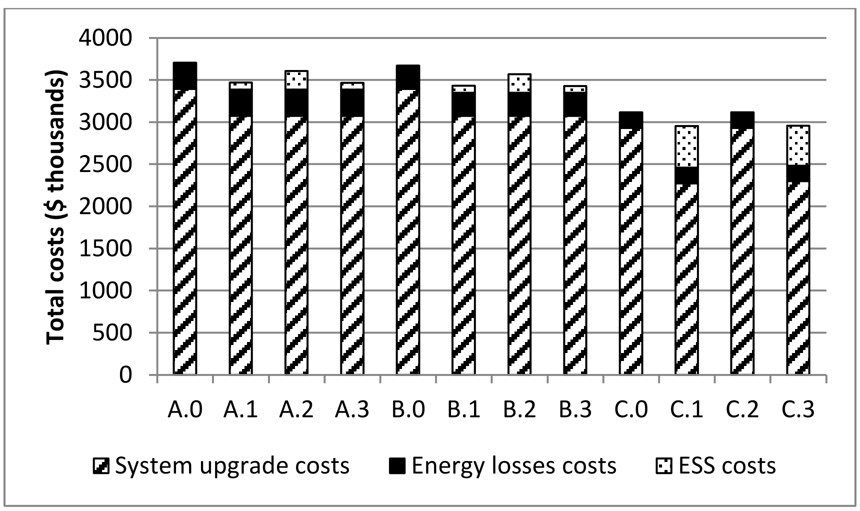

Figure 4-3 Results of the different scenarios

Table 4-5 Detailed results of the different scenarios

(a) Results for case A

Scenario		A.0	A.1	A.2	A.3
NPV of DS costs	**Capital costs ($)**	0	48,000	150,000	74,000
	Maintenance costs ($)	0	20,457	27,276	27,276
	Replacement costs ($)	0	13,720	41,546	0
	Total ($)	0	82,177	218,820	101,280
NPV of DS arbitrage value ($)		0	1,142	1,386	460
NPV of system upgrade costs ($)		3,395,200	3,076,500	3,076,500	3,076,500
% Savings		0.00%	9.39%	9.39%	9.39%
NPV of energy losses cost ($)		311,160	309,770	309,720	309,810
% Savings		0.00%	0.45%	0.46%	0.43%
Total cost ($)		3,706,360	3,467,305	3,603,654	3,487,130
% Total savings		0.00%	6.45%	2.77%	5.91%
Installed DS units (kW, kWh)	**Bus 16**	0	0	0	0
	Bus 17	0	100, 100	100, 100	100, 100
	Bus 21	0	0	0	0
	Bus 22	0	0	0	0
	Bus 25	0	0	0	0
	Bus 32	0	0	0	0

(b) Results for case B

Scenario		B.0	B.1	B.2	B.3
NPV of DS costs	Capital costs ($)	0	48,000	150,000	74,000
	Maintenance costs ($)	0	20,457	27,276	27,276
	Replacement costs ($)	0	13,720	41,546	0
	Total ($)	0	82,177	218,820	101,280
NPV of DS arbitrage value ($)		0	1,142	1,386	460
NPV of system upgrade costs ($)		3,395,200	3,076,500	3,076,500	3,076,500
% Savings		0.00%	9.39%	9.39%	9.39%
NPV of energy losses cost ($)		274,430	273,270	273,250	273,260
% Savings		0.00%	0.42%	0.43%	0.43%
Total cost ($)		3,669,630	3,430,805	3,567,184	3,450,580
% Total savings		0.00%	6.51%	2.79%	5.97%
Installed DS units (kW, kWh)	Bus 16	0	0	0	0
	Bus 17	0	100, 100	100, 100	100, 100
	Bus 21	0	0	0	0
	Bus 22	0	0	0	0
	Bus 25	0	0	0	0
	Bus 32	0	0	0	0

(c) Results for case C

Scenario		C.0	C.1	C.2	C.3
NPV of DS costs	Capital costs ($)	0	288,000	0	444,000
	Maintenance costs ($)	0	122,740	0	163,660
	Replacement costs ($)	0	82,319	0	0
	Total ($)	0	493,060	0	607,660
NPV of DS arbitrage value ($)		0	7,229	0	3,038
NPV of system upgrade costs ($)		2,929,100	2,275,200	2,929,100	2,275,200
% Savings		0.00%	22.32%	0.00%	22.32%
NPV of energy losses cost ($)		188,470	185,030	188,470	184,910
% Savings		0.00%	1.83%	0.00%	1.89%
Total cost ($)		3,117,570	2,946,061	3,117,570	3,064,732
% Total savings		0.00%	5.50%	0.00%	1.69%
Installed DS units (kW, kWh)	Bus 16	0	100, 100	0	100, 100
	Bus 17	0	500, 500	0	500, 500
	Bus 21	0	0	0	0
	Bus 22	0	0	0	0
	Bus 25	0	0	0	0
	Bus 32	0	0	0	0

4.5.1 No DG

In this case, the system is assumed to have no pre-allocated DGs. Scenario A.0 represents the base case in which the total cost is only comprised of the costs associated with the system upgrades and energy losses. The next three scenarios (A.1 to A.3) present the allocation of different storage technologies. The results of allocating DS units are the same for the three different technologies. Therefore, the cost of system upgrades is found similar; it is notably reduced from $3.40 million (base case) to $3.10 million, thus resulting in 9.39% saving. This reduction is due to deferring system upgrades to later years. However, the cost of the system losses is slightly decreased (i.e., ~0.45% saving) due to the demand management achieved. It is worthy to note that the costs of energy losses are different in each scenario based on the corresponding optimized DS operation, as given in Table 4-6. This table shows the optimal charging/discharging output powers at each load state for each storage technology. This table would be very useful for utilities' operators in controlling the DS operation, in order to achieve the maximum arbitrage benefit, based on the measurement of system load magnitude only, i.e., without any further utilization of advanced forecasting modules and controllers. Note that the difference in the operation of the various technologies is attributed to the different corresponding efficiencies.

Table 4-6 Optimal DS output power (in kW) at each load state

Load state no.	**DS status**	**LA**	**Na/S**	**VR**
1	Discharging	100	100	100
2	Discharging	24.29	24.41	27.73
3	Discharging	7.79	8.22	10.22
4	Discharging	1.98	1.88	1.07
5	Discharging	1.98	1.88	1.07
6	Discharging	2.00	1.90	1.09
7	Charging	0.00	0.00	0.09
8	Charging	42.94	40.16	48.08
9	Charging	15.41	17.16	13.53
10	Charging	27.58	28.39	27.69

With respect to the total cost in Table 4-5 (a), LA batteries are revealed to provide the least expensive solution: total costs are decreased from $3.71 million (base case) to $3.47 million, thus resulting in 6.45% total savings. It is worthwhile to mention that these costs are system dependent. More savings can be further achieved if other benefits of DS are taken into consideration, such as the enhancement of reliability and the mitigation of power quality problems.

As can be seen, the Na/S batteries represent an expensive option due to their high capital costs and low life time. On the other hand, although VR batteries have higher capital costs compared to LA ones, VR batteries have long life time and they do not need to be replaced during the planning period, thus reducing the NPV of DS costs to almost those of LA batteries.

With respect to the arbitrage benefit, it is clear that the more efficient the energy storage technology is, the higher the arbitrage benefit will be. Nevertheless, the highest arbitrage benefit is significantly less than the DS installation and maintenance costs. Therefore, according to the current costs of energy storage technologies, no private investors would install energy storage units in order to achieve this arbitrage benefit only.

4.5.2 Wind-Based DG Only

Only the wind-based DG (i.e., DG_2) is assumed existing in the system under study in order to study the impact of intermittent-based DGs on the allocation of DS units. As can be seen in the base case (B.0), the cost of system upgrades is the same of scenario (A.0) since the required upgrades are determined at the extreme power flow condition as mentioned earlier, which implies minimum output power from DG_2 (i.e., zero in this case) and maximum (peak) load. Consequently, the same allocation of DS units is depicted in this case. However, the cost of system losses is significantly reduced by 11% compared to scenario (A.0) due to the integration of wind-based DG.

4.5.3 Wind and Diesel-Based DGs

In this case, the system is assumed equipped with both dispatchable and intermittent DGs, i.e., DG_1 and DG_2, respectively. The results of the base case (C.0) show that the total cost, including the costs of system upgrades and energy losses, is significantly reduced by $0.59 million compared to scenario (A.0). This reduction is due to the two DGs installed in this case. The next three scenarios present the allocation of DS units for the three storage technologies. As can be seen, the number and sizes of DS units allocated are the same for LA and VR batteries, while Na/S batteries are found not economic for this case study. Moreover, the number and sizes of DS units allocated in scenarios (C.1) and (C.3) are higher than those of cases A and B. These results are attributed to the fact that the system costs are already decreased with the integration of the two DGs. Therefore, more energy storage units are needed in order to reduce the total cost.

Furthermore, the cost of system upgrades is significantly reduced from $2.93 million (C.0) to $2.28 million in scenarios (C.1) and (C.3), thus resulting in 22.32% saving. In scenarios (C.1) and (C.3), the losses are further decreased by almost 1.8%. The LA batteries are also shown to be the least expensive solution in this case. The deferral of system upgrades is shown in Table 4-7, which presents the first year of upgrading the distribution lines (feeders) for the different scenarios. For instance, upgrading line #7 is deferred from year 9, in the base case, to year 12, in scenarios (C.1) and (C.3). The other feeders are not needed to be upgraded within the planning period. In scenario (C.2), on the other hand, the upgrades are exactly the same as the base case since there are no DS units to be installed.

Table 4-7 First year of upgrading the distribution lines

Line number	C.0	C.1	C.2	C.3
1	4	6	4	6
2	4	6	4	6
4	8	11	8	11
6	9	12	9	12
7	9	12	9	12

4.6 Conclusions

In this chapter, a multi-year planning framework was proposed for the allocation of DS units in distribution systems in order to defer system upgrades, reduce energy losses, and take advantage of the arbitrage benefit. The NPV of DS installation and maintenance costs as well as system upgrade and energy losses costs were then minimized in order to determine the optimal size and location of DS units to be installed. Furthermore, a probabilistic approach, rather than time-series models used in the literature, was adopted in order to optimize the DS operation at each load state, and thus to achieve the maximum arbitrage benefit. The optimized DS operation allows utilities' operators simply control the DS units based on the measurement of system load magnitude only, i.e., without any further utilization of advanced forecasting modules and controllers. A sample case study was presented, and three different cases are discussed. Moreover, three storage technologies were compared and measured against a base case with no DS installation. The results were shown to be dependent on the system under study, e.g., type and size of existing DGs. Nevertheless, the results showed that integrating DS units with distribution systems reduces the total costs of utilities because of their capacity to shave peak load. However, the results might be more promising if storage costs become less in the future, or other benefits of ESS are considered, such as the improvement of distribution system reliability and the mitigation of power quality problems. Thus, combining the benefits of load management and enhancement of distribution system reliability will be discussed in the next chapter.

Chapter 5 Optimal ESS Allocation for Benefit Maximization in Distribution Networks

5.1 Introduction

In the previous two chapters, methodologies were proposed for allocating distributed storage units in distribution networks in order to achieve various benefits for distribution companies. Combining all of these benefits in one framework would thus ensure the effectiveness of the allocation strategy and increase the interest in deploying high penetration levels of energy storage in distribution systems. Thus, this chapter aims to present a new comprehensive planning framework for determining the size and location of DS units to be installed in distribution networks in order to improve distribution system reliability and to defer system upgrades using load management strategies.

Similar to the approach adopted in the previous chapters, a probabilistic approach is adopted that includes the consideration of the stochastic nature of system components. Such approach allows determining the optimal operation of distributed storage units at each load state. Moreover, contingency planning decisions, in the form of load points to be shed during contingencies, are identified through the methodology proposed.

In the next sections, the problem description, problem formulation, case study, and results are presented. Finally, some concluding remarks are discussed in the last section.

5.2 Problem Description

The rationale of the planning framework developed is to determine the investment decisions for distribution companies that may consider installing DS units in order to achieve several benefits. The main goal is to optimize the benefits of allocating DS units with respect to their installation and operation costs. In this section, the methodology proposed is described, and the benefits considered in this work are presented.

The input to the methodology proposed is the different models of load and DG units, average electricity rates, financial parameters, and the cost parameters of the different equipment. The output of this methodology is the optimal sizing and siting of DS units, as well as their optimized operation at each load state, and other contingency planning decisions, as will be described later on.

As discussed earlier, the various benefits that distribution companies can achieve from installing DS units at their networks are enumerated as follows:

- improving system reliability;
- arbitrage benefit;
- system upgrade deferral;
- energy losses reduction.

From the aforementioned discussion, the proposed work aims to find the optimal DS allocation in distribution systems that minimizes the NPV of system costs—i.e., system upgrades, energy losses, interruption costs, and DS installation and maintenance costs—and maximizes the NPV of arbitrage benefit. The methodology proposed includes determining the sizes and locations of DS units to be installed (planning decisions), the control strategy of those allocated DS units (operational decisions), and the load points to be shed during contingencies (contingency planning decisions). It is worth mentioning that the contingency planning decisions basically aim to increase the overall probability of successful islanding operation, and thus minimizing the total interruption cost.

5.3 Problem Formulation

This section presents the general methodology adopted in this chapter. A multi-stage model is proposed, in which GA and LP solvers are utilized for minimizing the objective function under study.

The main step of the methodology proposed is the chromosome encoding of GA. Each solution (chromosome) consists of integer variables that represent the discrete size of DS units to be installed and the loads to be shed during contingencies, as shown in Figure 5-1. For every population generated by GA, four steps are required to evaluate the objective (fitness) function of each individual, as summarized in Figure 5-2. Multi-year planning approach is further proposed in this work in order to evaluate the NPV of both system expenses and benefits. The first step adopts a discrete load model, which implies certain load states with their magnitudes and the associated probabilities, in optimizing the charging/discharging DS operation at each load state through a LP solver. The second step implies a load flow analysis at each system state in order to determine the required system upgrades and the corresponding energy losses. The third step performs a contingency analysis of the distribution system in order to determine how much power is required from each allocated DS unit in order to supply the demand power required for all possible island formations. Finally, a sequential MCS is performed, utilizing the output from the previous steps, in order to estimate the annual arbitrage benefit, EENS, and ECOST. These main steps are detailed in the next subsections and the associated mathematical formulations are presented.

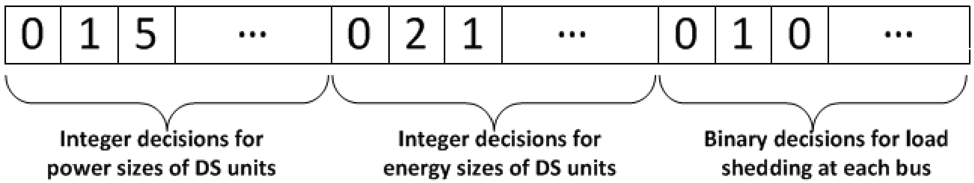

Figure 5-1 A sample structure of the chromosome encoding

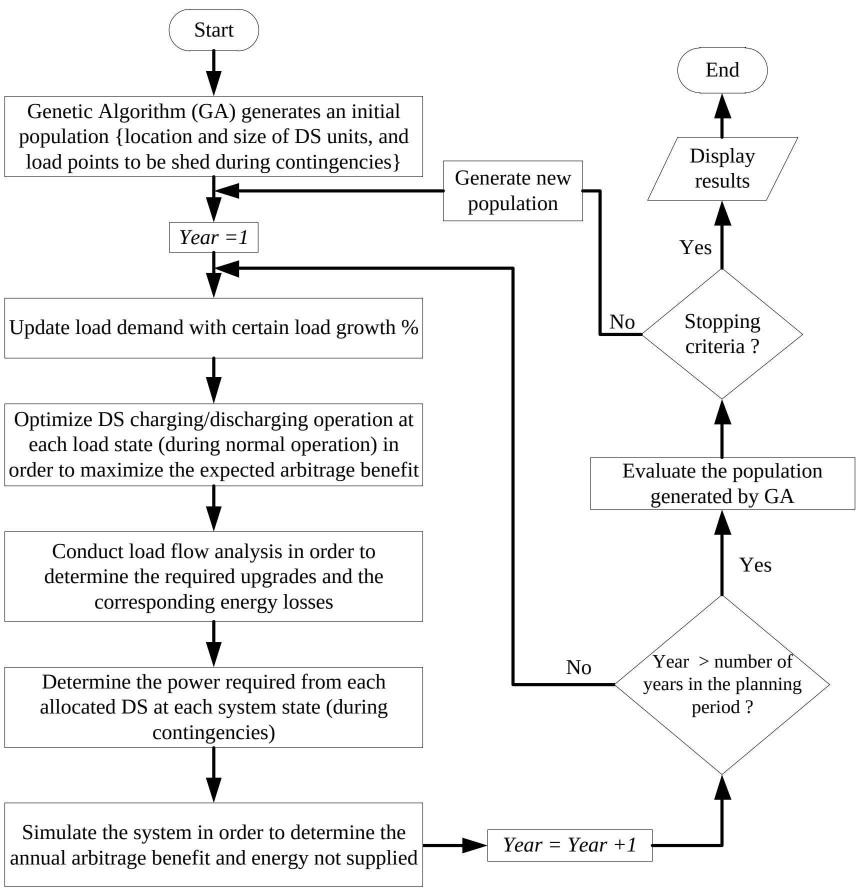

Figure 5-2 Flowchart of the proposed methodology

5.3.1 Optimize the Operation of DS Units during Normal Operation

This step involves determining the optimal DS charging/discharging power at each load state, as discussed earlier in section 4.3.1.

5.3.2 Evaluate System Upgrade and Energy Losses' Costs

In this step, a combined load-DG model is utilized as discussed in section 2.5. This step further applies multi-year probabilistic load flow analysis in order to evaluate system upgrade and energy losses' costs. The procedure for evaluating system upgrade and energy losses costs is presented in section 4.3.3.

5.3.3 Determine the Power Required From the Allocated DS Units during Contingencies

This step implies performing an N-1 contingency analysis that considers the failure of every single line in the distribution system. When such a disturbance occurs, the protection system isolates the faulty section so as to ensure the healthy operation of the rest of the system. This practice results in the formation of islands if DG and/or DS units are available and capable of supplying the load demand in those islands. The contingency analysis involves solving of the load flow equations for all possible islands in order to determine the power requirements from every DS unit for all combined load-DG states, taking into account the load-shedding decision variables at each bus. The complete analysis is explained in 3.4.1.

5.3.4 Determine the Annual Arbitrage Benefit, Number of Operation Cycles, and Interruption Cost

In this step, a sequential MCS is performed in order to estimate the annual arbitrage benefit, number of charging-discharging cycles per year, and EENS and ECOST indices. This simulation takes into account the DS operation from the foregoing stages. The procedure for performing MCS is described as follows:

1- Each year in the planning period is represented by N_y years, whereby the system state at every hour (*hr*) is generated through the generation of a uniformly distributed random number between 0 and 1, and rounding it to the nearest value in the CDF that corresponds to the combined load-DG probabilistic model.

2- As well, system feeders (lines) are represented using a two-state model (up state and down state), as discussed earlier in section 3.4.2.

3- For each hour, the system condition is checked to determine whether it operates in normal (grid connected) mode or in islanded mode. Based on the system state and condition at every hour, the DS output power at each state is recalled from the foregoing stages. Then, the energy stored at the DS (E_{ESS}) is calculated, taking into consideration the physical constraints of the DS at any time interval, via the following relations:

$$E_{ESS_{hr+1}} = E_{ESS_{hr}} + \eta \times P_{ESS_{hr}}^{ch} - P_{ESS_{hr}}^{dis} \qquad \forall hr \tag{5.1}$$

$$0 \le P_{ESS_{hr}}^{dis}, P_{ESS_{hr}}^{ch} \le S_{ESS}^{rated} \qquad \forall hr \tag{5.2}$$

$$0 \le E_{ESS_{hr}} \le E_{ESS}^{rated} \qquad \forall hr \tag{5.3}$$

4- Determine the annual arbitrage benefit as in (5.4) in which, at a certain hour, only one term has a value while the other term equals to zero. The first term, with negative sign, represents the energy purchased at off-peak periods, while the second term, with a positive sign, corresponds to the energy sold at peak times. The DS efficiency is used to accurately account for the energy purchased at energy storage terminals.

$$\frac{1}{N_y} \sum_{hr=1}^{8760*N_y} \left\{ -c_{\text{off-peak}} \times \max\left(0, E_{ESS_{hr+1}} - E_{ESS_{hr}}\right) / \eta + c_{\text{peak}} \times \max\left(0, E_{ESS_{hr}} - E_{ESS_{hr+1}}\right) \right\} \tag{5.4}$$

5- Calculate the number of annual operating (charge/discharge) cycles for each DS.

6- For every hour, the loads-shedding decision variables at every bus are set to zero during normal mode of operation. However, during islanded operation, they are adjusted based on the total generation, energy stored, and total demand at a given island.

7- Determine the EENS and ECOST per year as explained in section 3.4.2.

8- Stop if the ratio of the standard deviation of the sample mean of the index of interest (i.e., ECOST) to the sample mean of the same index becomes less than a predetermined tolerance, otherwise go to step 1.

9- At the end of the planning period, determine the NPV of the arbitrage benefit and ECOST as in (5.5) to (5.6)

$$NPV_{AR} = \text{Annual arbitrage benefit } \times PVF \tag{5.5}$$

$$NPV_{ECOST} = \sum_{yr=1}^{N_{yr}} \frac{ECOST_{yr}}{(1+IR')^{yr}} \tag{5.6}$$

5.3.5 Evaluate the Objective Function

In this step, the objective (fitness) function is presented that minimizes the aforementioned costs and maximizes the arbitrage benefit in (5.7), wherein the PVF is used to calculate the NPV of annual costs

$$\underset{x_i, y_i, z_i}{\text{Minimize}} \sum_{i=1}^{N} \left\{ \left(C_P + C_M \times PVF\right) \times S_{ESS_i}^{rated} + \left(C_E + C_R\right) \times E_{ESS_i}^{rated} \right\} + NPV_{UP} + NPV_{LO} + NPV_{ECOST} - NPV_{AR} + 10^8 \times \sum_{q=1}^{N_c} t_q \tag{5.7}$$

subject to

DS size constraints:

$$S_{ESS_i}^{rated} = x_i \times \text{certain discrete size} \qquad \forall i \in \mathcal{E} \tag{5.8}$$

$$E_{ESS_i}^{rated} = y_i \times \text{certain discrete size} \qquad \forall i \in \mathcal{E} \tag{5.9}$$

$$S_{ESS_i}^{rated} \le S_{ESS}^{\max} \qquad \forall i \in \mathcal{E} \tag{5.10}$$

$$E_{ESS_i}^{rated} \le E_{ESS}^{\max} \qquad \forall i \in \mathcal{E} \tag{5.11}$$

DS installation constraints:

$$x_i \text{ and } y_i = 0 \qquad \forall i \notin \mathcal{E} \tag{5.12}$$

Load shedding constraints:

$$P_{SH_i} = z_i \qquad \forall i \tag{5.13}$$

$$P_{SH_i} \le 1 \qquad \forall i \tag{5.14}$$

5.4 Case Study

The system under study is the same 33-bus radial distribution system shown in Figure 3-6. All system and financial parameters are assumed to be the same as in the previous two chapters. The distribution system is also assumed to contain a mix of 70% residential and 30% small commercial and industrial customers. These percentages are used for the estimation of the customers' WTP through the weighting of the corresponding CDFNs shown in Figure 3-1.

Again, lead-acid (LA), sodium-sulfur (Na/S), and vanadium-redox (VR) batteries are selected as the candidate storage technologies. It is assumed that the candidate storage technologies are available in discrete sizes in steps of 100 kW/kWh. Table 4-3 lists the capital and maintenance costs for the three candidate technologies. The candidate buses for DS installation are further assumed to be included in the set $\mathcal{E}$: (16, 17, 21, 22, 25, 32).

5.5 Results

This section summarizes the findings of this case study, in which DS units are optimally allocated in order to achieve the following benefits: improve system reliability, defer system upgrades, maximize the arbitrage benefit, and minimize system losses. The impact of pre-allocated DG types is studied in this section through three different cases: the system without any DG, the system with intermittent DG type only (i.e., DG_2), and the system with both intermittent and dispatchable DG types (i.e., DG_1 and DG_2).

In each case, several scenarios representing the base case (i.e., without DS units) and the three different storage technologies, as shown in Table 4-4, are compared. The NPV of total costs are summarized for each scenario in Figure 5-3, and the details are shown in Table 5-1. The load points to be shed, during contingencies, are also given in Table 5-1 for each scenario. Note that the percentage of savings in each scenario is calculated with respect to the corresponding base case.

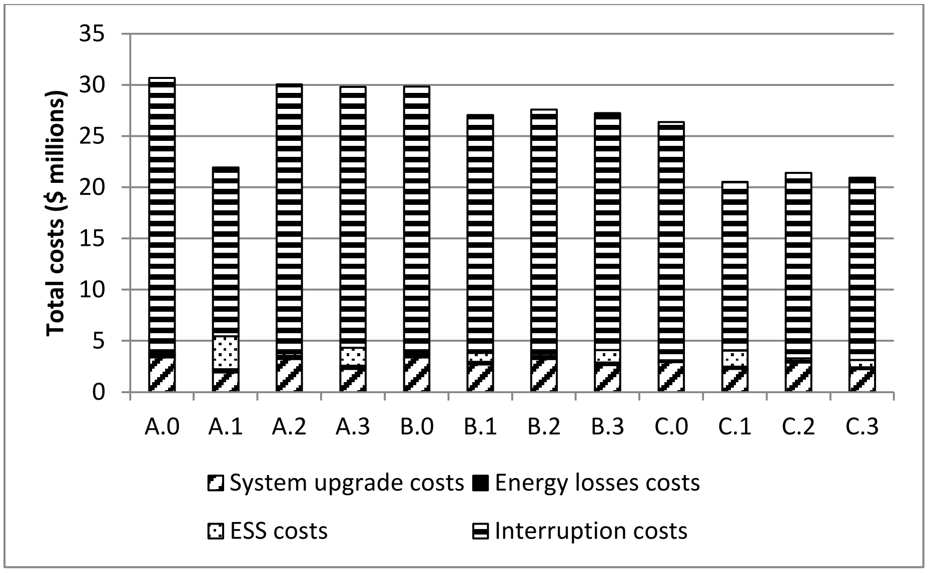

Figure 5-3 Results of the different scenarios

Table 5-1 Detailed results of the different scenarios

(a) Results for case A

Scenario		A.0	A.1	A.2	A.3
NPV of DS costs	Capital costs ($)	0	606,500	150,000	814,000
	Maintenance costs ($)	0	245,490	27,276	300,040
	Replacement costs ($)	0	143,700	51,116	0
	Total ($)	0	995,680	228,390	1,114,000
NPV of DS arbitrage value ($)		0	15,902	1,384	5,623
NPV of system upgrade costs ($)		3,395,200	2,269,500	3,234,400	2,331,700
% Savings		0.00%	33.16%	4.74%	31.32%
NPV of energy losses cost ($)		311,160	303,280	310,710	306,950
% Savings		0.00%	2.53%	0.14%	1.35%
NPV of interruption costs ($)		27,196,702	26,061,576	26,493,768	26,086,868
% Savings		0.00%	4.17%	2.58%	4.08%
Total cost ($)		30,903,062	29,614,134	30,265,884	29,833,895
% Total savings		0.00%	4.17%	2.06%	3.46%
Installed DS units (kW, kWh)	Bus 16	0	0	0	500, 500
	Bus 17	0	600, 600	0	500, 500
	Bus 21	0	0	0	0
	Bus 22	0	0	0	0
	Bus 25	0	100, 200	100, 100	100, 200
	Bus 32	0	500, 500	0	0
Load points to be shed		--	2, 6, 8-10, 13-15, 20, 23, 26, 29-32	4-6, 11, 14-16, 19, 20, 28-32	3, 5-8, 11, 13, 16, 17, 19, 20, 26, 30, 32, 33

(b) Results for case B

Scenario		B.0	B.1	B.2	B.3
NPV of DS costs	Capital costs ($)	0	528,000	150,000	888,000
	Maintenance costs ($)	0	225,030	27,276	327,310
	Replacement costs ($)	0	96,534	51,116	0
	Total ($)	0	849,560	228,390	1,215,300
NPV of DS arbitrage value ($)		0	13,308	1,384	5,812
NPV of system upgrade costs ($)		3,395,200	2,699,000	3,234,400	2,630,200
% Savings		0.00%	20.51%	4.74%	22.53%
NPV of energy losses cost ($)		274,430	269,090	274,000	270,140
% Savings		0.00%	1.95%	0.16%	1.56%
NPV of interruption costs ($)		26,176,492	23,241,630	23,842,020	23,115,616
% Savings		0.00%	11.21%	8.92%	11.69%
Total cost ($)		29,846,122	27,045,972	27,577,426	27,225,445
% Total savings		0.00%	9.38%	7.60%	8.78%
Installed DS units (kW, kWh)	Bus 16	0	0	0	0
	Bus 17	0	0	0	0
	Bus 21	0	0	0	0
	Bus 22	0	0	0	200, 200
	Bus 25	0	500, 500	100, 100	400, 400
	Bus 32	0	600, 600	0	600, 600
Load points to be shed		--	5, 7, 10-16, 18, 20-24, 28-31, 33	2-4, 6-11, 14-16, 23, 24, 27, 29-31, 33	2, 4-13, 16-18, 21, 23, 24, 26, 27, 30

(c) Results for case C

Scenario		C.0	C.1	C.2	C.3
NPV of DS costs	Capital costs ($)	0	1,203,000	150,000	518,000
	Maintenance costs ($)	0	122,740	27,276	190,930
	Replacement costs ($)	0	245,110	51,116	0
	Total ($)	0	1,570,900	228,390	708,930
NPV of DS arbitrage value ($)		0	48,601	1,384	3,382
NPV of system upgrade costs ($)		2,929,100	2,275,200	2,894,500	2,243,300
% Savings		0.00%	22.32%	1.18%	23.41%
NPV of energy losses cost ($)		188,470	209,300	188,060	185,810
% Savings		0.00%	-11.05%	0.22%	1.41%
NPV of interruption costs ($)		23,235,774	16,484,542	18,090,104	17,783,020
% Savings		0.00%	29.06%	22.15%	23.47%
Total cost ($)		26,353,344	20,491,341	21,399,670	20,917,678
% Total savings		0.00%	22.24%	18.80%	20.63%
Installed DS units (kW, kWh)	Bus 16	0	0	0	0
	Bus 17	0	600, 3600	0	600, 600
	Bus 21	0	0	0	0
	Bus 22	0	0	0	0
	Bus 25	0	0	100, 100	100, 100
	Bus 32	0	0	0	0
Load points to be shed		--	4, 6, 7, 9, 14, 15, 19-22, 24, 25, 28, 30, 32	6, 7, 9, 10, 12-15, 18, 20, 22-24, 27, 32	4-8, 10, 13-15, 19, 24, 26-29

5.5.1 No DG

In this case, the system is assumed to have no pre-allocated DGs. Scenario A.0 represents the base case in which the total cost comprises the costs associated with the system upgrades, customer interruptions, and energy losses. The next three scenarios (A.1 to A.3) present the allocation of different storage technologies. In Table 5-1 (a), LA batteries are revealed to provide the least expensive solution: total costs are reduced from $30.9 million (base case) to $29.6 million, thus resulting in 4.17% total savings. This reduction is due to deferring system upgrades to later years, and thus reducing upgrade costs by 33.16%, and improving system reliability, and thus reducing interruption costs by 4.17%. The energy losses were further reduced by 2.53%.

With respect to the arbitrage benefit, the highest arbitrage benefit is significantly less than the DS installation and maintenance costs. Therefore, according to the current costs of energy storage technologies, no private investors would install energy storage units in order to achieve this arbitrage benefit only.

As an example, Figure 5-4 shows a graphical representation of LA battery allocation during a failure at the line between buses 6 and 7. The DS unit allocated at bus 17 is utilized in order to supply the island formed. Further, load points 8 to 10 and 13 to 15 should be disconnected by the utility operator in a timely manner in order to guarantee the highest successful islanding operation for the isolated system.

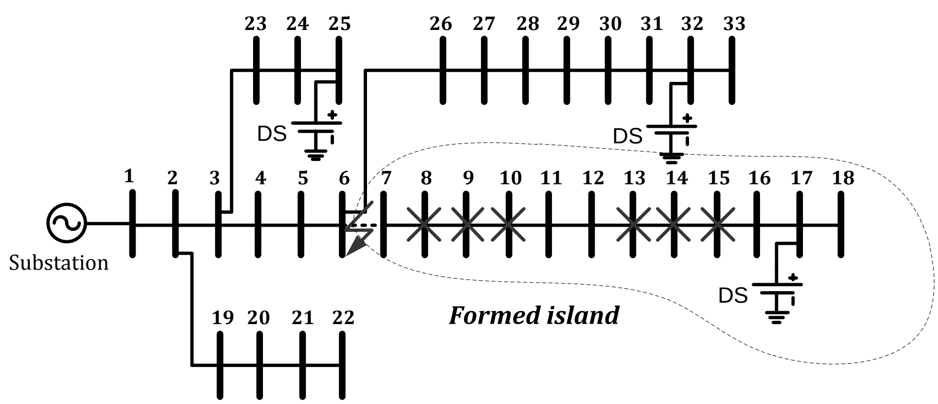

Figure 5-4 Graphical representation of DS allocation and load shedding during a contingency at the line between buses 6 and 7

5.5.2 Wind-Based DG Only

In this case, the system is assumed equipped with wind-based DG only (i.e., DG_2) in order to study the impact of intermittent-based DGs on the allocation of DS units. As observed in the base case (B.0), the cost of system upgrades is the same of scenario (A.0) since the required upgrades are determined at the extreme power flow condition as mentioned earlier, which implies minimum output power from DG_2 (i.e., zero in this case) and maximum (peak) load. However, the interruption costs of scenario (B.0) are reduced by $1.02 million compared to scenario (A.0) due to the DG integration. Nevertheless, LA batteries are also found the least expensive technology in this case, where the total cost is reduced by 12.48% compared to scenario (A.0).

5.5.3 Wind and Diesel-Based DGs

In this case, both dispatchable and intermittent DGs, i.e., DG_1 and DG_2, respectively, are assumed existing in the system under study. The results of the base case (C.0) show that the total cost, including the costs of system upgrades, energy losses, and interruption costs, is significantly reduced by $4.55 million compared to scenario (A.0). The next three scenarios present the allocation of DS units for the three storage technologies. It is clear that the impact of DS integration on reducing the interruption costs, and thus the total costs, is significant with the presence of DG units compared to the first case without any DG units.

Table 5-1 (c) further shows that LA batteries are the most economic technology; total costs are reduced from $30.9 million (scenario A.0) to $20.49 million, thus resulting in 33.69% in total savings. Moreover, the cost of upgrades and customer interruptions are notably reduced by almost 33% and 39%, respectively, compared to scenario (A.0). However, the cost of energy losses has been increased only in the case of LA battery due to the large size of battery installed. This increase is attributed to the fact that the cost of energy losses is not significant compared to the costs of system upgrades and the costs of interruptions. Therefore, a large battery was found more cost effective in reducing the costs of interruption and deferring system upgrades, even at the expense of adding more energy losses.

As an example, Table 5-2 gives the optimal operation of DS units for the different scenarios. This table shows the optimal charging/discharging output powers at each load state for each storage technology. This table would be very useful for utilities' operators in controlling the DS operation, in order to achieve the maximum arbitrage benefit, based on the measurement of system load magnitude only, i.e., without any further utilization of advanced forecasting modules and controllers. Note that the difference in the operation of the various technologies is attributed to the different sizes and their corresponding efficiencies.

Table 5-2 Optimal DS output power (in kW) at each load state

Load state no.	**DS status**	**LA (bus #17)**	**Na/S (bus #25)**	**VR (bus #25)**
1	Discharging	600.00	100.00	100.00
2	Discharging	270.75	24.41	27.73
3	Discharging	225.39	8.22	10.22
4	Discharging	212.11	1.88	1.07
5	Discharging	212.11	1.88	1.07
6	Discharging	213.79	1.90	1.09
7	Charging	597.92	0.00	0.09
8	Charging	598.00	40.16	48.08
9	Charging	599.28	17.16	13.53
10	Charging	595.63	28.39	27.69

5.6 Conclusions

In this chapter, a comprehensive planning framework was proposed for allocating DS units in distribution systems in order to improve system reliability, defer system upgrades, reduce energy losses, and take advantage of the arbitrage benefit. The NPV of DS installation and maintenance costs as well as interruption costs, system upgrade and energy losses costs were minimized in order to determine the optimal size and location of DS units to be installed. A sample case study was presented, and three storage technologies were compared against each other and against a base case with no DS installation. Like the work presented in Chapter 4, the results were shown to be dependent on the system under study, e.g., type and size of existing DGs. Nevertheless, the results showed that integrating DS units with distribution systems reduces the total costs of utilities because of their capacity to improve system reliability and defer system upgrades.

Chapter 6 Impact of Energy Storage Systems on Electricity Market Equilibrium

6.1 Introduction

In the previous chapters, a planning framework was developed for the allocation of DS units in distribution systems. This chapter presents an energy-market tool for electricity markets incorporating large-scale ESSs. Controlling the operation of energy storage usually depends on electricity-market prices so as to charge when the price is low and discharge when the price is high. On the other hand, the market-clearing price itself is determined based on the net demand, i.e., including energy storage output, at every hour. Therefore, it is crucial to develop a mathematical model to determine the optimal ESS operation as well as the market-clearing prices, as proposed in this chapter. The problem is formulated as a mixed complementarity problem (MCP) that allows the representation of special (incentive) prices, which cannot be represented in a single optimization model. The proposed model is useful for power system operators to determine the optimal storage dispatch simultaneously with the market-clearing price in addition to the conventional generation dispatch. The impact of energy storage size and location on market price, total generation cost, energy storage arbitrage benefit, and total consumer payment is further investigated in this chapter. The latter analysis provides some guidelines for power system planners to identify the optimal size and location for installing large-scale ESSs.

The main contributions of the work presented in this chapter are summarized as follows:

- This chapter presents a novel mathematical model for determining the optimal operation strategy of an ESS and the market-clearing price simultaneously in a perfectly competitive environment, even if special incentives make it impossible to formulate a single optimization model.
- The model proposed is used to address the impact of the ESS location and size on electricity-market equilibrium.

In the next sections, the problem formulation, case study, and simulation results are presented. Finally, some concluding remarks are discussed in the last section.

6.2 Problem Formulation

As discussed earlier, governments may consider special incentives for ESSs in order to encourage private investment. For some forms of special incentives, it is impossible to represent market equilibrium as a single optimization model, e.g., if an ESS is to receive a fixed multiple (greater than one) of the ordinary market price for its discharged output [76]. In such cases, however, an MCP formulation can be used. The work presented in this chapter includes consideration of one special incentive whereby the ESS would receive or pay the highest locational marginal price (LMP) among all the buses in the system.

The rationale behind this research work is to solve two dependent problems, i.e., social welfare maximization, given the energy storage operational decisions, and energy storage arbitrage benefit maximization, given the highest LMP, during charging and discharging, as a special incentive for the ESS. Before discussing how to solve the whole model as an MCP, the three optimization models are defined in the following paragraphs. The MCP is outlined at the end of this section, and it appears in detail in Appendix B.

The single auction market structure is considered in this work whereby the electricity price is settled based on the net demands at buses, i.e., after accounting for ESS charging and discharging, and the bids offered by the generators. Social welfare maximization under such a structure is achieved by minimizing the total generation cost function as follows [77], [78]

$$\text{minimize } F_1 = \sum_{hr=1}^{24} \sum_{i \in \mathcal{G}} \alpha_i P_{g_{i,hr}}^2 + \beta_i P_{g_{i,hr}} + \gamma_i \tag{6.1}$$

It is worth mentioning that the above cost function neglects startup costs since the representation of these costs requires binary variables, which cannot be considered in the MCP formulation used in this study. Therefore, we assume that unit commitment decisions have already been made in an earlier stage, and the committed generators are only considered in F_1. When deciding on unit commitments, the system operator would require an estimate of the charging and discharging schedule of the ESS, as the ESS operation could affect the need for some generation units. An estimate of the ESS schedule could be based on experience, to start, and the estimate could be updated after running the MCP model described in this chapter, in an iterative process. In this work, we focus on the MCP model only, and leave the extension to the unit commitment process for future research.

Moreover, if the power rating of the ESS is less than or equal to the capacity of the smallest generator (i.e., minimum spinning reserve), which is usually the case since the capacities of ESS are small compared to those of bulky generators, the ESS would be charged without the need for starting up another offline generator. Consequently, considering the startup costs would not affect the storage scheduling under the above condition. The amount of spinning reserve would be further unchanged, if we neglected the losses in the ESS, since a part of the reserve would be stored in the ESS in this case [79].

Nevertheless, F_1 is minimized under system constraints such as power flow constraints, generation limits, and voltage limits, as given in (6.2) to (6.9). Note that the variables for ESS charging and discharging are treated as parameters in this optimization model; dual variables are in parentheses.

$$P_{g_{i,hr}} - P_{D_{i,hr}} - P^{ch}_{ESS_{i,hr}} + P^{dis}_{ESS_{i,hr}} = \sum_{j=1}^{N} V_{i,hr} \times V_{j,hr} \times \left(G_{ij}\cos\delta_{ij,hr} + B_{ij}\sin\delta_{ij,hr}\right) \quad \left(\lambda_{i,hr}\right) \quad \forall i, hr \tag{6.2}$$

$$Q_{g_{i,hr}} - Q_{D_{i,hr}} = \sum_{j=1}^{N} V_{i,hr} \times V_{j,hr} \times \left(G_{ij}\sin\delta_{ij,hr} - B_{ij}\cos\delta_{ij,hr}\right) \quad \left(\mu_{i,hr}\right) \quad \forall i, hr \tag{6.3}$$

$$P_{flow_{ij,hr}} = V_{i,hr} \times \left\{ -G_{ij} \times V_{i,hr} + G_{ij} \times V_{j,hr} \times \cos\delta_{ij,hr} + B_{ij} \times V_{j,hr} \times \sin\delta_{ij,hr} \right\} \le P^{\max}_{flow_{ij}} \quad \left(ww_{ij,hr}\right) \quad \forall i \ne j, hr \tag{6.4}$$

$$P_{g_{i,\min}} \le P_{g_{i,hr}} \le P_{g_{i,\max}} \quad \left(aa_{i,hr}, bb_{i,hr}\right) \quad \forall i \in \mathcal{G}, hr \tag{6.5}$$

$$Q_{g_{i,\min}} \le Q_{g_{i,hr}} \le Q_{g_{i,\max}} \quad \left(cc_{i,hr}, dd_{i,hr}\right) \quad \forall i \in \mathcal{G}, hr \tag{6.6}$$

$$V_{min} \le V_{i,hr} \le V_{max} \quad \left(ee_{i,hr}, ff_{i,hr}\right) \quad \forall i \notin \mathcal{G}, hr \tag{6.7}$$

$$V_{i,hr} = \text{constant} \quad \left(gg_{i,hr}\right) \quad \forall i \in \mathcal{G}, hr \tag{6.8}$$

$$-\pi \le \delta_{i,hr} \le \pi \quad \left(kk_{i,hr}, ll_{i,hr}\right) \quad \forall i, hr \tag{6.9}$$

In this work, all generators and customers receive and pay the LMPs at every hour, i.e., the bus dual variables ($\lambda_{i,hr}$) corresponding to (6.2), respectively. However, the hourly electricity price (Λ_{hr}) that ESSs pay or receive for the energy stored or delivered, respectively, is set to be the highest bus dual variable as in (6.10), as motivated by [77], [78]

$$\Lambda_{hr} = \max_{i}\left(\lambda_{i,hr}\right) \qquad \forall hr \tag{6.10}$$

Taking the highest bus dual variable is justified as an incentive for promoting energy storage implementation. There tends to be much smaller differences among LMPs during off-peak, low-price, times when the ESS would charge, and so the "highest price" is close to all LMPs. The special incentive occurs when the "highest price" is very high during peak periods, and the ESS sells its discharged output. Applying this proposed incentive requires that the ESS pays the highest LMP during off-peak times, whereas the power authority compensates the ESS with the difference between its LMP and the highest LMP in the system during peak periods. This proposed incentive is basically one of many other possible incentives that may be offered to the storage owners. Other incentives could be, e.g., to use a weighted average of the LMP at the ESS connection, and the highest LMP, or to use the LMP, but the government pays a constant subsidy as an added amount on the selling price during discharging.

It is worthwhile to mention that if the LMP corresponding to the ESS location were used, then in the case study of sections 6.3 and 6.4, the energy storage would not be dispatched unless the ESS is located at the bus corresponding to the highest market-clearing price. This phenomenon is attributed to the fact that the difference between off-peak and peak price should be large enough in order to justify the ESS operation and maintenance cost, and thus to economically operate the ESS. This condition is not satisfied in the case when using the LMP. However, this conclusion depends on the system data and parameters. In other words, utilizing the LMP might lead to an economic dispatch with other systems of different data.

Equation (6.10) is implemented via a mathematical device that fits into the framework for developing an MCP: the system operator has a second objective (in addition to social welfare maximization) to minimize the electricity price (Λ_{hr}) at every hour, subject to the constraint that Λ_{hr} exceeds or equals the dual variable at every bus as follows (note that $\lambda_{i,hr}$ are treated as parameters in this optimization model):

$$\text{minimize } F_2 = \sum_{hr=1}^{24} \Lambda_{hr} \tag{6.11}$$

subject to

$$\Lambda_{hr} \geq \lambda_{i,hr} \quad \left(mm_{i,hr}\right) \quad \forall i, hr \tag{6.12}$$

The arbitrage benefit maximization problem associated with the energy storage is mathematically represented as minimizing the following objective function, where the electricity prices at every hour are treated as parameters in this model:

$$\text{minimize } F_3 = \sum_{hr=1}^{24} \sum_{i \in \mathcal{E}} \left\{ \left(P_{ESS_{i,hr}}^{ch} + P_{ESS_{i,hr}}^{dis} \right) \times C_O - \left(P_{ESS_{i,hr}}^{dis} - P_{ESS_{i,hr}}^{ch} \right) \times \Lambda_{hr} \right\} \quad (6.13)$$

In the above objective function, the first term represents the direct operation and maintenance cost associated with the ESS due to hourly charging and discharging, whereas the second term represents the arbitrage value. Indirect costs of losses are represented implicitly in (6.14) below, through the charging and discharging efficiency parameters. This formulation thus prevents dispatching the ESS for a zero arbitrage benefit since the arbitrage benefit should be at least equal to the cost of operating and maintaining the ESS. F_3 is to be minimized under the energy storage constraints as given in (6.14) to (6.17)

$$E_{ESS_{i,hr}} = E_{ESS_{i,hr-1}} + \eta^{ch} \times P_{ESS_{i,hr}}^{ch} - P_{ESS_{i,hr}}^{dis} / \eta^{dis} \qquad \left(nn_{i,hr} \right) \quad \forall i \in \mathcal{E}, hr \qquad (6.14)$$

$$0 \le P_{ESS_{i,hr}}^{ch} \le P_{ESS_i}^{rated} \qquad \left(oo_{i,hr}, pp_{i,hr} \right) \quad \forall i \in \mathcal{E}, hr \qquad (6.15)$$

$$0 \le P_{ESS_{i,hr}}^{dis} \le P_{ESS_i}^{rated} \qquad \left(qq_{i,hr}, rr_{i,hr} \right) \quad \forall i \in \mathcal{E}, hr \qquad (6.16)$$

$$0 \le E_{ESS_{i,hr}} \le E_{ESS_i}^{rated} \qquad \left(ss_{i,hr}, tt_{i,hr} \right) \quad \forall i \in \mathcal{E}, hr \qquad (6.17)$$

If the ESS was to pay and receive the LMP at its bus ($\lambda_{i,hr}$ instead of Λ_{hr}), then the OPF problem (6.1) to (6.9) could be combined with (6.14) to (6.17) in a single OPF that minimizes generation costs in (6.1) plus ESS costs in the first term of (6.13). However, such a formulation cannot be used to determine the optimal dispatch of the ESS with the special (incentive) price in (6.10). In other words, conventional market models cannot take into consideration the formulations introduced in (6.11) to (6.17) while solving for the 24-hour OPF problem in (6.1) to (6.9). Therefore, we propose a novel method that determines the optimal operation strategy of ESS and the special price that ESS will pay or receive at each hour, in addition to the conventional dispatch variables, i.e., the generation power levels at each hour. As a result, the main challenge of this work is to solve the aforementioned three dependent problems together.

In order to solve the three dependent problems simultaneously, for equilibrium, they are formulated as an MCP. In such a formulation, the Karush-Kuhn-Tucker (KKT) conditions of all optimization problems are combined together to form a square set of equations, inequalities, and complementarity conditions. However, any solution to those KKT conditions is not guaranteed to give the optimal solutions to the three problems unless certain sufficiency conditions are met, e.g., the objective function is a continuously differentiable convex function, and the constraints constitute a convex set [76]. By examining the three problems under study, we can conclude that the objective functions are convex functions since the first one is a quadratic function with non-negative parameters, whereas the second and third objectives are linear. However, all constraints are linear functions, i.e., convex, except the power flow equations which are non-convex functions in most cases [80]. Consequently, the obtained solutions are only guaranteed to be local optima.

6.3 Case Study

In all case studies, the system under study consists of a 6-bus transmission system and a 3-bus distribution system, as shown in Figure 6-1 [77]. The distribution system is interconnected to the transmission system through a 100-MVA transformer. Transmission and distribution lines' data are given in Table C.1, Appendix C [77]. Two generating stations (G1 and G2) are connected at buses 1 and 3; their cost function parameters, generation limits, and daily peak demand are given in Table C.2, Appendix C [77]. This system is simple enough to be solved in a short time, i.e., nearly one minute on a personal computer. Therefore, the model can be run several times, in a good timely manner, in order to provide a sensitivity analysis for the impact of the ESS location and size on market equilibrium. However, the IEEE 14 and 30 bus systems are also used in the first case study in order to demonstrate the performance of the model developed in solving larger real systems. The system layouts and data of the IEEE 14 and 30 bus systems are given in Appendix D and Appendix E, respectively [81].

The demand profile at each node is assumed to follow the IEEE-RTS summer load profile in Table F.1, Appendix F [61], which provides the hourly load magnitude as a percentage of the daily peak demand. However in real case studies, one-day ahead forecasted load demand profile as in [74] can be utilized in the developed model to set the market price and determine the optimal operation of allocated ESSs. On the other hand, the size and the location of the energy storage will be varied as will be discussed later on in section 6.4. The ESS charging and discharging efficiencies are assumed to be 90% (i.e., 81% round trip efficiency) in all case studies [57]. The operational cost of ESS (C_O) is assumed to be 0.6 cents/kWh [82].

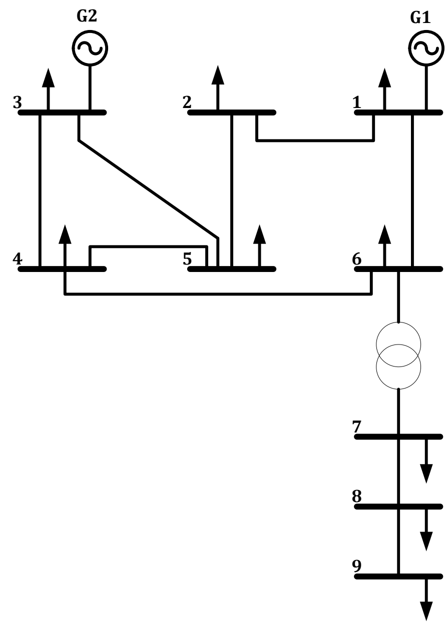

Figure 6-1 System under study

6.4 Simulation Results

The aforementioned MCP is solved by means of the PATH solver in the General algebraic modeling system (GAMS) environment. Several case studies are presented in this section; the first one shows the significance of the proposed MCP model to power system operators, i.e., to determine the optimal ESS dispatch and the highest market-clearing price in a perfectly competitive market. Afterwards, other case studies are discussed to show the impact of ESS size and location on the highest market-clearing price, total generation cost and benefit, energy storage arbitrage benefit, and total consumer payments. The simulation results are discussed in the next subsections. For all case studies, we report only the highest market-clearing price (Λ_{hr}), but not all nine LMPs, to save space.

6.4.1 Impact of energy storage operation

Basically, the ESS size is defined by two parameters: rated charging/discharging rate (in MW) and rated storage capacity (in number of discharge hours at rated discharging rate), which correspond to PCS and energy reservoir sizes, respectively.

In this case study, the 9 bus system is utilized first, and it is assumed that one ESS is allocated at the distribution system (bus #7) with a rating of 100 MW and 2 discharge hours, i.e., $P_{ESS}^{rated} = 100$ MW, and $E_{ESS}^{rated} = 200$ MWh. The proposed MCP model is utilized to determine the optimal ESS dispatch and the highest market-clearing price for one day ahead.

The highest market-clearing price is presented in Figure 6-2 with and without the ESS integration to the system. With the presence of the ESS, the electricity prices become almost leveled during off-peak and peak periods. Furthermore, it is clear that the prices are increased during off-peak times, while they are reduced during peak periods. This is because of the optimal ESS charging and discharging during off-peak and peak times, respectively, as shown in Figure 6-3, which shows the ESS output power as a percentage of the rated charging/discharging rate (i.e., 100 MW in this case study).

Moreover, the model proposed is used to solve the IEEE 14 and 30 bus systems in order to assess the increase in computational time as the model grows in size. The run times corresponding to the systems used in this study are summarized in Table 6-1. Although it seems that the model developed could scale up to solve larger systems, it is worth mentioning that for larger real-world systems, faster computer equipment and possibly specialized algorithms such as decomposition, as discussed at chapter 9 in [76], might be needed, to be solvable within a reasonable amount of time for day-ahead markets.

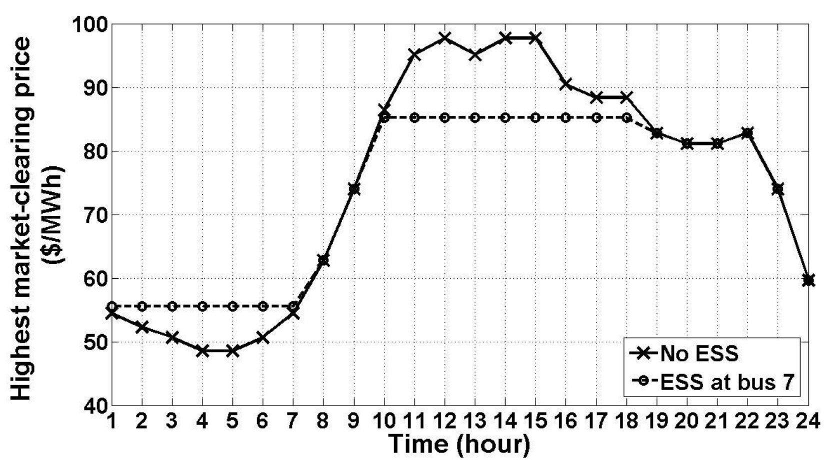

Figure 6-2 Highest market-clearing price with and without ESS integration

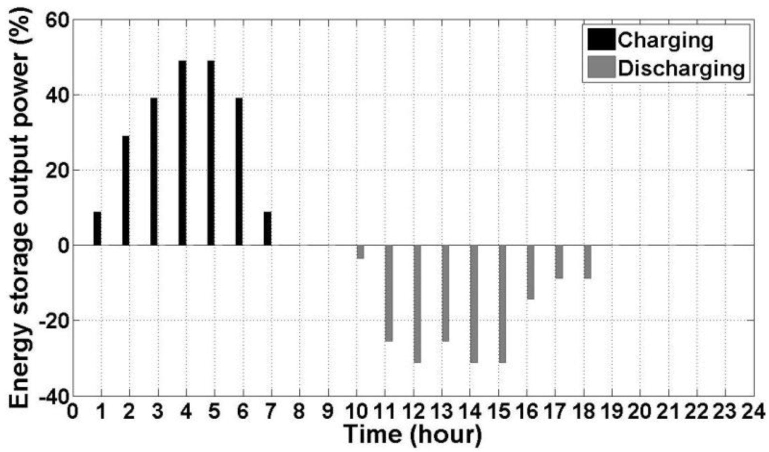

Figure 6-3 Optimal ESS dispatch

Table 6-1 Complexity analysis of the MCP model developed

System size	Run time (in seconds)
9 bus	50
14 bus	74
30 bus	206

6.4.2 Impact of energy storage size

This case study investigates the impact of energy storage size on the highest market-clearing price, total generation cost and benefit, arbitrage benefit, and total consumer payments. Like the previous case study, one ESS is assumed connected to bus #7. Firstly, the PCS size is fixed at 40 MW, while the reservoir size is varied between 2 and 6 discharge hours in steps. Afterwards, the PCS size is changed in steps between 40-80 MW, while the reservoir size is kept constant at 2 discharge hours.

Figure 6-4 shows the highest market-clearing prices for the different energy reservoir sizes compared to the case of no energy storage in the system. With the increase of energy storage capacity, the ESS can exchange more power with the generating stations during the day. Therefore, the market prices are settled at higher prices during low demand periods and at lower prices, on the other hand, when the demand is high. Similar results are obtained when the PCS size is increased from 40 MW to 80 MW, as shown in Figure 6-5.

The total generation cost profiles are presented in Figure 6-6 and Figure 6-7 for the different ESS sizes adopted in this case study. Figure 6-6 reveals that up to 20% higher generation costs are incurred during off-peak periods, whereas generation costs can be reduced by 10% during peak times.

With respect to the energy storage arbitrage benefit (in Figure 6-8), it is clear that the arbitrage benefit increases with an increment of the energy storage size up to a certain size. The arbitrage benefit then becomes steady at the maximum value since the optimal ESS operation does not change beyond this point. The maximum arbitrage benefit depicted is almost $3,100 per day, which can be achieved with different combinations between the PCS and reservoir sizes. For example, 80MW-4 discharge hours and 40 MW-6 discharge hours ESSs result in the same (maximum) arbitrage benefit. Therefore, the ESS owner needs to calculate the economic size to be installed that maximizes the present value of the arbitrage benefit over the lifetime of the ESS, minus the installation cost.

Moreover, Figure 6-9 and Figure 6-10 show total consumer payments and total generation benefit for the different ESS sizes, respectively, where total generation benefit is calculated by subtracting total generation cost from total generation revenue. It can be noticed that consumer payments and generation benefits are reduced with the increase of ESS size.

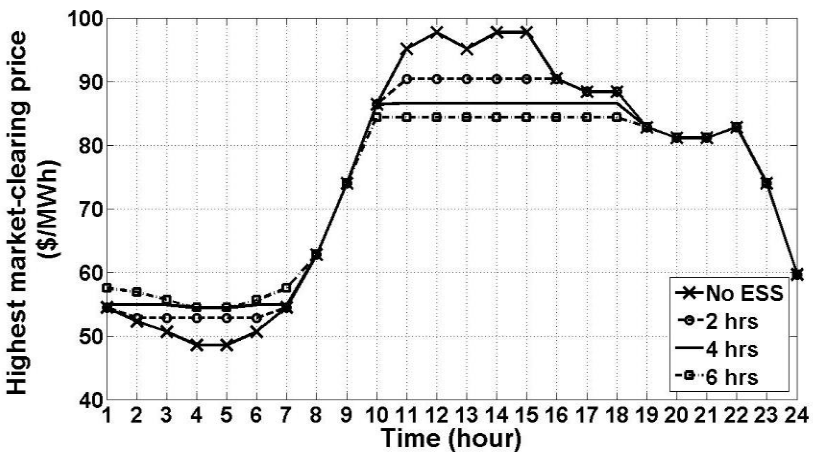

Figure 6-4 Highest market-clearing price for different energy storage reservoir sizes

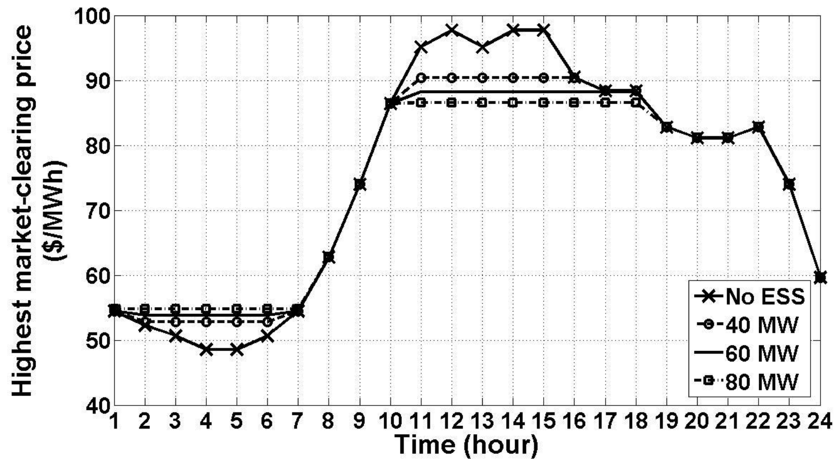

Figure 6-5 Highest market-clearing price for different PCS sizes

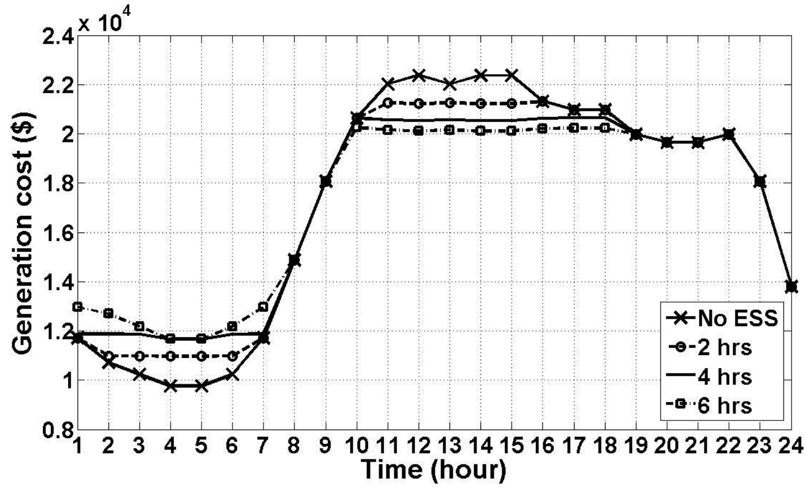

Figure 6-6 Total generation cost for different energy storage reservoir sizes

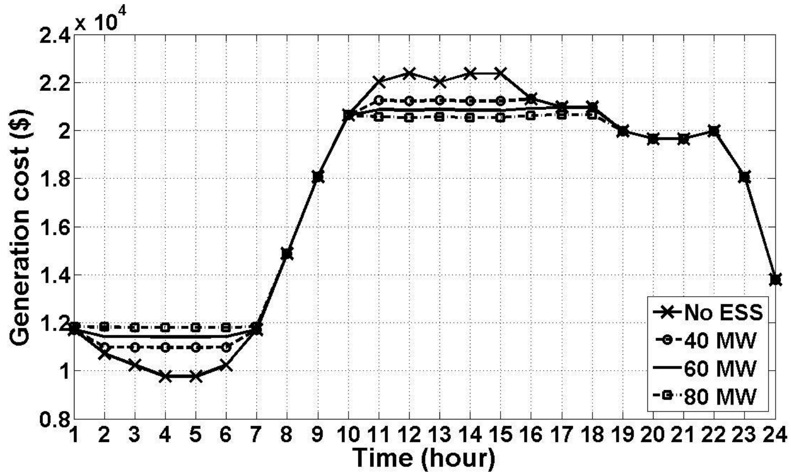

Figure 6-7 Total generation cost for different PCS sizes

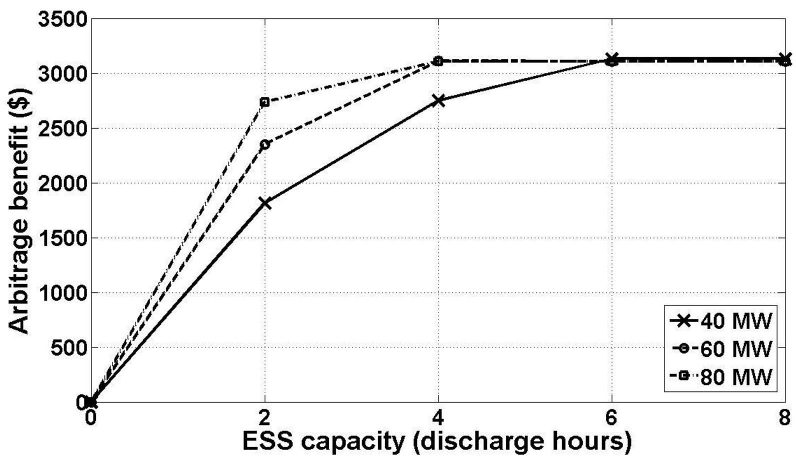

Figure 6-8 Arbitrage benefit for different ESS sizes

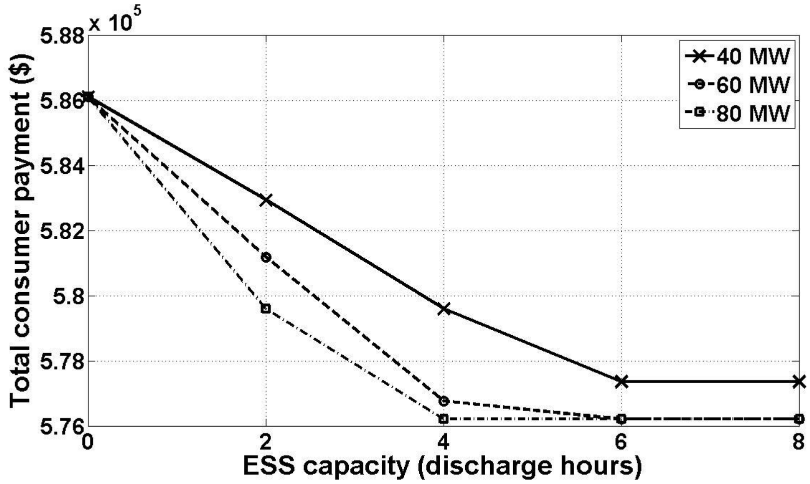

Figure 6-9 Total consumer payments for different ESS sizes

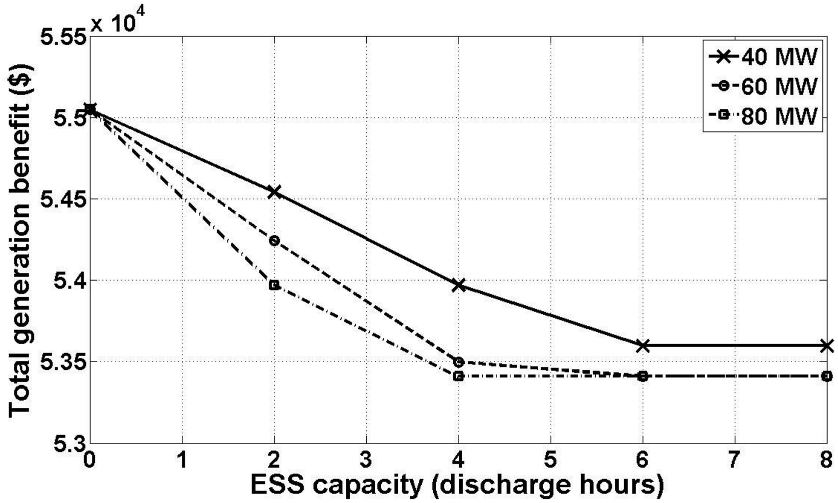

Figure 6-10 Total generation benefit for different ESS sizes

6.4.3 Impact of energy storage location

The impact of energy storage installation location is analyzed in this case study. Two possible locations are considered as follows: bus #5 (in the transmission system) and bus #8 (in the distribution system). In this case study, the size of ESS installed is fixed at 40 MW-4 discharge hours.

As shown in Figure 6-11, the energy storage location has an impact on the highest market-clearing price. When the ESS is installed in the transmission system (bus #5), the differences between off-peak and peak market prices are higher than those depicted when installing the same ESS in the distribution system (bus #8). This observation is attributed to the fact that the market prices are higher when more power losses are incurred in the system and vice versa. Therefore, when ESS units are installed in the distribution system, the system power losses are increased during charging periods of ESS, while they are reduced during discharging periods of ESS, thus increasing and decreasing the market prices during off-peak and peak periods, respectively.

Furthermore, the arbitrage value associated with transmission system installation equals $2,947 (per day), which is almost two times the value of the distribution system installation. As a result, it is more profitable for the ESS owner to install the ESS in the transmission system in order to achieve higher arbitrage benefit. On the other hand, Figure 6-12 reveals that total generation costs are larger with transmission system installation during off-peak times, while they are smaller when the load is high, compared to installing the same ESS in the distribution system. This observation can be explained as generation costs depend on the net system demand shown in Figure 6-13. The net system demand is calculated taking into consideration the optimal ESS operation in each case.

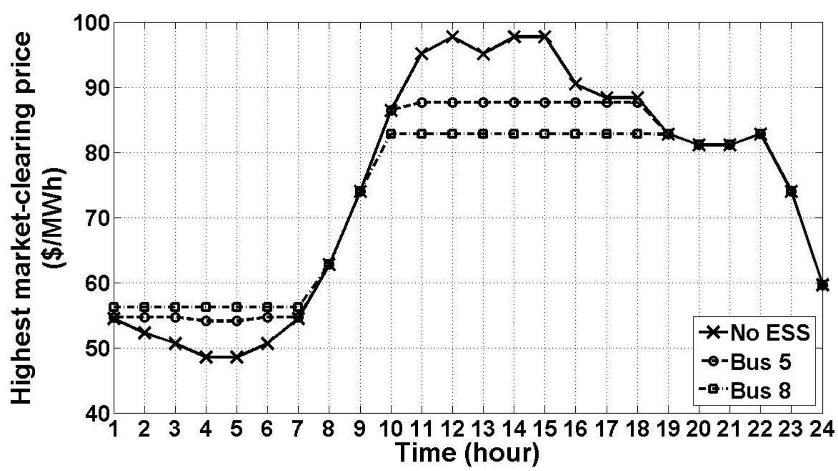

Figure 6-11 Highest market-clearing price (case study 3)

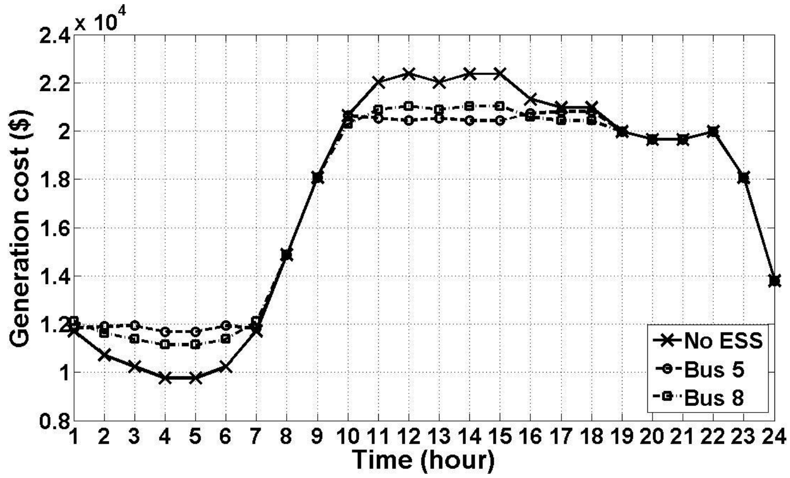

Figure 6-12 Total generation cost (case study 3)

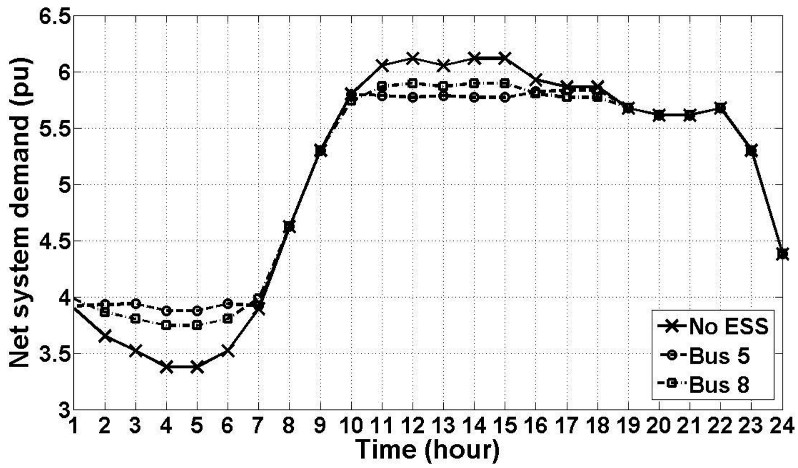

Figure 6-13 Net system demand (case study 3)

Moreover, the impact of energy storage location is further studied during congestion in the system. As an example, congestion in the transmission system is simulated through reducing the power-flow limit of selected lines that are shaded in Table 6-2. Afterwards, the impact of installing the same ESS at buses #5 and #8 is investigated; the highest market-clearing prices and total generation costs are shown in Figure 6-14 and Figure 6-15. As observed, the ESS location has the same impact on the market prices and generation costs even during congestion in the transmission system. This conclusion is explained by noting that the ESS does not stress the system infrastructure since it is charged during off-peak periods, when the lines are lightly loaded, and discharged during peak times, thus relieving the congestion in the system. As shown in Table 6-2, the lines 3-4 and 3-5, for example, were congested before the ESS was installed in the system; however, these congestions are alleviated after connecting the ESS at either bus #5 or bus #8.

Table 6-2 Power flow values during congestion in the system

Line between buses	**Rated power flow (pu)***	**Maximum power flow**		
		No ESS	**ESS at bus 5**	**ESS at bus 8**
1-2	2	1.83	1.81	1.84
1-6	1.7	1.70	1.70	1.70
2-5	1.0	1.00	1.00	1.00
3-4	0.3	0.30	0.23	0.22
3-5	0.55	0.55	0.42	0.40
4-5	0.2	0.01	0.06	0.00
4-6	1.8	0.58	0.56	0.54
6-7	1	0.76	0.74	0.74
7-8	0.9	0.77	0.77	0.71
8-9	0.5	0.31	0.31	0.31
*Base power = 100 MVA				

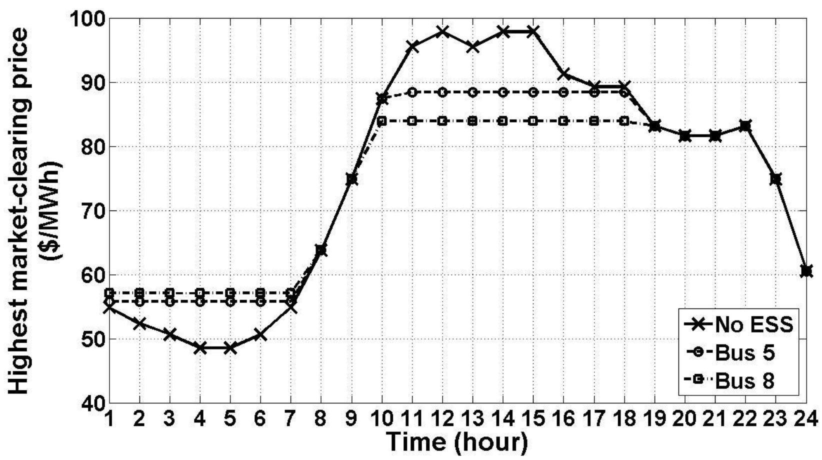

Figure 6-14 Highest market-clearing price (under congestion in the system)

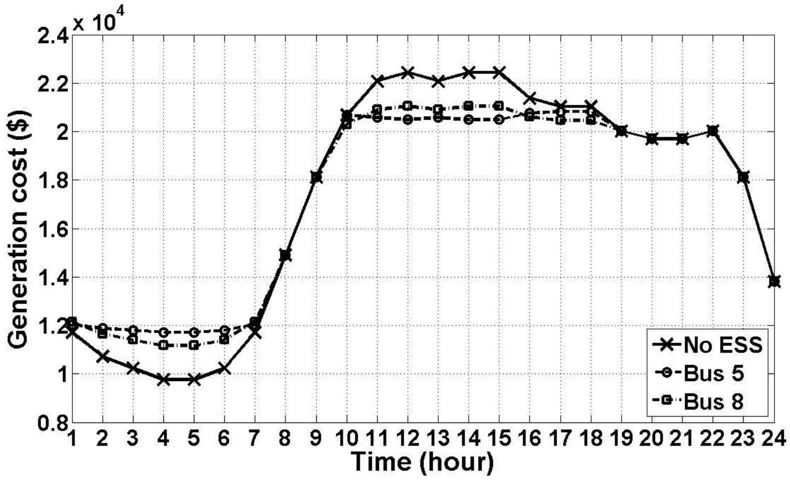

Figure 6-15 Total generation cost (under congestion in the system)

6.4.4 Central vs. distributed storage

This case study investigates the difference between central and distributed implementation of energy storage. The installation of one ESS (60 MW-2 discharge hours) at bus #8 is compared to the installation of three ESSs (each is 20 MW- 2 discharge hours) at buses #7, #8, and #9.

It is shown in Figure 6-16 that the highest market-clearing prices are exactly the same with both implementations since the power losses in the transmission network, constituting the major part of total system losses, are independent of the storage location in the distribution system. However, the arbitrage benefit associated with the distributed storage is found to be slightly higher than that with the central storage case. Therefore, it may be more desirable for the ESS owner to install distributed storage facility than installing central energy storage. Similarly, total generation costs are found to be slightly influenced by central/distributed storage implementation, as shown in Figure 6-17, since the ESS operation is almost the same in both cases.

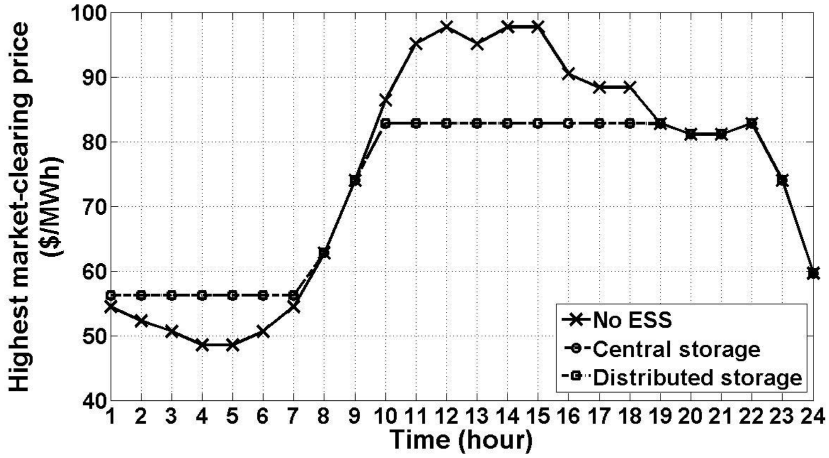

Figure 6-16 Highest market-clearing price (case study 4)

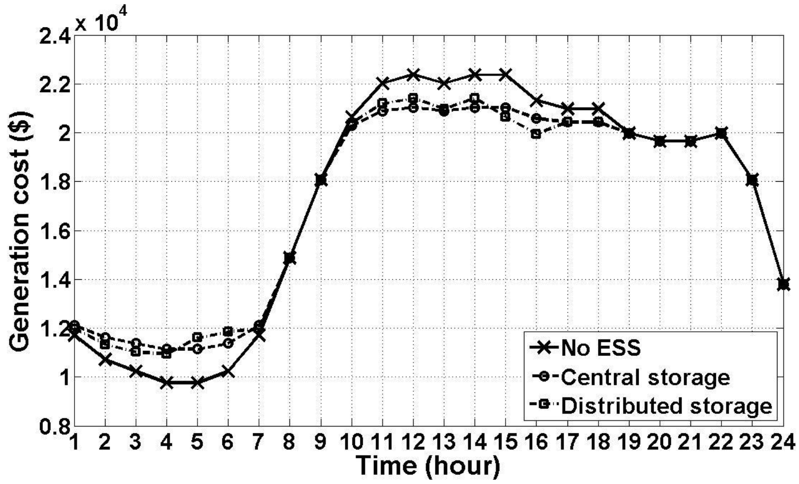

Figure 6-17 Total generation cost (case study 4)

6.5 Conclusions

In this chapter, a mathematical model was developed for determining the optimal operation strategy of ESSs simultaneously with the optimal market prices in a perfectly competitive environment, modified with special incentive pricing for ESSs based on the highest LMP in the system. The problem formulation solves two dependent problems, social welfare and energy storage arbitrage benefit maximization. Moreover, this chapter investigated the impact of energy storage size and location on market price, total generation cost and benefit, arbitrage benefit, and total consumer payments, through several case studies.

Due to ESS operation, the highest market-clearing price became almost leveled during off-peak and peak intervals. The larger the energy storage size, the less difference between off-peak and peak prices. The total generation costs were also affected by the energy storage size; for larger sizes, higher costs were observed during low demand, while lower costs were incurred when the demand is high. With respect to the arbitrage benefit, it increased up to a certain maximum value when it was plotted versus the storage capacity size. Furthermore, consumer payments and generation benefits were reduced with the increase of arbitrage benefit.

Regarding the impact of energy storage location, a higher difference between off-peak and peak prices was noticed in the case of connecting the energy storage to the transmission system compared to the case of installing the same ESS in the distribution system. Thus, the arbitrage benefit was higher in the case of transmission system installation. Therefore, the ESS owner is economically encouraged to install the ESS in the transmission system. Moreover, central and distributed energy storage implementations were compared in this chapter. The results showed that the highest market-clearing price and the generation costs are almost not influenced by central/distributed implementation; however, the arbitrage benefit associated with distributed storage was slightly higher than that found in the case of central storage. As a result, distributed storage may be desirable to be implemented in power systems, from the ESS owner's perspective.

In conclusion, energy storage size and location have a direct impact on electricity-market prices and arbitrage benefit. The conclusions are very useful for power system planners in allocating large-scale ESSs. Moreover, the proposed mathematical model is helpful for power system operators to determine the optimal charging/discharging strategy of ESSs and the optimal market prices in a perfect competition.

Chapter 7 Concluding Remarks

7.1 Summary and Conclusions

In this thesis, a comprehensive planning framework was developed for the allocation of DS units in distribution network. An energy-marked based tool was further proposed for determining the optimal charging/discharging of energy storage as well as the market prices in a perfectly competitive environment. The planning framework was presented in stages through Chapters 3, 4, and 5, whereas the market model was presented in Chapter 6.

As a first step, a mathematical formulation was introduced for the allocation of DS units and load shedding in distribution systems as cost-effective means of improving distribution system reliability. In this formulation, a value-based reliability approach was adopted that includes consideration of customers' WTP as the reliability value benefit of improving system reliability. The formulation introduced was used with several case studies, in Chapter 3, and the results showed that integrating DS units with distribution systems reduces the utilities' annual costs because of their capacity to enable successful islanding and to minimize interruption costs. Moreover, the sensitivity analysis conducted in Chapter 3 proved that the optimal DS allocation and load points to be shed are dependent on the value of the interruption cost.

In the second step, a multi-year planning framework was proposed for ascertaining the most cost-effective siting and sizing of DS units in order to defer system upgrades, reduce energy losses, and take advantage of the arbitrage benefit. The results of this framework were shown to be dependent on the system under study, e.g., type and size of existing DGs, as presented in Chapter 4. Nevertheless, the results showed that integrating DS units with distribution systems reduces the total costs of utilities because of their capacity to shave the peak load. The interesting output of the approach proposed is the optimized operation of DS units at each load state, which allows utilities control the DS units based on the measurement of the system load magnitude only, i.e., without any further utilization of advanced forecasting modules and controllers.

The third step implies combining the mathematical formulations proposed in the previous steps in one comprehensive planning framework, as introduced in Chapter 5. The output of this framework is the sizes and locations of DS units to be installed (planning decisions), the control strategy of those allocated DS units (operational decisions), and the load points to be shed during contingencies (contingency planning decisions).

Finally, a mathematical model was developed for determining the optimal operation strategy of ESSs simultaneously with the optimal market prices in a perfectly competitive environment. This model would replace the conventional market models when large-scale ESSs are integrated into power systems in the future. Moreover, the model developed was used to investigate the impact of energy storage size and location on the market prices and arbitrage benefit. The results showed that energy storage size and location significantly affects the market-clearing prices and arbitrage benefit, as given in Chapter 6.

7.2 Contributions

The main contribution of this thesis is the development of comprehensive planning framework and market model for ESSs as discussed in the previous section. The findings of the work presented in this thesis can be summarized as follows:

- The developed planning framework takes into account all possible islanding scenarios in the allocation of DS units. The planning framework further includes determining contingency planning decisions, i.e., load points to be shed during contingencies, which basically aim to increase the overall probability of successful islanding operation, and thus to minimize the total interruption cost.
- A probabilistic approach is adopted in order to consider the uncertainty of system components, unlike the previous studies that applied time-series patterns for optimizing the size of DS units. In the probabilistic approach, the available historical data of the system components are used to derive a probabilistic model, for each component, that incorporates certain number of states along with their associated probabilities. This probabilistic representation allowed determining the control strategy of DS units, in the form of a look-up table, as an output from the planning framework.
- A novel comprehensive planning framework is developed in this thesis that takes into account several benefits for distribution companies (i.e., improving system reliability, deferring system upgrades, reducing energy losses, and taking advantage of the price arbitrage during peak and off-peak times).
- A new electricity-market model is developed for determining the optimal operation of ESSs simultaneously with the market-clearing price. The model is based on MCP formulation that combines the KKT conditions of dependent optimization problems.

7.3 Directions for Future Research

The following studies can be conducted as an extension to the work presented in this thesis:

- Assessing the cost effectiveness of using ESSs for mitigating power quality issues. The utility statistics of power quality events and the monetary value associated with the interruption or damage caused by these events will be necessary for conducting this study.
- Investigating the challenges and economics of ESSs for demand management in remote communities. These communities are usually characterized with high variability in the power demand and high-penetration levels of renewable sources integrated into the system.
- Developing a multiagent system for the coordinated energy management of DERs and plug-in electric vehicles (PEVs) in smart microgrids. In this context, ESSs will play an important role in matching the characteristics of both RESs and PEVs without imposing on the distribution network infrastructure. That is to charge the ESS when there is a generation surplus from the RESs, and to disseminate the energy stored when PEVs need to be charged during peak times.

Appendix A The 34-bus system data

Table A-1 Feeder and load data [72]

Line number	Sending bus	Receiving bus	Resistance (Ω)	Reactance (Ω)	Rated load at receiving end		Rated power flow of the line (MVA)
					Active power (kW)	Reactive power (kVAR)	
1	1	2	0.0922	0.0477	100.00	60.00	4.50
2	2	3	0.4930	0.2511	90.00	40.00	3.84
4	3	4	0.3660	0.1864	120.00	80.00	3.18
6	4	5	0.3811	0.1941	60.00	30.00	3.18
7	5	6	0.8190	0.7070	60.00	20.00	3.18
8	6	7	0.1872	0.6188	200.00	100.00	3.18
10	7	8	1.7114	1.2351	200.00	100.00	3.18
11	8	9	1.0300	0.7400	60.00	20.00	3.18
12	9	10	1.0400	0.7400	60.00	20.00	3.18
13	10	11	0.1966	0.0650	45.00	30.00	3.18
14	11	12	0.3744	0.1238	60.00	35.00	3.18
15	12	13	1.4680	1.1550	60.00	35.00	3.18
16	13	14	0.5416	0.7129	120.00	80.00	3.18
17	14	15	0.5910	0.5260	60.00	10.00	3.18
18	15	16	0.7463	0.5450	60.00	20.00	3.18
19	16	17	1.2890	1.7210	60.00	20.00	3.18
20	17	18	0.7320	0.5740	90.00	40.00	3.18
3	2	19	0.1640	0.1565	90.00	40.00	3.18
21	19	20	1.5042	1.3554	90.00	40.00	3.18
22	20	21	0.4095	0.4784	90.00	40.00	3.18
23	21	22	0.7089	0.9373	90.00	40.00	3.18
5	3	23	0.4512	0.3083	90.00	50.00	3.18
24	23	24	0.8980	0.7091	420.00	200.00	3.18
25	24	25	0.8960	0.7011	420.00	200.00	3.18
9	6	26	0.2030	0.1034	60.00	25.00	3.18
26	26	27	0.2842	0.1447	60.00	25.00	3.18
27	27	28	1.0590	0.9337	60.00	20.00	3.18
28	28	29	0.8042	0.7006	120.00	70.00	3.18
29	29	30	0.5075	0.2585	200.00	100.00	3.18
30	30	31	0.9744	0.9630	150.00	70.00	3.18
31	31	32	0.3105	0.3619	210.00	100.00	3.18
32	32	33	0.3410	0.5302	60.00	40.00	3.18

Appendix B The MCP model of Chapter 6

KKT conditions can be derived by taking derivatives of Lagrangian functions $\left(\mathcal{L}_1,\, \mathcal{L}_2, \text{ and } \mathcal{L}_3\right)$ that correspond to F_1, F_2, and F_3, respectively, with respect to the primal variables and the Lagrangian multipliers (dual variables) associated with equality constraints, and setting those derivatives equal to zero. KKT conditions further include the complementarity conditions associated with inequality constraints and their dual variables. The complete MCP model is then given as follows:

$$\frac{\partial \mathcal{L}_1}{\partial P_{g_{i,hr}}}:\quad 2\alpha_i \times P_{g_{i,hr}} + \beta_i - \lambda_{i,hr} - aa_{i,hr} + bb_{i,hr} = 0 \qquad \forall i \in \mathcal{G}, hr \tag{B.1}$$

$$\frac{\partial \mathcal{L}_1}{\partial Q_{g_{i,hr}}}:\quad -\mu_{i,hr} - cc_{i,hr} + dd_{i,hr} = 0 \qquad \forall i \in \mathcal{G}, hr \tag{B.2}$$

$$\begin{aligned}
&\frac{\partial \mathcal{L}_1}{\partial V_{i,hr}}:\quad \lambda_{i,hr}\sum_{j=1}^{N}\left\{V_{j,hr}\times\begin{pmatrix}G_{ij}\cos\delta_{ij,hr}+\\ B_{ij}\sin\delta_{ij,hr}\end{pmatrix}\right\}+\sum_{j=1}^{N}\left\{\begin{matrix}\lambda_{j,hr}\times V_{j,hr}\times\\ \begin{pmatrix}G_{ij}\cos\delta_{ij,hr}-\\ B_{ij}\sin\delta_{ij,hr}\end{pmatrix}\end{matrix}\right\}+\\
&\mu_{i,hr}\sum_{j=1}^{N}\left\{\begin{matrix}V_{j,hr}\times\\ \begin{pmatrix}G_{ij}\sin\delta_{ij,hr}-\\ B_{ij}\cos\delta_{ij,hr}\end{pmatrix}\end{matrix}\right\}+\sum_{j=1}^{N}\left\{\begin{matrix}\mu_{j,hr}\times V_{j,hr}\times\\ \begin{pmatrix}-G_{ij}\sin\delta_{ij,hr}-\\ B_{ij}\cos\delta_{ij,hr}\end{pmatrix}\end{matrix}\right\}+\sum_{\substack{j=1\\ j\neq i}}^{N}\left\{\begin{matrix}ww_{ji,hr}\times V_{j,hr}\times\\ \begin{pmatrix}G_{ij}\cos\delta_{ij,hr}-\\ B_{ij}\sin\delta_{ij,hr}\end{pmatrix}\end{matrix}\right\}+\\
&\sum_{\substack{j=1\\ j\neq i}}^{N}\left\{ww_{ij,hr}\times\begin{pmatrix}-2G_{ij}\times V_{i,hr}+V_{j,hr}\times\\ \begin{pmatrix}G_{ij}\cos\delta_{ij,hr}+\\ B_{ij}\sin\delta_{ij,hr}\end{pmatrix}\end{pmatrix}\right\}-ee_{i,hr}+ff_{i,hr}=0 \qquad \forall i\notin\mathcal{G}, hr
\end{aligned} \tag{B.3}$$

$$\frac{\partial \mathcal{L}_1}{\partial V_{i,hr}}: \quad \lambda_{i,hr}\sum_{j=1}^{N}\left\{V_{j,hr}\times\begin{pmatrix}G_{ij}\cos\delta_{ij,hr}+\\ B_{ij}\sin\delta_{ij,hr}\end{pmatrix}\right\}+\sum_{j=1}^{N}\left\{\begin{matrix}\lambda_{j,hr}\times V_{j,hr}\times\\ \begin{pmatrix}G_{ij}\cos\delta_{ij,hr}-\\ B_{ij}\sin\delta_{ij,hr}\end{pmatrix}\end{matrix}\right\}+$$

$$\mu_{i,hr}\sum_{j=1}^{N}\left\{\begin{matrix}V_{j,hr}\times\\ \begin{pmatrix}G_{ij}\sin\delta_{ij,hr}-\\ B_{ij}\cos\delta_{ij,hr}\end{pmatrix}\end{matrix}\right\}+\sum_{j=1}^{N}\left\{\begin{matrix}\mu_{j,hr}\times V_{j,hr}\times\\ \begin{pmatrix}-G_{ij}\sin\delta_{ij,hr}-\\ B_{ij}\cos\delta_{ij,hr}\end{pmatrix}\end{matrix}\right\}+\sum_{\substack{j=1\\ j\neq i}}^{N}\left\{\begin{matrix}ww_{ji,hr}\times V_{j,hr}\times\\ \begin{pmatrix}G_{ij}\cos\delta_{ij,hr}-\\ B_{ij}\sin\delta_{ij,hr}\end{pmatrix}\end{matrix}\right\}+$$

$$\sum_{\substack{j=1\\ j\neq i}}^{N}\left\{ww_{ij,hr}\times\begin{pmatrix}-2G_{ij}\times V_{i,hr}+V_{j,hr}\times\\ \begin{pmatrix}G_{ij}\cos\delta_{ij,hr}+\\ B_{ij}\sin\delta_{ij,hr}\end{pmatrix}\end{pmatrix}\right\}+gg_{i,hr}=0 \qquad \forall i\in\mathcal{G},hr \tag{B.4}$$

$$\frac{\partial \mathcal{L}_1}{\partial \delta_{i,hr}}: \quad V_{i,hr}\times\left[\lambda_{i,hr}\sum_{j=1}^{N}\left\{\begin{matrix}V_{j,hr}\times\\ \begin{pmatrix}-G_{ij}\sin\delta_{ij,hr}+\\ B_{ij}\cos\delta_{ij,hr}\end{pmatrix}\end{matrix}\right\}+\sum_{j=1}^{N}\left\{\begin{matrix}\lambda_{j,hr}\times V_{j,hr}\times\\ \begin{pmatrix}-G_{ij}\sin\delta_{ij,hr}\\ -B_{ij}\cos\delta_{ij,hr}\end{pmatrix}\end{matrix}\right\}+\right.$$

$$\mu_{i,hr}\sum_{j=1}^{N}\left\{\begin{matrix}V_{j,hr}\times\\ \begin{pmatrix}G_{ij}\cos\delta_{ij,hr}+\\ B_{ij}\sin\delta_{ij,hr}\end{pmatrix}\end{matrix}\right\}+\sum_{j=1}^{N}\left\{\begin{matrix}\mu_{j,hr}\times V_{j,hr}\times\\ \begin{pmatrix}-G_{ij}\cos\delta_{ij,hr}+\\ B_{ij}\sin\delta_{ij,hr}\end{pmatrix}\end{matrix}\right\}+\sum_{\substack{j=1\\ j\neq i}}^{N}\left\{\begin{matrix}ww_{ij,hr}\times V_{j,hr}\times\\ \begin{pmatrix}-G_{ij}\sin\delta_{ij,hr}+\\ B_{ij}\cos\delta_{ij,hr}\end{pmatrix}\end{matrix}\right\}+$$

$$\left.\sum_{\substack{j=1\\ j\neq i}}^{N}\left\{\begin{matrix}ww_{ji,hr}\times V_{j,hr}\times\\ \begin{pmatrix}-G_{ij}\sin\delta_{ij,hr}-\\ B_{ij}\cos\delta_{ij,hr}\end{pmatrix}\end{matrix}\right\}\right]-kk_{i,hr}+ll_{i,hr}=0 \qquad \forall i,hr \tag{B.5}$$

$$\frac{\partial \mathcal{L}_1}{\partial \lambda_{i,hr}}: \quad \sum_{j=1}^{N}\left\{V_{i,hr}\times V_{j,hr}\times\begin{pmatrix}G_{ij}\cos\delta_{ij,hr}+\\ B_{ij}\sin\delta_{ij,hr}\end{pmatrix}\right\}-P_{g_{i,hr}}+P_{D_{i,hr}}+$$

$$P_{ESS_{i,hr}}^{ch}-P_{ESS_{i,hr}}^{dis}=0 \qquad \forall i,hr \tag{B.6}$$

$$\frac{\partial \mathcal{L}_1}{\partial \mu_{i,hr}}: \quad \sum_{j=1}^{N}\left\{V_{i,hr}\times V_{j,hr}\times\begin{pmatrix}G_{ij}\sin\delta_{ij,hr}-\\ B_{ij}\cos\delta_{ij,hr}\end{pmatrix}\right\}-Q_{g_{i,hr}}+Q_{D_{i,hr}}=0 \qquad \forall i,hr \tag{B.7}$$

$$\frac{\partial \mathcal{L}_1}{\partial gg_{i,hr}}: \quad V_{i,hr}=\text{constant} \qquad \forall i\in\mathcal{G},hr \tag{B.8}$$

$$\frac{\partial \mathcal{L}_2}{\partial \Lambda_{hr}}: \quad \sum_{i=1}^{N} mm_{i,hr} = 1 \qquad \forall hr \tag{B.9}$$

$$\frac{\partial \mathcal{L}_3}{\partial P^{ch}_{ESS\,i,hr}}: \quad C_O + \Lambda_{hr} - nn_{i,hr} \times \eta^{ch}_{ESS} - oo_{i,hr} + pp_{i,hr} = 0 \qquad \forall i \in \mathcal{E}, hr \tag{B.10}$$

$$\frac{\partial \mathcal{L}_3}{\partial P^{dis}_{ESS\,i,hr}}: \quad C_O - \Lambda_{hr} + nn_{i,hr} / \eta^{dis}_{ESS} - qq_{i,hr} + rr_{i,hr} = 0 \qquad \forall i \in \mathcal{E}, hr \tag{B.11}$$

$$\frac{\partial \mathcal{L}_3}{\partial E_{ESS\,i,hr}}: \quad nn_{i,hr} - nn_{i,hr+1} - ss_{i,hr} + tt_{i,hr} = 0 \qquad \forall i \in \mathcal{E}, hr \tag{B.12}$$

$$\frac{\partial \mathcal{L}_3}{\partial nn_{i,hr}}: \quad E_{ESS_{i,hr}} - E_{ESS_{i,hr-1}} - \eta^{ch}_{ESS} \times P^{ch}_{ESS\,i,hr} + P^{dis}_{ESS\,i,hr} / \eta^{dis}_{ESS} = 0 \qquad \forall i \in \mathcal{E}, hr \tag{B.13}$$

$$0 \le P^{\max}_{flow_{ij}} - P_{flow_{ij,hr}} \perp ww_{ij,hr} \ge 0 \qquad \forall i \ne j, hr \tag{B.14}$$

$$0 \le P_{g_{i,hr}} - P_{g_{i,min}} \perp aa_{i,hr} \ge 0 \qquad \forall i \in \mathcal{G}, hr \tag{B.15}$$

$$0 \le P_{g_{i,\max}} - P_{g_{i,hr}} \perp bb_{i,hr} \ge 0 \qquad \forall i \in \mathcal{G}, hr \tag{B.16}$$

$$0 \le Q_{g_{i,hr}} - Q_{g_{i,min}} \perp cc_{i,hr} \ge 0 \qquad \forall i \in \mathcal{G}, hr \tag{B.17}$$

$$0 \le Q_{g_{i,\max}} - Q_{g_{i,hr}} \perp dd_{i,hr} \ge 0 \qquad \forall i \in \mathcal{G}, hr \tag{B.18}$$

$$0 \le V_{i,hr} - V_{min} \perp ee_{i,hr} \ge 0 \qquad \forall i \notin \mathcal{G}, hr \tag{B.19}$$

$$0 \le V_{max} - V_{i,hr} \perp ff_{i,hr} \ge 0 \qquad \forall i \notin \mathcal{G}, hr \tag{B.20}$$

$$0 \le \delta_{i,hr} + \pi \perp kk_{i,hr} \ge 0 \qquad \forall i, hr \tag{B.21}$$

$$0 \le \pi - \delta_{i,hr} \perp ll_{i,hr} \ge 0 \qquad \forall i, hr \tag{B.22}$$

$$0 \le \Lambda_{hr} - \lambda_{i,hr} \perp mm_{i,hr} \ge 0 \qquad \forall i, hr \tag{B.23}$$

$$0 \le P^{ch}_{ESS\,i,hr} \perp oo_{i,hr} \ge 0 \qquad \forall i \in \mathcal{E}, hr \tag{B.24}$$

$$0 \le P_{ESS_{i,rated}} - P^{ch}_{ESS\,i,hr} \perp pp_{i,hr} \ge 0 \qquad \forall i \in \mathcal{E}, hr \tag{B.25}$$

$$0 \le P^{dis}_{ESS\,i,hr} \perp qq_{i,hr} \ge 0 \qquad \forall i \in \mathcal{E}, hr \tag{B.26}$$

$$0 \le P_{ESS_{i,rated}} - P^{dis}_{ESS\,i,hr} \perp rr_{i,hr} \ge 0 \qquad \forall i \in \mathcal{E}, hr \tag{B.27}$$

$$0 \le E_{ESS_{i,hr}} \perp ss_{i,hr} \ge 0 \qquad \forall i \in \mathcal{E}, hr \tag{B.28}$$

$$0 \le E_{ESS_{i,rated}} - E_{ESS_{i,hr}} \perp tt_{i,hr} \ge 0 \qquad \forall i \in \mathcal{E}, hr \tag{B.29}$$

Appendix C The 9-bus system data

Table C.1 Network data

Line between buses	Resistance (pu)	Reactance (pu)
1-2	0.0210	0.1097
1-6	0.0824	0.2732
2-5	0.1070	0.3185
3-4	0.0945	0.2987
3-5	0.0662	0.1804
4-5	0.0639	0.1792
4-6	0.0340	0.0980
6-7	0.0000	0.1000
7-8	0.0540	0.0820
8-9	0.0540	0.0820

Table C.2 Generation and load data

Bus	α_i (\$/MWh^2)	β_i (\$/MWh)	Υ_i (\$/h)	$P_{g,min}$ (pu)*	$P_{g,max}$ (pu)*	$Q_{g,min}$ (pu)*	$Q_{g,max}$ (pu)*	P_d (pu)*	Q_d (pu)*
1	0.01	25.5	9	1	5	-0.2	3	0.92	0.29
2	0	0	0	0	0	0	0	0.78	0.39
3	0.05	8.5	5	0.5	2.5	-0.2	3	0.73	0.19
4	0	0	0	0	0	0	0	0.67	0.24
5	0	0	0	0	0	0	0	1.12	0.31
6	0	0	0	0	0	0	0	0.26	0.12
7	0	0	0	0	0	0	0	0.2	0.05
8	0	0	0	0	0	0	0	0.4	0.2
9	0	0	0	0	0	0	0	0.3	0.13
* Base power = 100 MVA									

Appendix D The 14-bus system data

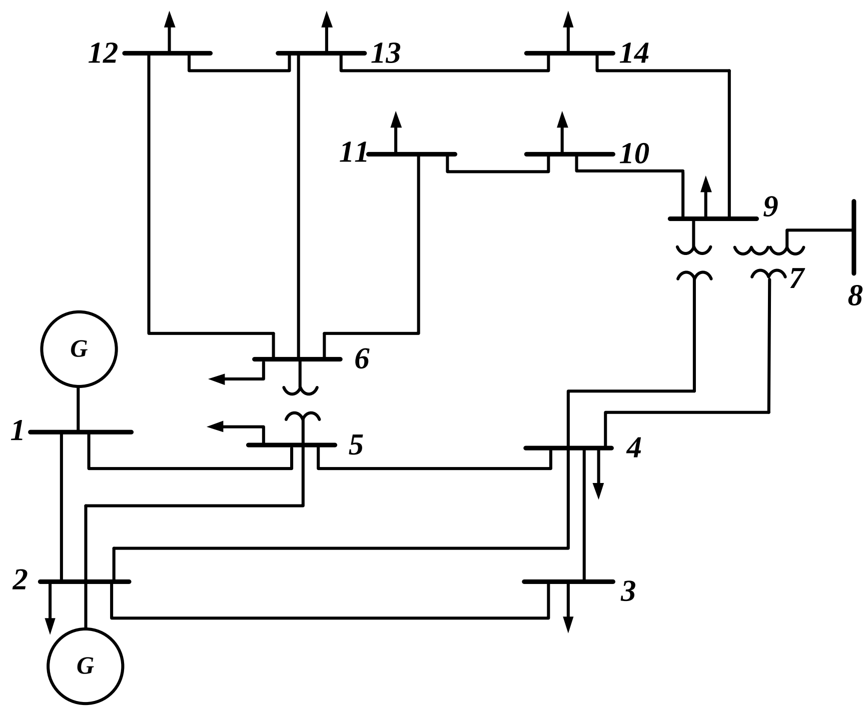

Figure D.1 IEEE 14-bus system layout

Table D.1 Network data

Line between buses	Resistance (pu)	Reactance (pu)	Line between buses	Resistance (pu)	Reactance (pu)
1-2	0.0194	0.0592	6-11	0.0950	0.1989
1-5	0.0540	0.2230	6-12	0.1229	0.2558
2-3	0.0470	0.1980	6-13	0.0662	0.1303
2-4	0.0581	0.1763	7-8	0.0000	0.1762
2-5	0.0570	0.1739	7-9	0.0000	0.1100
3-4	0.0670	0.1710	9-10	0.0318	0.0845
4-5	0.0134	0.0421	9-14	0.1271	0.2704
4-7	0.0000	0.2091	10-11	0.0821	0.1921
4-9	0.0000	0.5562	12-13	0.2209	0.1999
5-6	0.0000	0.2520	13-14	0.1709	0.3480

Table D.2 Generation and load data

Bus	**α_i (\$/MWh^2)**	**β_i (\$/MWh)**	**γ_i (\$/h)**	**$P_{g,min}$ (pu)***	**$P_{g,max}$ (pu)***	**$Q_{g,min}$ (pu)***	**$Q_{g,max}$ (pu)***	**P_d (pu)***	**Q_d (pu)***
1	0.01	25.5	9	1.2	6	-0.2	1	0	0
2	0.05	8.5	5	0.1	0.45	-0.2	0.50	0.217	0.127
3	0	0	0	0	0	0	0	0.942	0.19
4	0	0	0	0	0	0	0	0.478	0
5	0	0	0	0	0	0	0	0.076	0.016
6	0	0	0	0	0	0	0	0.112	0.075
7	0	0	0	0	0	0	0	0	0
8	0	0	0	0	0	0	0	0	0
9	0	0	0	0	0	0	0	0.295	0.166
10	0	0	0	0	0	0	0	0.09	0.058
11	0	0	0	0	0	0	0	0.035	0.018
12	0	0	0	0	0	0	0	0.061	0.016
13	0	0	0	0	0	0	0	0.135	0.058
14	0	0	0	0	0	0	0	0.149	0.05
* Base power = 100 MVA									

Appendix E The 30-bus system data

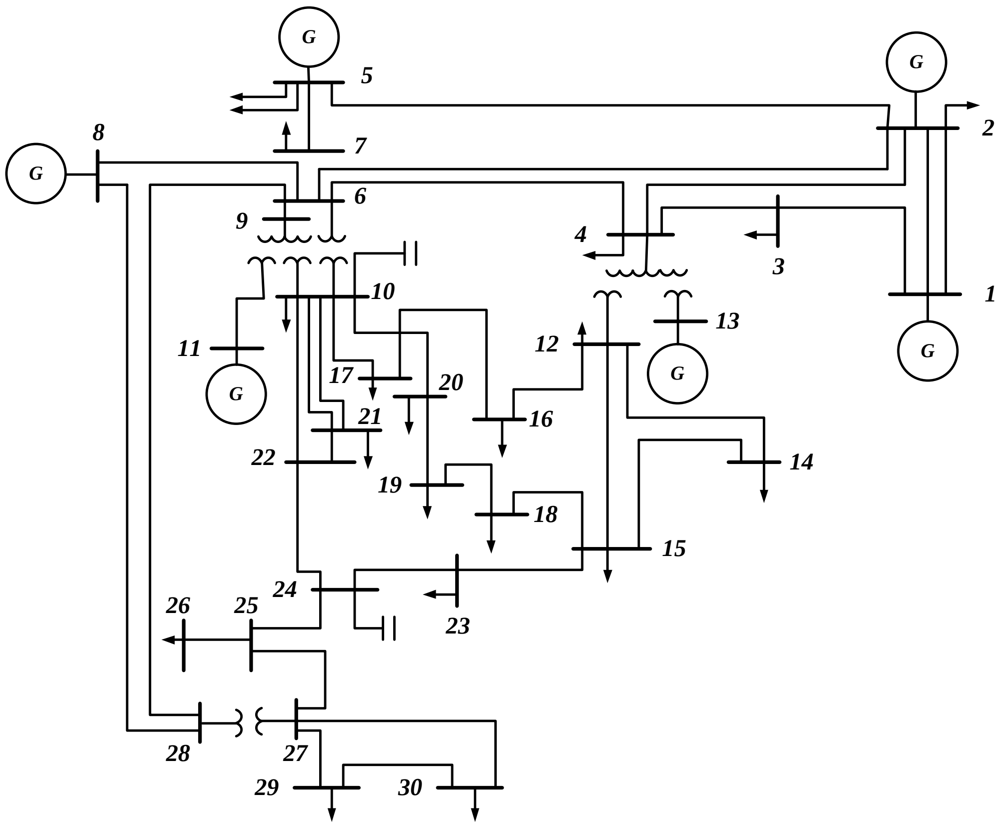

Figure E.1 IEEE 30-bus system layout

Table E.1 Network data

Line between buses	**Resistance (pu)**	**Reactance (pu)**	**Line between buses**	**Resistance (pu)**	**Reactance (pu)**
1-2	0.0192	0.0575	15-18	0.1070	0.2185
1-3	0.0452	0.1852	18-19	0.0639	0.1292
2-4	0.0570	0.1737	19-20	0.0340	0.0680
3-4	0.0132	0.0379	10-20	0.0936	0.2090
2-5	0.0472	0.1983	10-17	0.0324	0.0845
2-6	0.0581	0.1763	10-21	0.0348	0.0749
4-6	0.0119	0.0414	10-22	0.0727	0.1499
5-7	0.0460	0.1160	21-22	0.0116	0.0236
6-7	0.0267	0.0820	15-23	0.1000	0.2020
6-8	0.0120	0.0142	22-24	0.1150	0.1790
6-9	0.0000	0.2080	23-24	0.1320	0.2700
6-10	0.0000	0.5560	24-25	0.1885	0.3292
9-11	0.0000	0.2080	25-26	0.2544	0.3800
9-10	0.0000	0.1100	25-27	0.1093	0.2087
4-12	0.0000	0.2560	28-27	0.0000	0.3960
12-13	0.0000	0.1400	27-29	0.2198	0.4153
12-14	0.1231	0.2559	27-30	0.3202	0.6027
12-15	0.0662	0.1304	29-30	0.2399	0.4533
12-16	0.0945	0.1987	8-28	0.0636	0.2000
14-15	0.2210	0.1997	6-28	0.0169	0.0599
16-17	0.0824	0.1932			

Table E.2 Generation and load data

Bus	α_i **(\$/MWh^2)**	β_i **(\$/MWh)**	γ_i **(\$/h)**	$P_{g,min}$ **(pu)***	$P_{g,max}$ **(pu)***	$Q_{g,min}$ **(pu)***	$Q_{g,max}$ **(pu)***	P_d **(pu)***	Q_d **(pu)***
1	0.00375	2	1	0.5	2	-0.4	2.5	0	0
2	0.0175	1.75	2	0.2	0.8	-0.2	1	0.217	0.127
3	0	0	0	0	0	0	0	0.024	0.012
4	0	0	0	0	0	0	0	0.076	0.016
5	0.0625	1	0	0.15	0.5	-0.1	0.8	0.942	0.19
6	0	0	0	0	0	0	0	0	0
7	0	0	0	0	0	0	0	0.228	0.109
8	0.00834	3.25	4	0.1	0.35	-0.1	0.6	0.3	0.3
9	0	0	0	0	0	0	0	0	0
10	0	0	0	0	0	0	0	0.058	0.02
11	0.025	3	4	0.1	0.3	-0.1	0.5	0	0
12	0	0	0	0	0	0	0	0.112	0.075
13	0.025	3	4	0.12	0.4	-0.1	0.6	0	0
14	0	0	0	0	0	0	0	0.062	0.016
15	0	0	0	0	0	0	0	0.082	0.025
16	0	0	0	0	0	0	0	0.035	0.018
17	0	0	0	0	0	0	0	0.09	0.058
18	0	0	0	0	0	0	0	0.032	0.009
19	0	0	0	0	0	0	0	0.095	0.034
20	0	0	0	0	0	0	0	0.022	0.007
21	0	0	0	0	0	0	0	0.175	0.112
22	0	0	0	0	0	0	0	0	0
23	0	0	0	0	0	0	0	0.032	0.016
24	0	0	0	0	0	0	0	0.087	0.067
25	0	0	0	0	0	0	0	0	0
26	0	0	0	0	0	0	0	0.035	0.023
27	0	0	0	0	0	0	0	0	0
28	0	0	0	0	0	0	0	0	0
29	0	0	0	0	0	0	0	0.024	0.009
30	0	0	0	0	0	0	0	0.106	0.019

* Base power = 100 MVA

Appendix F The summer load profile of IEEE-RTS

Table F.1 Load demand at every hour as percentage of the peak load

Hour	Load demand	Hour	Load demand
12-1 AM	0.64	12-1	0.99
1-2	0.60	1-2	1.00
2-3	0.58	2-3	1.00
3-4	0.56	3-4	0.97
4-5	0.56	4-5	0.96
5-6	0.58	5-6	0.96
6-7	0.64	6-7	0.93
7-8	0.76	7-8	0.92
8-9	0.87	8-9	0.92
9-10	0.95	9-10	0.93
10-11	0.99	10-11	0.87
11-12 PM	1.00	11-12	0.72

Bibliography

[1] A. Ipakchi and F. Albuyeh, "Grid of the future," *IEEE Power and Energy Magazine*, vol. 7, no. 2, pp. 52-62, Mar.-Apr. 2009.

[2] K. Moslehi and R. Kumar, "A Reliability Perspective of the Smart Grid," *IEEE Transactions on Smart Grid*, vol. 1, no. 1, pp. 57-64, Jun. 2010.

[3] J. Eyer and G. Corey, "Energy Storage for the Electricity Grid: Benefits and Market Potential Assessment Guide," *Prepared by Sandia National Laboratories*, February 2010.

[4] H. Ibrahim, A. Ilinca, and J. Perron, "Energy storage systems—Characteristics and comparisons," *Renewable and Sustainable Energy Reviews*, vol. 12, no. 5, pp. 1221-1250, 2008.

[5] *Field battery energy storage project*, Available: https://www.bchydro.com/energy-in-bc/projects/field-battery.html

[6] (2013). *Introducing the first urban community energy storage project*, Available: http://www.torontohydro.com/sites/electricsystem/powerup/Pages/CommunityEnergyStorage.aspx

[7] (2014). *Ontario's long-term energy plan*, Available: http://www.energy.gov.on.ca/en/ltep/#.UzywOqj1mE4

[8] B. P. Roberts, "Deploying battery energy storage in the utility distribution grid," in *IEEE Power and Energy Society General Meeting*, pp. 1-2, 25-29 Jul. 2010.

[9] (2013). *California's First-in-Nation Energy Storage Mandate*, Available: http://spectrum.ieee.org/energywise/energy/renewables/californias-firstinnation-energy-storage-mandate

[10] MHC, "Energy Storage in Australia," report submitted to Clean Energy Council, Nov. 2012.

[11] S. Schoenung and C. Burns, "Utility energy storage applications studies," *IEEE Transactions on Energy Conversion*, vol. 11, no. 3, pp. 658-665, Sep. 1996.

[12] I. Hadjipaschalis, A. Poullikkas, and V. Efthimiou, "Overview of current and future energy storage technologies for electric power applications," *Renewable and Sustainable Energy Reviews*, vol. 13, no. 6–7, pp. 1513-1522, 2009.

[13] S. S. Choi, K. J. Tseng, D. M. Vilathgamuwa, and T. D. Nguyen, "Energy storage systems in distributed generation schemes," in *IEEE Power and Energy Society General Meeting*, pp. 1-8, 20-24 Jul. 2008.

[14] T. Sels, C. Dragu, T. Van Craenenbroeck, and R. Belmans, "Overview of new energy storage systems for an improved power quality and load managing on distribution level," in *16th International Conference and Exhibition on Electricity Distribution*, p. 5 pp. vol.4, 18-21 Jun. 2001.

[15] R. B. Schainker, "Executive overview: energy storage options for a sustainable energy future," in *IEEE Power Engineering Society General Meeting*, pp. 2309-2314 Vol.2, 10 Jun. 2004.

[16] J. D. Boyes and N. H. Clark, "Technologies for energy storage. Flywheels and super conducting magnetic energy storage," in *IEEE Power Engineering Society Summer Meeting*, pp. 1548-1550 vol. 3, 16-20 Jul. 2000.

[17] S. C. Smith, P. K. Sen, and B. Kroposki, "Advancement of energy storage devices and applications in electrical power system," in *IEEE Power and Energy Society General Meeting*, pp. 1-8, 20-24 Jul. 2008.

[18] Y. Bo, Y. Makarov, J. Desteese, V. Viswanathan, P. Nyeng, B. McManus, and J. Pease, "On the use of energy storage technologies for regulation services in electric power systems with

significant penetration of wind energy," in *5th International Conference on European Electricity Market*, pp. 1-6, 28-30 May 2008.

[19] M. H. Ali, W. Bin, and R. A. Dougal, "An Overview of SMES Applications in Power and Energy Systems," *IEEE Transactions on Sustainable Energy,* vol. 1, no. 1, pp. 38-47, Apr. 2010.

[20] M. A. Guerrero, E. Romero, F. Barrero, M. I. Milanes, and E. Gonzalez, "Overview of medium scale energy storage systems," in *Compatibility and Power Electronics*, pp. 93-100, May 2009.

[21] R. Hooshmand and M. Moazzami, "Optimal design of adaptive under frequency load shedding using artificial neural networks in isolated power system," *International Journal of Electrical Power & Energy Systems,* vol. 42, no. 1, pp. 220-228, Nov. 2012.

[22] "IEEE Guide for Design, Operation, and Integration of Distributed Resource Island Systems with Electric Power Systems", IEEE Std. 1547.4-2011, pp. 1-54, 2011

[23] A. Pregelj, M. Begovic, and A. Rohatgi, "Recloser allocation for improved reliability of DG-enhanced distribution networks," *IEEE Transactions on Power Systems*, vol. 21, no. 3, pp. 1442-1449, Aug. 2006.

[24] B. Banerjee and S. M. Islam, "Reliability based optimum location of distributed generation," *International Journal of Electrical Power & Energy Systems,* vol. 33, no. 8, pp. 1470-1478, Oct. 2011.

[25] C. L. T. Borges and D. M. Falcão, "Optimal distributed generation allocation for reliability, losses, and voltage improvement," *International Journal of Electrical Power & Energy Systems,* vol. 28, no. 6, pp. 413-420, Jul. 2006.

[26] M. F. Shaaban, Y. M. Atwa, and E. El-Saadany, "DG Allocation for Benefit Maximization in Distribution Networks," *IEEE Transactions on Power Systems,* vol. 28, no. 2, pp. 639-649, May 2013.

[27] Y. M. Atwa and E. F. El-Saadany, "Reliability evaluation for distribution system with renewable distributed generation during islanded mode of operation," *IEEE Transactions on Power Systems*, vol. 24, no. 2, pp. 572-581, May 2009.

[28] W. R. Lachs and D. Sutanto, "Battery storage plant within large load centres," *IEEE Transactions on Power Systems,* vol. 7, no. 2, pp. 762-767, May 1992.

[29] D. Aming, A. Rajapakse, T. Molinski, and E. Innes, "A Technique for Evaluating the Reliability Improvement Due to Energy Storage Systems," in *Canadian Conference on Electrical and Computer Engineering*, pp. 413-416, 22-26 Apr. 2007.

[30] J. Mitra, "Reliability-Based Sizing of Backup Storage," *IEEE Transactions on Power Systems*, vol. 25, no. 2, pp. 1198-1199, May 2010.

[31] X. Yixing and C. Singh, "Distribution systems reliability and economic improvement with different electric energy storage control strategies," in *IEEE Power and Energy Society General Meeting,* Detroit, Michigan, USA, pp. 1-8, 26-28 Jul. 2011.

[32] X. Yixing and C. Singh, "Adequacy and Economy Analysis of Distribution Systems Integrated With Electric Energy Storage and Renewable Energy Resources," *IEEE Transactions on Power Systems*, vol. 27, no. 4, pp. 2332-2341, Nov. 2012.

[33] S. A. Arefifar, Y. A. I. Mohamed, and T. H. M. El-Fouly, "Supply-Adequacy-Based Optimal Construction of Microgrids in Smart Distribution Systems," *IEEE Transactions on Smart Grid,* vol. 3, no. 3, pp. 1491-1502, Sept. 2012.

[34] F. A. Chacra, P. Bastard, G. Fleury, and R. Clavreul, "Impact of energy storage costs on economical performance in a distribution substation," *IEEE Transactions on Power Systems,* vol. 20, no. 2, pp. 684-691, May 2005.

[35] R.-C. Leou, "An economic analysis model for the energy storage system applied to a distribution substation," *International Journal of Electrical Power & Energy Systems,* vol. 34, no. 1, pp. 132-137, Jan. 2012.
[36] T. K. A. Brekken, A. Yokochi, A. Von Jouanne, Z. Z. Yen, H. M. Hapke, and D. A. Halamay, "Optimal Energy Storage Sizing and Control for Wind Power Applications," *IEEE Transactions on Sustainable Energy,* vol. 2, no. 1, pp. 69-77, Jan. 2011.
[37] Y. M. Atwa and E. F. El-Saadany, "Optimal Allocation of ESS in Distribution Systems With a High Penetration of Wind Energy," *IEEE Transactions on Power Systems,* vol. 25, no. 4, pp. 1815-1822, Nov. 2010.
[38] A. Keane, L. F. Ochoa, C. L. T. Borges, G. W. Ault, A. D. Alarcon-Rodriguez, R. A. Currie, F. Pilo, C. Dent, and G. P. Harrison, "State-of-the-Art Techniques and Challenges Ahead for Distributed Generation Planning and Optimization," *IEEE Transactions on Power Systems,* vol. 28, no. 2, pp. 1493-1502, May 2013.
[39] D. Q. Hung, N. Mithulananthan, and R. Bansal, "Analytical expressions for DG allocation in primary distribution networks," *IEEE Transactions on Energy Conversion,* vol. 25, no. 3, pp. 814-820, Sept. 2010.
[40] Y. M. Atwa and E. F. El-Saadany, "Probabilistic approach for optimal allocation of wind-based distributed generation in distribution systems," *IET Renewable Power Generation,* vol. 5, no. 1, pp. 79-88, Jan. 2011.
[41] T. Niknam and H. Doagou-Mojarrad, "Multiobjective economic/emission dispatch by multiobjective θ-particle swarm optimisation," *IET Generation, Transmission & Distribution,* vol. 6, no. 5, pp. 363-377, May 2012.
[42] C. Chen, S. Duan, T. Cai, B. Liu, and G. Hu, "Optimal allocation and economic analysis of energy storage system in microgrids," *IEEE Transactions on Power Electronics,* vol. 26, no. 10, pp. 2762-2773, Oct. 2011.
[43] M. F. Akorede, H. Hizam, I. Aris, and M. Z. A. Ab Kadir, "Effective method for optimal allocation of distributed generation units in meshed electric power systems," *IET Generation, Transmission & Distribution,* vol. 5, no. 2, pp. 276-287, Feb. 2011.
[44] C. Chen, S. Duan, T. Cai, B. Liu, and G. Hu, "Smart energy management system for optimal microgrid economic operation," *IET Renewable Power Generation,* vol. 5, no. 3, pp. 258-267, May 2011.
[45] S. Kannan, S. M. R. Slochanal, and N. P. Padhy, "Application and comparison of metaheuristic techniques to generation expansion planning problem," *IEEE Transactions on Power Systems,* vol. 20, no. 1, pp. 466-475, Feb. 2005.
[46] P. Hu, R. Karki, and R. Billinton, "Reliability evaluation of generating systems containing wind power and energy storage," *IET Generation, Transmission & Distribution,* vol. 3, no. 8, pp. 783-791, Aug. 2009.
[47] A. Soroudi, M. Ehsan, and H. Zareipour, "A practical eco-environmental distribution network planning model including fuel cells and non-renewable distributed energy resources," *Renewable Energy,* vol. 36, no. 1, pp. 179-188, 2011.
[48] HydroOne. *Distributed generation technical interconnection requirements*, Available: http://www.hydroone.com/Generators/Pages/TechnicalRequirements.aspx
[49] Y. M. Atwa, E. F. El-Saadany, M. M. A. Salama, and R. Seethapathy, "Optimal Renewable Resources Mix for Distribution System Energy Loss Minimization," *IEEE Transactions on Power Systems,* vol. 25, no. 1, pp. 360-370, Feb. 2010.
[50] R. Herman and J. J. Kritzinger, "The statistical description of grouped domestic electrical load currents," *Electric Power Systems Research,* vol. 27, no. 1, pp. 43-48, May 1993.

[51] A. Seppälä, *Load research and load estimation in electricity distribution*, Technical Research Centre of Finland, 1996.
[52] D. H. O. McQueen, P. R. Hyland, and S. J. Watson, "Monte Carlo simulation of residential electricity demand for forecasting maximum demand on distribution networks," *IEEE Transactions on Power Systems,* vol. 19, no. 3, pp. 1685-1689, Aug. 2004.
[53] C. Singh and Y. Kim, "An efficient technique for reliability analysis of power systems including time dependent sources," *IEEE Transactions on Power Systems,* vol. 3, no. 3, pp. 1090-1096, Aug. 1988.
[54] H. Lund, G. Salgi, B. Elmegaard, and A. N. Andersen, "Optimal operation strategies of compressed air energy storage (CAES) on electricity spot markets with fluctuating prices," *Applied Thermal Engineering,* vol. 29, no. 5–6, pp. 799-806, Apr. 2009.
[55] J. Usaola, "Operation of concentrating solar power plants with storage in spot electricity markets," *IET Renewable Power Generation,* vol. 6, no. 1, pp. 59-66, Jan. 2012.
[56] J. Garcia-Gonzalez, R. M. R. de la Muela, L. M. Santos, and A. M. Gonzalez, "Stochastic Joint Optimization of Wind Generation and Pumped-Storage Units in an Electricity Market," *IEEE Transactions on Power Systems,* vol. 23, no. 2, pp. 460-468, May 2008.
[57] A. D. Lamont, "Assessing the economic value and optimal structure of large-scale electricity storage," *IEEE Transactions on Power Systems,* vol. 28, no. 2, pp. 911-921, May 2013.
[58] R. Sioshansi, P. Denholm, T. Jenkin, and J. Weiss, "Estimating the value of electricity storage in PJM: Arbitrage and some welfare effects," *Energy Economics,* vol. 31, no. 2, pp. 269-277, Mar. 2009.
[59] B. Nyamdash and E. Denny. (2011). *The impact of electricity storage on wholesale electricity prices,* Available: http://mpra.ub.uni-muenchen.de/34941/
[60] A. A. Chowdhury and D. O. Koval, "Current practices and customer value-based distribution system reliability planning," *IEEE Transactions on Industry Applications,* vol. 40, no. 5, pp. 1174-1182, Sept.-Oct. 2004.
[61] Y. M. Atwa, E. F. El-Saadany, M. M. A. Salama, R. Seethapathy, M. Assam, and S. Conti, "Adequacy Evaluation of Distribution System Including Wind/Solar DG During Different Modes of Operation," *IEEE Transactions on Power Systems,* vol. 26, no. 4, pp. 1945-1952, Nov. 2011.
[62] P. Wang, Y. Ding, and L. Goel, "Reliability assessment of restructured power systems using optimal load shedding technique," *IET Generation, Transmission & Distribution,* vol. 3, no. 7, pp. 628-640, Jul. 2009.
[63] G. Wacker and R. Billinton, "Customer cost of electric service interruptions," *Proceedings of the IEEE,* vol. 77, no. 6, pp. 919-930, 1989.
[64] M. J. Sullivan, M. G. Mercurio, and J. A. Schellenberg, "Estimated Value of Service Reliability for Electric Utility Customers in the United States," *LBNL Research Project Final Report,* June 2009.
[65] J. Hetzer, D. C. Yu, and K. Bhattarai, "An Economic Dispatch Model Incorporating Wind Power," *IEEE Transactions on Energy Conversion,* vol. 23, no. 2, pp. 603-611, Jun. 2008.
[66] C. Grigg, P. Wong, P. Albrecht, R. Allan, M. Bhavaraju, R. Billinton, Q. Chen, C. Fong, S. Haddad, S. Kuruganty, W. Li, R. Mukerji, D. Patton, N. Rau, D. Reppen, A. Schneider, M. Shahidehpour, and C. Singh, "The IEEE Reliability Test System-1996. A report prepared by the Reliability Test System Task Force of the Application of Probability Methods Subcommittee," *IEEE Transactions on Power Systems,* vol. 14, no. 3, pp. 1010-1020, Aug. 1999.
[67] L. Goel and R. Billinton, "Determination of reliability worth for distribution system planning," *IEEE Transactions on Power Delivery,* vol. 9, no. 3, pp. 1577-1583, Jul. 1994.

[68] S. Yan, H. Nai-Shan, and S. Zhi-Yuan, "Power Flow Calculation Method for Islanded Power Network," in *Asia-Pacific Power and Energy Engineering Conference (APPEEC)*, Wuhan, China, pp. 1-5, 28–31 March 2009.

[69] B. Craenen, A. Eiben, and E. Marchiori, "How to handle constraints with evolutionary algorithms," *Practical Handbook of Genetic Algorithms: Applications,* pp. 341-361, 2001.

[70] Y. G. Hegazy, M. M. A. Salama, and A. Y. Chikhani, "Adequacy assessment of distributed generation systems using Monte Carlo Simulation," *IEEE Transactions on Power Systems,* vol. 18, no. 1, pp. 48-52, Feb. 2003.

[71] G. M. Masters, *Renewable and Efficient Electric Power Systems*, NY: IEEE/Wiley Interscience, 2004.

[72] B. Venkatesh, R. Ranjan, and H. B. Gooi, "Optimal reconfiguration of radial distribution systems to maximize loadability," *IEEE Transactions on Power Systems,* vol. 19, no. 1, pp. 260-266, Feb. 2004.

[73] P. Poonpun and W. T. Jewell, "Analysis of the Cost per Kilowatt Hour to Store Electricity," *IEEE Transactions on Energy Conversion,* vol. 23, no. 2, pp. 529-534, Jun. 2008.

[74] *Market Summaries*, Available: http://www.ieso.ca/imoweb/marketdata/marketSummary.asp

[75] S. Wong, K. Bhattacharya, and J. D. Fuller, "Electric power distribution system design and planning in a deregulated environment," *IET Generation, Transmission & Distribution,* vol. 3, no. 12, pp. 1061-1078, Dec. 2009.

[76] S. A. Gabriel, A. J. Conejo, J. D. Fuller, B. F. Hobbs, and C. Ruiz, *Complementarity Modeling in Energy Markets* Springer 2013.

[77] T. H. M. El-Fouly, H. H. Zeineldin, E. F. El-Saadany, and M. M. A. Salama, "Impact of wind generation control strategies, penetration level and installation location on electricity market prices," *IET Renewable Power Generation,* vol. 2, no. 3, pp. 162-169, Sept. 2008.

[78] H. H. Zeineldin, K. Bhattacharya, E. F. El-Saadany, and M. M. A. Salama, "Impact of intentional islanding of distributed generation on electricity market prices," *IEE Proceedings, Generation, Transmission and Distribution,* vol. 153, no. 2, pp. 147-154, Mar. 2006.

[79] S. X. Chen, H. B. Gooi, and M. Q. Wang, "Sizing of Energy Storage for Microgrids," *IEEE Transactions on Smart Grid,* vol. 3, no. 1, pp. 142-151, Mar. 2012.

[80] Y. V. Makarov, D. Zhao-Yang, and D. J. Hill, "On Convexity of Power Flow Feasibility Boundary," *IEEE Transactions on Power Systems*, vol. 23, no. 2, pp. 811-813, May 2008.

[81] *Power system test case archive*, Available: http://www.ee.washington.edu/research/pstca/

[82] M. Kintner-Meyer, J. Chunlian, P. Balducci, M. Elizondo, G. Xinxin, T. Nguyen, F. Tuffner, and V. Viswanathan, "Energy storage for variable renewable energy resource integration — A regional assessment for the Northwest Power Pool (NWPP)," in *IEEE/PES Power Systems Conference and Exposition (PSCE)*, pp. 1-7, 20–23 Mar. 2011.